University of the Aegean
Department of Environment
Biodiversity Conservation Laboratory

DOCTORAL THESIS

Assessing the health state of arboreal vegetation in urban, rural, and natural ecosystems, using non–destructive phenotypic techniques: implications for conservation and management

Yiannis G. Zevgolis


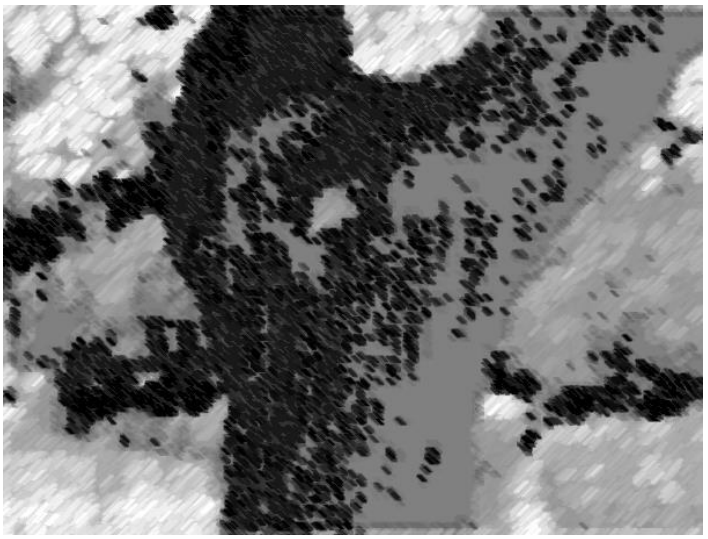

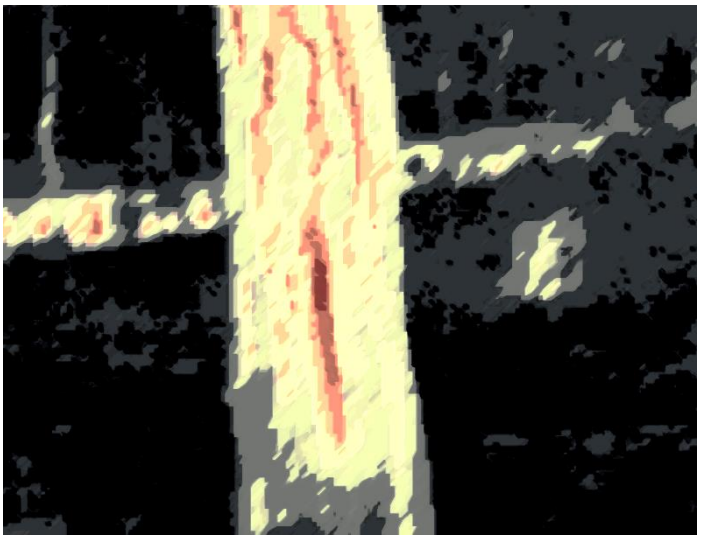

Mytilene, 2022

Assessing the health state of arboreal vegetation in urban, rural, and natural ecosystems, using non–destructive phenotypic techniques: implications for conservation and management

Yiannis G. Zevgolis

Biodiversity Conservation Laboratory, Department of Environment

Doctoral Thesis

University of the Aegean, Mytilene, Greece

Assessing the health state of arboreal vegetation in urban, rural, and natural ecosystems, using non–destructive phenotypic techniques: implications for conservation and management

Synopsis

Conservation of urban, rural, and natural ecosystems, through effective monitoring of their health state, is crucial both at a tree and at a population level. In this thesis, a comprehensive methodological framework for estimating the health state of arboreal vegetation was established, by considering the trees' fundamental phenotypic, spectral, spatial, thermal, and humidity traits. A set of 910 trees from nine different species was evaluated, by obtaining phenotypic information from (a) 334 urban trees (*Robinia pseudoacacia, Morus alba, Melia azedarach*), 80 olive trees (*Olea europaea*), and 496 pine trees (*Pinus brutia*). The effect of different disturbances such as structural defects and fungal presence, which can compromise the trees' mechanical integrity, health, and productivity, was detected, quantified, and mapped, with the use of non–destructive phenotypic techniques. Results showed that combining the trees' phenotypic traits and indices, can sufficiently (a) estimate decay severity, (b) classify hazardous trees, (c) identify fungal presence, and (e) predict the trees' growth rate and productivity. All of these can contribute to tree health assessment, by offering significant information in monitoring urban, rural, and natural ecosystems' dynamics.

Keywords: *traditional agroecosystems; phenotypic traits; infrared thermography; Lesvos; Olea europaea var. pyriformis; urban trees; tree risk assessment; R. pseudoacacia; M. alba; M.azedarach; spatial statistics; hotspot analysis; kriging geostatistical procedure; pine forests; P. brutia; resin extraction process; hemispherical imaging, thermal and humidity indices*

Author's address**:** Yiannis G. Zevgolis, Biodiversity Conservation Laboratory, Department of Environment, University of the Aegean, Mytilene 81100, Greece.
E–mail: zevgolis@env.aegean.gr

Funding: This research received no external funding.

Data Availability Statement: The data that support the findings of this thesis are available from the author, [Y.G.Z.], upon reasonable request.

Scientific Board of Examiners

Professor **Andreas Y. Troumbis**
Department of Environment, University of the Aegean, Supervisor

Professor **Panayiotis G. Dimitrakopoulos**
Department of Environment, University of the Aegean, Doctoral Advisory Committee

Professor **Ioannis G. Matsinos**
Department of Environment, University of the Aegean, Doctoral Advisory Committee

Assistant Professor **Triantaphyllos Akriotis**
Department of Environment, University of the Aegean, Member

Assistant Professor **Nikolaos M. Fyllas**
Department of Environment, University of the Aegean, Member

Associate Professor **Georgios Kokkoris**
Department of Marine Sciences, University of the Aegean, Member

Assistant Professor **Georgios G. Adamidis**
Biology Department, University of Patras, Member

To my parents, George and Irene,
who are always by my side, loving, caring and supporting

Some thoughts…

Somewhere here this journey is coming to an end. It was quite a journey!!! What an experience….

I was extremely fortunate to have landed into a department that is friendly and supportive. To have come this far, there were people who supported, advised, and guided me throughout this journey. The least I can do is to say a huge and sincere thank you…

First of all, I would like to express my sincere gratitude to my supervisor Prof. Andreas Y. Troumbis for giving me the opportunity to pursue and finally finish a Ph.D. concerning my own interests. Thank you very much for the trust, the teaching opportunities, and the space that you provided me. Thank you for not judging my failures and setbacks, thank you for not emphasizing my few accomplishments…All of these, helped me to fight for everything, to learn things on my own, to find solutions where they did not exist, and to avoid situations that bothered me…After all, as you always said 'a Ph.D. student is self–created'… and I think that I did so at every level…

Additionally, I would like to express my gratitude to Prof. Panayiotis G. Dimitrakopoulos for his support and guidance for issues concerning not only this doctoral dissertation but academia in general. Thank you for being supportive and very helpful at critical times…I will never forget it…

I would also like to express my sincere thanks to Assistant Prof. Triantaphyllos Akriotis, who believed in me and supported me in a variety of different ideas and thoughts that I had regarding interdisciplinary issues and approaches that were apart (but not so far) from this dissertation. Thank you for everything, I wholeheartedly wish that the help that you offered me will be given by me to others accordingly.

I would also like to thank Prof. Ioannis G. Matsinos who agreed to be on the Doctoral Advisory Committee and for the enjoyable academic discussions at the very early stages of this dissertation. I also like to thank Associate Prof. Georgios Kokkoris, who agreed to be in the seven–member Board of Examiners for the assessment of this thesis. Thank you very much for your statistical courses when I was an undergraduate student. I would like to offer my sincere thanks to Assistant Prof. Nikolaos M. Fyllas for his support and advice in general, but especially for his help during the field sampling in the coniferous forests. Last but not least, I would like to thank Assistant Prof. Georgios C. Adamidis who agreed to be in the seven–member Board of Examiners, for the assessment of this thesis, and also for his support when I was starting the field sampling in the urban parks.

I want to say a big thank you to Dr. Alexandros Galanidis with whom we have been together in the Biodiversity Conservation Laboratory for so many years…Thank you for still tolerating me, thank you for not judging and for being humble, thank you for not boasting your accomplishments.

I would also like to thank all the students of the undergraduate and postgraduate study program of the Department of Environment with whom I collaborated in the context of their dissertations: Akrivi Palmou (2016), Konstantinos Chaintarlis (2016), Chrysoniki Metaxa (2017), Despoina Chrysafi and Eleni Savvidou (2017), Maria–Zinovia Alsamail (2018), Vasiliki Michail (2019), Alexandros–Dimitrios Kouris (2020), Venetia Grammenou (2020), Maria Lykogeorgou (2020), Olga Mikroni (2020), Dimitra Kafetsi (2021), and Marios Leros (2021). You must know

that all of you have helped me a lot and you have been an important factor concerning my Ph.D.

Many friends and colleagues have helped in many ways during the past years. I would like to thank Efstratios Kamatsos, Andreas Masouras, and Lazaros Tsiridis, for their constant psychological support and boosting; Chrysanthi Michelaki, for yelling at me every time that I had a setback or a "new" innovative idea; Christodoulos Sazeides, for being so good in discussing new ideas (Chrysanthi was not present), future projects and more; Stylianos Zannetos, for wakening me up and for his help during the field sapling in the pine forests and many more.

Finally, I would like to thank Taxiarchoula for just being there, and my parents, George and Irene, for the support that they have given me. Thank you for being there whenever I needed it, and even when I thought I didn't need it. Thank you for teaching me respect, confidence, and proper manners.

Mom, I am proud to say I got my love of learning, from you. I am truly a follower in your footsteps of thorough and practical thinking.

Dad, thank you for teaching me perseverance. You've helped me to be strong even through the hard times. Thank you for letting me find my own way…I will always keep in mind and follow your quote (in Greek) "Η τιμή, τιμή δεν έχει και χαρά στον που την έχει"…

Thank you all!!!

Mytilene, January 2022
Yiannis G. Zevgolis

Table of Contents

List of Publications

This thesis is based on the work contained in the following publications:

Scientific Journal

I. **Zevgolis Y.G.,** Kamatsos E., Akriotis T., Dimitrakopoulos P.G., Troumbis A.Y. (2022), **Estimating productivity, detecting biotic disturbances, and assessing the health state of traditional olive groves, using non–destructive phenotypic techniques**, *Sustainability*, 14(1), 391, https://doi.org/10.3390/su14010391

International Conference Proceedings

i. **Zevgolis Y.G.,** Zannetos S.P., Sazeides C.I, Fyllas N.M, Troumbis A.Y, (2021), **Non-destructive diagnostics for estimating fungal infection in resin-tapped and non-tapped pine trees**, In: "Proceedings of the 17th International Conference on Environmental Science And Technology", 01–04/09/2021, Athens, Greece.

ii. **Zevgolis Y.G.,** Troumbis A.Y., (2021), **Quantifying and mapping urban trees' decay severity using thermal and spatial indices: implications for tree hazard assessment and management**, In: "Proceedings of the 17th International Conference on Environmental Science And Technology", 01–04/09/2021, Athens, Greece.

iii. **Zevgolis Y.G.,** Troumbis A.Y., (2020), **Hot spots, cluster detection, and spatial outlier analysis for estimating trees' structural defects**, In: "Abstracts book of the 20th International Symposium of MESAEP on Environmental Pollution and its Impact on Life in the Mediterranean Region", pp. 205, 26–27/10/20, Athens, Greece.

iv. **Zevgolis Y.G.,** Alsamaail M.Z., Zannetos S.P., Troumbis A.Y., (2020), **Geospatial analysis for tree hazard assessment using screening tools: implications for urban forest management**, In: "Abstracts book of the 20th International Symposium of MESAEP on Environmental Pollution and its Impact on Life in the Mediterranean Region", pp. 204, 26–27/10/20, Athens, Greece.

v. **Zevgolis Y.G.,** Grammenou V., Zannetos S.P., Troumbis A.Y., (2020), **Evaluating the effectiveness of infrared techniques in quantifying disturbances of post harvested pine forest systems**, In: "Abstracts book of the 20th International Symposium of MESAEP on Environmental Pollution and its Impact on Life in the Mediterranean Region", pp. 203, 26–27/10/20, Athens, Greece.

vi. **Zevgolis Y.G.**, Zannetos S.P., Christopoulos A., Glezou I. (2020), **Assessment of High Nature Value farmlands with ground thermal imaging techniques: the case of Mediterranean olive groves in Naxos Island, Greece**, In: "Abstracts book of the 20th International Symposium of MESAEP on Environmental Pollution and its Impact on Life in the Mediterranean Region", pp. 179, 26–27/10/20, Athens, Greece.

vii. Alsamaail M.Z.I., **Zevgolis Y.G.,** Vasios G.K., Troumbis A.Y. (2018), **Thermal imaging as a diagnostic tool for stress detection in urban trees**, In: "Abstracts book of the 11th International Conference of the Hellenic Geographical Society (ICHGS – 2018)", 12–15/04/18, Lavrion, Greece.

viii. **Zevgolis Y.G.,** Vasios G.K., Troumbis A.Y. (2017), **Detection of woody vegetation structural stress in urban forests using thermal imaging**, In: "Abstracts book of the 19th International Symposium of MESAEP on Environmental Pollution and its Impact on Life in the Mediterranean Region", pp. 49–50, 04–06/10/17, Rome, Italy.

ix. **Zevgolis Y.G.,** Vasios G.K., Troumbis A.Y. (2017), **Precision Conservation of *Olea europaea* with thermal imaging techniques**, In: "Proceedings of the 15th International Conference on Environmental Science And Technology", 31/08–02/09/2017, Rhodes, Greece.

x. **Zevgolis Y.G.,** Vasios G.K, Kyriakidis P.C., Troumbis A.Y. (2015), **Thermal map analysis of tree trunks in urban parks with spatial statistics**, In: "Abstracts book of the 18th International Symposium of MESAEP on Environmental Pollution and its Impact on Life in the Mediterranean Region", pp. 255, 26–30/09/15, Crete, Greece.

Hellenic Conference Proceedings

i. **Zevgolis Y.G.,** Kamatsos E., Sazeides C.I., Petousi I., Troumbis A.Y. (2021), **Estimating productivity and detecting biotic and abiotic disturbances in traditional olive groves, using phenotypic indices**, In: "Abstracts book of the 9th Panhellenic Conference on Ecology, pp. 164, 10–14/10/21, Ioannina, Greece.

ii. **Zevgolis Y.G.,** Sazeides C.I., Zannetos S.P., Fyllas N.M., Troumbis A.Y. (2021), **Investigation of the effect of resin extraction process on the growth of the Brutia pine**, In: "Abstracts book of the 9th Panhellenic Conference on Ecology, pp. 161, 10–14/10/21, Ioannina, Greece.

iii. **Zevgolis Y.G.,** Alsamail M.Z. Zannetos P.S., Troumbis A.Y. (2019), **Assessment of the structural stability of woody vegetation species in urban ecosystems using non–invasive methods**, In: "Abstracts book of the 16th Panhellenic Scientific Conference of the Hellenic Botanical Society, pp. 68, 10–13/10/2019, Athens, Greece.

iv. **Zevgolis Y.G.,** Alsamaail M.Z.I., Vasios G.K., Troumbis A.Y., (2018), **Development of a methodological framework for woody vegetation species disturbance assessment using thermal indicators,** In: "Abstracts book of the 9th Panhellenic Conference on Ecology, 04–07/10/18, pp. 248, Herakleion, Greece.

v. Grammenou V., **Zevgolis Y.G.,** Zannetos P.S., Troumbis A.Y., (2018), **Thermal imaging as a tool for estimating disturbances in *Pinus brutia* forest systems after resin extraction**, In: "Abstracts book of the 9th Panhellenic Conference on Ecology, pp. 167, 04–07/10/18, Herakleion, Greece.

vi. Skoura C., **Zevgolis Y.G.,** Zannetos P.S., Troumbis A.Y., (2018), **The effect of canopy cover in regeneration and biomass subfloor of brutia forests after resin extraction,** In: "Abstracts book of the 9th Panhellenic Conference on Ecology, pp. 229, 04–07/10/18, Herakleion, Greece.

vii. **Zevgolis Y.G.,** Vasios G.K., Troumbis A.Y., (2015), **Detection of thermal signature of species *Robinia pseudoacacia* using spatial statistical methods,** In: "Abstracts book of the 14th Panhellenic Scientific Conference of the Hellenic Botanical Society, pp. 58–59, 08–11/10/2015, Patra, Greece.

Εισαγωγή

Οι ραγδαίες αλλαγές που παρατηρούνται στο κλίμα της Γης έχουν μεταβάλλει δραστικά τον πλανήτη και έχουν επιφέρει σημαντικές επιπτώσεις στα είδη και στα οικοσυστήματα (Parmesan, 2006). Οι προβλέψεις δεν είναι τόσο αισιόδοξες καθώς θεωρείται σχεδόν βέβαιο ότι θα υπάρξουν ακόμη πιο δραστικές μεταβολές στην κατάσταση των οικοσυστημάτων καθώς, η παγκόσμια μέση ετήσια θερμοκρασία προβλέπεται να αυξηθεί από 1.1 έως και 6.4 ^{o}C μέχρι το 2100 (IPCC, 2007b). Πολλά οικολογικά συστήματα εμφανίζουν ήδη τις επιπτώσεις των πρόσφατων κλιματικών αλλαγών (Parmesan and Yohe, 2003; Parmesan, 2006), με καλύτερα τεκμηριωμένες τις μεταβολές που παρουσιάζονται στη φαινολογία, τις κατανομές και τη φυσιολογία των ειδών. Υπό το πρίσμα των επικείμενων επιπτώσεων της κλιματικής αλλαγής και λόγω της αβεβαιότητας που διακρίνει τις προβλέψεις, γίνεται αντιληπτή η δυσκολία διαχείρισης των οικοσυστημάτων, η απώλεια των οποίων θεωρείται πρωταρχική αιτία απειλής για τη βιοποικιλότητα και τις οικοσυστημικές υπηρεσίες που απορρέουν από αυτή. Επιπλέον, η συνεχής τροποποίησή τους περιορίζει τη δυνατότητά τους να στηρίξουν ενδημικά είδη (Seastedt *et al*., 2008), ενώ παράλληλα, το 60% των παγκόσμιων οικοσυστημικών υπηρεσιών έχουν υποστεί υποβάθμιση, καθώς η ανθρωπογενής πίεση εκτείνεται στο 83% της επιφάνειας της γης (Sanderson *et al*., 2002) και στο 100% των ωκεανών (Halpern *et al*., 2008). Πλέον επιβεβαιώνεται η παραδοχή ότι το «ανθρώπινο αποτύπωμα» στη φύση έχει αυξηθεί σε τέτοιο βαθμό που θεωρείται σχεδόν βέβαιο ότι δεν υπάρχει οικοσύστημα στη Γη που να έχει διαφύγει από άμεση ή έμμεση ανθρώπινη επίδραση. Ως εκ τούτου,, η έννοια των αδιατάρακτων οικοσυστημάτων δεν υφίσταται καθώς από τη δεκαετία του 1990 οι φυσικές περιοχές μετατρέπονται σε ανθρωπογενείς με ρυθμό 11.4% (Balmford *et al*. 2002).

Παράλληλα, σημαντικός είναι και ο ρόλος των διαταραχών τόσο στη διαμόρφωση του τοπίου όσο και στην επίδραση που έχουν στα οικοσυστήματα. Πλήθος διαταραχών, φυσικές και ανθρωπογενείς, όπως φωτιές, πλημμυρικά φαινόμενα, εισαγωγή παρασίτων, βιολογικοί εισβολείς, κατακερματισμός ενδιαιτημάτων κ.ά., ασκούν πίεση στα οικοσυστήματα σε ένα ευρύ φάσμα χωρικών και χρονικών κλιμάκων. Ως διαταραχή ορίζεται οποιοδήποτε σχετικά διακριτό συμβάν στο χρόνο που διαταράσσει το οικοσύστημα, την κοινότητα, ή τη δομή του πληθυσμού και μεταβάλλει τη διαθεσιμότητα των φυσικών πόρων (White and Pickett, 1985). Οι διαταραχές καλύπτουν διαφορετικά μεγέθη και συχνότητες, χαρακτηρίζονται από συγκεκριμένη χωρική κατανομή, συχνότητα, προβλεψιμότητα και ένταση (White and Pickett, 1985) ενώ ταυτόχρονα απαιτείται ο σαφής προσδιορισμός τόσο των χωροχρονικών κλιμάκων του συστήματος μελέτης όσο και της ίδιας της διαταραχής. Οι όροι που περιγράφουν τη διαταραχή ενός οικοσυστήματος, - υποβάθμιση, βλάβη, καταστροφή - αντιπροσωπεύουν τον βαθμό απόκλισης από την επιθυμητή κατάστασή του (SER, 2002; Day *et al*., 2006), που ουσιαστικά μπορεί να περιγραφεί από τον όρο «υγεία του οικοσυστήματος».

Η έννοια της «υγείας του οικοσυστήματος» (Su *et al*., 2010), περιλαμβάνει όλα εκείνα τα χαρακτηριστικά που την καθορίζουν όπως (α) η ζωτικότητα, η ελαστικότητα και η ανθεκτικότητα (Rapport, 1989), (β) η «απουσία ασθένειας» σε κλίμακα οικοσυστήματος, είδους, πληθυσμού και ατόμου (Rapport, 1992) και (γ) η ικανότητα παροχής οικοσυστημικών υπηρεσιών (Su *et al*. 2010). Επιπλέον, η έννοια αυτή περιλαμβάνει τόσο οικολογική όσο και κοινωνικοοικονομική προοπτική που μελετάται, εδώ και χρόνια, από μία πληθώρα διακριτών ερευνητικών πεδίων. Τα χαρακτηριστικά αυτά, ορίζουν την ικανότητα ενός συστήματος να παραμένει αμετάβλητο απέναντι σε εξωτερικές πιέσεις, να ανακάμπτει από διαταραχές και να ανταπεξέρχεται σε γεγονότα πίεσης (Walker *et al*., 2004; Cumming and Collier, 2005). Άλλωστε, τα υγιή, πλήρως λειτουργικά οικοσυστήματα, είναι περισσότερο ανθεκτικά σε περιβαλλοντικές πιέσεις και συνεπώς περισσότερο ευέλικτα, όσον αφορά την προσαρμογή τους στις επιπτώσεις εξωτερικών πιέσεων.

Στα αστικά, αγροτικά και δασικά οικοσυστήματα, οι ανθρωπογενείς πιέσεις που παρατηρούνται αποτελούν παράγοντες υποβάθμισής τους, οι οποίοι και ενισχύονται από διαταραχές που προκύπτουν τόσο από βιοτικούς όσο και από αβιοτικούς παράγοντες, οι οποίοι και επιδρούν αρνητικά τόσο στα οικοσυστήματα όσο και στα είδη που περικλείονται σε αυτά (Boa, 2003) (**Πίνακας 1**).

Πίνακας 1. Κατηγορίες βιοτικών και αβιοτικών διαταραχών σε αστικά, αγροτικά και δασικά οικοσυστήματα

Βιοτικοί παράγοντες	**Συμπτώματα**	**Αβιοτικοί παράγοντες**	**Συμπτώματα**
Μύκητες	Κιτρινίσματα ή/και ξηράνσεις φυλλαρίων. Στα τελικά στάδια παρατηρούνται σχισίματα στον κορμό	Φυτοφάρμακα/ ζιζανιοκτόνα	Κίτρινα σημάδια στα φύλλα, αποχρωματισμός, νέκρωση ριζικού συστήματος
Βακτήρια	Αποξηράνσεις κλάδων και ολόκληρων δέντρων	Μηχανικά μέσα	Κοιλότητες, αποκοπή κλάδων, αποφλοίωση, σήψη, είσοδος μυκήτων
Ιοί	Πλήρης ξήρανση σε μερικούς μήνες ανάλογα την περίπτωση	Εδαφικές συνθήκες	Υπερβολική διαθεσιμότητα /ανεπάρκεια θρεπτικών, κακή αποστράγγιση, αναστολή ανάπτυξης ριζικού συστήματος
Έντομα	Σημαντική μείωση στην ετήσια προσαύξηση των δέντρων, αποφλοίωση, νέκρωση καταπονημένων δέντρων	Κλιματικές συνθήκες	Οι επιπτώσεις του κλίματος στην υγεία των δένδρων δεν είναι άμεσες (εξαίρεση τα ακραία καιρικά φαινόμενα)
Ακάρεα	Απομύζηση των φύλλων και καρπών	Διαθεσιμότητα νερού	Τα δέντρα διαφέρουν ως προς την ικανότητα αντοχής στην υπερβολική διαθεσιμότητα/έλλειψη νερού.
Παρασιτικά φυτά	Αποδυνάμωση του ξενιστή από τον οποίο εξασφαλίζουν τα απαραίτητα θρεπτικά συστατικά.		
Ζώα	Αποδυνάμωση του δέντρων λόγω απώλειας φλοιού και φυλλώματος.		

Στα αστικά οικοσυστήματα, η αύξηση των επιπέδων ρύπανσης στις αστικές περιοχές, η αύξηση του πληθυσμού και η ολοένα αυξανόμενη οδική πυκνότητα, επηρεάζουν άμεσα ή έμμεσα την ξυλώδη βλάστηση και ιδιαίτερα τα αστικά δέντρα, μειώνοντας την ανάπτυξή τους και διαφοροποιώντας τα φαινοτυπικά χαρακτηριστικά τους (λ.χ. απόκτηση ρωγμών, σχισμών, κοιλοτήτων), οδηγώντας στην αύξηση της πιθανότητας αποσύνθεσής τους. Στα αγροτικά οικοσυστήματα, η εντατικοποίηση της γεωργίας, η εγκατάλειψη της αγροτικής γης και η ολοένα και αυξανόμενη χρήση φυτοφαρμάκων και ζιζανιοκτόνων δρουν συνεργατικά τόσο με αβιοτικούς παράγοντες, όπως η υδρογεωλογική αστάθεια, η υδατική καταπόνηση, η απώλεια οργανικής ύλης του εδάφους και η διάβρωση (Salvati and Ferrara, 2015; Dunjó *et al*., 2003), όσο και με βιοτικούς (μύκητες, βακτήρια, ιοί). Οι παράγοντες αυτοί, ασκούν επιπρόσθετη πίεση που επηρεάζει άμεσα τη δυναμική αυτών των οικοσυστημάτων, μειώνοντας την παραγωγικότητά τους, και κατ' επέκταση την υγεία τους και το προσδόκιμο ζωής τους. Στα δασικά οικοσυστήματα, η συχνότητα, η διάρκεια και η σοβαρότητα καταπονήσεων που προκαλούνται από ακραία καιρικά φαινόμενα, άμεσα σχετιζόμενα με την κλιματική αλλαγή, μπορεί να μεταβάλλει τη δασική σύνθεση, τη δομή και τη βιογεωγραφία των δασών σε πολλές περιοχές (Allen *et al*., 2010), ενώ οι ανθρωπογενείς πιέσεις που παρατηρούνται όπως η αλλαγή χρήσεων γης, η υπερβόσκηση, η αυξανόμενη ζήτηση ξυλείας καθώς και η εν γένει συγκομιδή δασικών προϊόντων, αποτελούν παράγοντες υποβάθμισης που δυνητικά μπορεί να οδηγήσουν στη μεταβολή της διαθεσιμότητας των φυσικών πόρων, στη διαφοροποίηση των δασικών εκτάσεων και στη μείωση της παραγωγικότητας και της αναγέννησής τους.

Υπό αυτό το πρίσμα, η παρακολούθηση και η αξιολόγηση της υγείας οικοσυστημάτων και ειδών, καθώς και η ποσοτικοποίηση των διαταραχών που τους ασκούνται σε επίπεδο τοπίου, οικοσυστήματος και είδους, αποτελεί πρόκληση τόσο σε επίπεδο συλλογής πρωτογενών δεδομένων όσο και σε επίπεδο ανάλυσής τους, ενώ παράλληλα οι πληροφορίες αυτές είναι κρίσιμης σημασίας, προκειμένου να αναπτυχθούν αποτελεσματικά σχέδια διαχείρισης τόσο για την προστασία όσο και για τη διατήρησή τους.

Στη διεθνή επιστημονική βιβλιογραφία, η κύρια τάση παρακολούθησης και ποσοτικοποίησης της υγείας, σε επίπεδο τοπίου και οικοσυστήματος, αφορά μεθοδολογίες που συνδυάζουν δεδομένα πεδίου καθώς και πολυφασματικούς αισθητήρες διαφορετικής χωρικής ανάλυσης, όπως δορυφορικές, εναέριες και επίγειες εικόνες (Zhang, 2010). Σε επίπεδο τοπίου και οικοσυστήματος, οι μεθοδολογίες αυτές συνδυάζουν δεδομένα από αισθητήρες υψηλής ανάλυσης οι οποίοι μεταξύ άλλων δίδουν τη δυνατότητα ταχείας ανίχνευσης μεταβολών των χρήσεων γης και υποβάθμισης των οικοσυστημάτων (Hansen *et al*., 2008; Eva *et al*., 2010). Ταυτόχρονα, ένα ευρύ φάσμα τηλεπισκοπικών δεδομένων (υπερφασματικών, πολυφασματικών, θερμικών) και δεικτών που προκύπτουν από αυτά (π.χ. δείκτες βλάστησης) έχουν αρχίσει να χρησιμοποιούνται ευρύτατα για την παρακολούθηση των οικοσυστημάτων και την αξιολόγηση των πιέσεων που τους ασκούνται (Nagendra *et al*., 2013). Οι πολυφασματικές και υπερφασματικές εικόνες σε συνδυασμό με δεδομένα ακτινοβολίας, έχουν βελτιώσει τη χαρτογράφηση, την εκτίμηση της κατάστασης και την παρακολούθηση των ενδιαιτημάτων, αυξάνοντας την ακρίβεια στη μέτρηση μεταβλητών σχετικών με τα λειτουργικά τους χαρακτηριστικά, τα οποία μπορεί να σχετίζονται με σημαντικές ιδιότητες των ενδιαιτημάτων, συμπεριλαμβανομένης της βιομάζας ή και της ηλικίας των μελετώμενων συστημάτων (Boyd and Danson, 2005). Οι θερμικές εικόνες τηλεπισκοπικών δεδομένων προσφέρουν επίσης σημαντικές πληροφορίες σχετικές με τις θερμοκρασιακές κατανομές και τις επιφανειακές ενεργειακές ροές (εκτίμηση της εξατμισοδιαπνοής και της υγρασίας του εδάφους), οι οποίες αποτελούν αναπόσπαστο μέρος των διαδικασιών κατανόησης του τοπίου (Quattrochi and Luvall, 1999; Kerr and Ostrovsky, 2003).

Σε επίπεδο είδους αλλά και ατόμου, ιδιαίτερα σε ότι αφορά την ξυλώδη βλάστηση, η αξιολόγηση και ποσοτικοποίηση των διαταραχών απαιτεί υψηλή ακρίβεια και ως εκ τούτου η χρήση διαγνωστικών συσκευών θεωρείται επιβεβλημένη. Οι μεθοδολογίες που ανιχνεύουν τα επίπεδα υγείας των υπό εξέταση ειδών χαρακτηρίζονται ως καταστρεπτικές και μη-καταστρεπτικές, ανάλογα με (Johnstone *et al*., 2010): (α) τη διεισδυτικότητα και τη βλάβη που προκαλείται στους ιστούς των υπό μελέτη ειδών, (β) την ακρίβεια εκτίμησης διαταραχών σε συνθήκες πεδίου και (γ) την ευκολία χρήσης και ερμηνείας των πρωτογενών (μη-επεξεργασμένων) δεδομένων. Τα εργαλεία αυτά ταξινομούνται ανάλογα με την ταχύτητα μέτρησης, την ανάλυση και την ακρίβειά τους σε (Vidal and Pitarma, 2019) (**Πίνακας 2**):

- εργαλεία προβολής (screening tools) - γρήγορη αλλά χαμηλής ανάλυσης αξιολόγηση
- εργαλεία αξιολόγησης (evaluation tools) - ενδιάμεσα των εργαλείων προβολής και διάγνωσης
- εργαλεία διάγνωσης (diagnostic tools) - αργή αλλά υψηλής ανάλυσης αξιολόγηση για την έκταση των μελετούμενων διαταραχών

Πίνακας 2. Μεθοδολογίες και τεχνικές ανίχνευσης της κατάστασης των δέντρων

Μεθοδολογία	Εργαλεία	Κύρια σημεία
Καταστρεπτική	Προσαυξητική τρυπάνη	Κοινό εργαλείο εξαγωγής πυρήνων από ένα δέντρο για τον προσδιορισμό του ρυθμού αύξησης, της ηλικίας και της ευρωστίας τους.
Καταστρεπτική	Ενδοσκοπική κάμερα	Δημιουργία οπής με ηλεκτρικό τρυπανίδιο όπου εισάγεται η κάμερα

Καταστρεπτική	Resistograph	Εισαγωγή μικρής τρυπάνης/βελόνας στο δέντρο και καταγραφή της αντίσταση διάτρησης. Δεν ανιχνεύει πρόωρα έως και ενδιάμεσα στάδια αποσύνθεσης.
Καταστρεπτική	Shigometer	Δημιουργία οπής και εισαγωγή παλμικού συνεχούς ρεύματος, το οποίο πηγαίνει στο ξύλο ή στο φλοιό του δέντρου και καταγράφει την ηλεκτρική αντίσταση
Καταστρεπτική	Fractometer	Προσδιορίζει την αντοχή στην κάμψη και στην θλίψη πυρήνων ξύλου
Μη καταστρεπτική	Stress wave velocity	Μέτρηση της διάδοσης ηχητικού κύματος (stress wave) στο ξύλο. Η ταχύτητα του κύματος σχετίζεται άμεσα με τις φυσικές και μηχανικές ιδιότητες του ξύλου.
Μη καταστρεπτική	Τεχνικές τομογραφίας	Εντοπισμός της θέσης των ανωμαλιών και εκτίμηση των μεγεθών, των σχημάτων και των χαρακτηριστικών τους σε ότι αφορά τις μηχανικές τους ιδιότητες.
Μη καταστρεπτική	Electronic nose	Διακρίνει το υγιές και το ξύλο σε αποσύνθεση μέσω αλλαγών στις πτητικές οργανικές ενώσεις που απελευθερώνονται από τους μύκητες από τη φθορά του ξύλου.

Σε επίπεδο είδους αλλά και ατόμου, μια μέθοδος που μπορεί να υποστηρίξει τη μελέτη των διαταραχών και την εν γένει αξιολόγηση της υγείας φυτικών ειδών, είναι μια μη καταστροφική μέθοδος, που ονομάζεται υπέρυθρη θερμογραφία (Ouis, 2003). Η υπέρυθρη θερμογραφία (infrared thermography) είναι μια ταχέως αναπτυσσόμενη τεχνική η οποία ανήκει στον ευρύτερο τομέα της τηλεπισκόπησης και ορίζεται ως: η τεχνική απεικόνισης ενός αντικειμένου χρησιμοποιώντας τη θερμική ακτινοβολία που εκπέμπει το αντικείμενο αυτό. Τα θερμικά δεδομένα, που εξάγονται από τη μέθοδο αυτή, αποτελούν χρήσιμους, μη-επεμβατικούς δείκτες για την απόκτηση αξιόπιστων δεδομένων χωρίς να επηρεάζονται άμεσα τα οικοσυστήματα και τα είδη που περικλείουν, καθώς οπτικοποιούν τη διαφοροποίηση της επιφανειακής θερμοκρασίας ενός αντικειμένου μέσω της ανίχνευσης της υπέρυθρης ακτινοβολίας που εκπέμπεται από αυτό (Dragavtsev and Nartov, 2015). Η υπέρυθρη θερμογραφία, έχει χρησιμοποιηθεί για τη μέτρηση της βιωσιμότητας σπόρων και δενδρυλλίων, την αναγνώριση διαταραχών, την εκτίμηση της ανάπτυξης φυτικών ειδών (Dragavtsev and Nartov, 2015) και την παρακολούθηση της φυσιολογικής κατάστασης των φυτών (Chaerle *et al*., 1999; Chaerle *et al*., 2001; Lenthe *et al*., 2007). Επιπλέον, η παρακολούθηση της θερμοκρασίας με υπέρυθρες τεχνικές συνεισφέρει στην αναγνώριση αβιοτικών και βιοτικών καταπονήσεων (stress) των ειδών που σχετίζονται με τη θερμική φυσιολογία τους (McCafferty, 2013; Briscoe *et al*., 2014), με την απώλεια νερού (Jones *et al*., 2009; Eitel *et al*., 2010; García-Tejero *et al*., 2012; Ballester *et al*., 2013), με την ανίχνευση ασθενειών σε αγροτικές καλλιέργειες (Oerke *et al*., 2006; Stoll *et al*., 2008) και δασικά συστήματα (Eitel *et al*., 2010; García-Tejero *et al*., 2012), με την εκτίμηση της αλατότητας του εδάφους (Dragavtsev and Nartov, 2015) και με την αξιολόγηση της υγείας συγκεκριμένων ειδών βλάστησης (Zevgolis *et al*., 2022; Catena and Catena, 2008).

Γενικά σε ότι αφορά την ξυλώδη βλάστηση, η κατανομή της επιφανειακής θερμοκρασίας δείχνει το αποτέλεσμα των συνθηκών υγείας του είδους και την παρουσία ή απουσία αποσύνθεσης μέσα σε αυτό (Burcham *et al*., 2012). Στα ιστάμενα δέντρα, οι ξυλοσηπτικοί μύκητες, καταστρέφουν το εγκάρδιο ξύλο, διακόπτουν την αγωγιμότητα σε ένα υγιές κομμάτι του κορμού, με αποτέλεσμα της διακοπή της ροής της θερμότητας. Όσο μεγαλύτερη είναι η έκταση της διαταραχής, τόσο μεγαλύτερη είναι η επίδραση στην επιφανειακή θερμοκρασία (Catena and Catena, 2008). Αν δεν υπάρχουν ασυνέχειες ή εσωτερική αποσύνθεση, η κατανομή της θερμοκρασίας στην επιφάνεια του εξεταζόμενου είδους είναι ενιαία. Μια μεταβαλλόμενη κατανομή της θερμοκρασίας της επιφάνειας του σώματος υπό μελέτη επισημαίνει ένα ελάττωμα μέσα στο σώμα. Αυτή η διαφορά θερμοκρασίας της επιφάνειας μεταξύ υγιών και κατεστραμμένων περιοχών εξαρτάται από την διαφορετική θερμική αγωγιμότητα τους. Στα δέντρα, η επιφανειακή τους θερμοκρασία είναι αποτέλεσμα της κίνησης της θερμικής ενέργειας στην επιφάνειά τους, ως αποτέλεσμα του πρώτου και δεύτερου νόμου της θερμοδυναμικής (η θερμότητα τείνει να κινηθεί από περιοχές υψηλής ενέργειας σε περιοχές χαμηλής ενέργειας) (Atkins and de Paula, 2006). Η θερμότητα κινείται μέσα από το «σύστημα» δέντρο από θερμότερες περιοχές σε ψυχρότερες περιοχές (Hunt *et al*., 2008). Η αγωγιμότητα του ξύλου είναι συνάρτηση τόσο σύνθεσής του όσο και της μορφολογίας των κυττάρων του (Potter and Andresen, 2002). Όταν υπάρχει μικρή διαταραχή στη δομή των κυττάρων

τότε η αγωγιμότητα είναι βέλτιστη, ενώ σε περίπτωση μεταβολής της δομής των κυττάρων (ιδιαίτερα εάν εισάγεται αέρας μέσα στο σύστημα) τότε η αγωγιμότητα μειώνεται σημαντικά.

Μαζί με την υπέρυθρη θερμογραφία, οι δείκτες φασματικής ανάκλασης του φαινότυπου των φυτών που σχετίζονται με τη φωτοσυνθετική τους ικανότητα και κατάσταση, όπως η συγκέντρωση χλωροφύλλης στα φύλλα και στην κόμη (Li *et al*., 2019; Obeidat *et al*., 2018; Guo *et al*., 2016; Wang *et al*., 2015), λαμβανόμενες σε συνθήκες πεδίου μη επεμβατικά, μπορεί να αντικατοπτρίζουν την κατάσταση της υγείας των φυτών. Εξάλλου, η χλωροφύλλη ως βασική φωτοσυνθετική χρωστική από την οποία εξαρτώνται η ανάπτυξη και η παραγωγικότητα των φυτών (Li *et al*., 2019), θεωρείται χαρακτηριστικός δείκτης για την εκτίμηση της υγείας τους (Almansoori *et al*., 2021; Pavlovic *et al*., 2014; Steele *et al*., 2008). Χαμηλή περιεκτικότητα σε χλωροφύλλη μπορεί να σημαίνει έκθεση σε βιοτικές και/ή αβιοτικές καταπονήσεις, ασθένειες και γήρανση (Sánchez–Reinoso *et al*., 2019; Mishra *et al*., 2016; Richardson *et al*., 2002), ενώ η εκτίμησή της παράσχει σημαντικές πληροφορίες για τη φωτοσυνθετική δραστηριότητα και την πρωτογενή παραγωγικότητα.

Οι παραπάνω μη-επεμβατικές τεχνικές παρακολούθησης, μπορούν να βελτιωθούν περαιτέρω με την υποστήριξη παραδοσιακών μεθόδων μέτρησης των δομικών και λειτουργικών χαρακτηριστικών των υπό εξέταση φυτών, όπως το ύψος, η διάμετρος, η φυλλική επιφάνεια και οι σχετικοί δείκτες της (π.χ. δείκτης επιφάνειας φύλλων-LAI), καθώς και η αρχιτεκτονική της κόμης. Συγκεκριμένα ο δείκτης φυλλικής επιφάνειας θεωρείται ένα από τα θεμελιώδη βιοφυσικά χαρακτηριστικά και συνδέεται άμεσα, μεταξύ άλλων, με την ανάπτυξη και την παραγωγικότητα των φυτών (Musau *et al*., 2016) και με την περιγραφή της δομής του οικοσυστήματος (Zarate-Valdez *et al*., 2012) καθώς ελέγχει το μικροκλίμα εντός και κάτω από την κόμη των δέντρων ρυθμίζοντας ταυτόχρονα τις ροές νερού και άνθρακα (Bréda, 2003).

Ένας συνδυασμός αυτών των μεθοδολογιών, μετρήσεων και τεχνικών μπορεί να παράσχει ένα ολοκληρωμένο μεθοδολογικό πλαίσιο δημιουργώντας και χρησιμοποιώντας μια ποικιλία διαφορετικών σύνθετων δεικτών και εξισώσεων που περιγράφουν τη συνολική κατάσταση της υγείας των δέντρων σε αστικά, αγροτικά και δασικά οικοσυστήματα, σε επίπεδο είδους, πληθυσμού και ατόμου. Προς τούτο, η παρούσα διδακτορική διατριβή φιλοδοξώντας να προσφέρει στη διασύνδεση αυτών των διακριτών μεθόδων και τεχνικών, χρησιμοποίησε μία πληθώρα διαφορετικών μη-επεμβατικών μεθόδων, εργαλείων, τεχνικών τα οποία περιγράφονται εκτενώς στη μεθοδολογία του κάθε κεφαλαίου, για τη διερεύνηση της κατάσταση της υγείας 910 ιστάμενων δέντρων, από 9 διαφορετικά είδη, σε αστικά, αγροτικά και δασικά συστήματα.

Συγκεκριμένα, σε ότι αφορά τα αστικά δέντρα (βλέπε: ***A. Detecting, quantifying and mapping urban trees' structural defects using non–destructive diagnostics: implications for tree hazard assessment and management***), ανιχνεύθηκαν και ποσοτικοποιήθηκαν τα δομικά ελαττώματά τους με τη συνδυασμένη χρήση θερμικών δεδομένων, χωρικών στατιστικών μεθόδων και λειτουργικών χαρακτηριστικών τους. Συνολικά εξετάσθηκαν 334 δέντρα από 9 διαφορετικά είδη που περικλείονται στα τέσσερα αστικά πάρκα της πόλης της Μυτιλήνης, Λέσβος, Ελλάδα. Αναπτύχθηκαν θερμικοί δείκτες και υπολογίσθηκε η χωρική τους εξάρτηση από τη θερμοκρασία στον κορμό κάθε δέντρου. Παράλληλα, αξιολογήθηκαν στατιστικά σημαντικές χωρικές συστάδες σε επίπεδο ατόμου, είδους και πληθυσμού χρησιμοποιώντας στατιστικές χωρικής αυτοσυσχέτισης. Διερευνήθηκαν οι σχέσεις μεταξύ δεικτών σταθερότητας των δέντρων, των θερμικών και χωρικών δεικτών χρησιμοποιώντας μοντέλα γραμμικής και λογιστικής παλινδρόμησης. Τέλος, χρησιμοποιήθηκε ο στατιστικός δείκτης Getis–Ord Gi* για την αναγνώριση των δυνητικά επικίνδυνων δέντρων στα αστικά πάρκα με την παράλληλη εφαρμογή γεωστατιστικών μεθόδων που στόχο είχε τη χαρτογράφηση της χωρικής τους εξάπλωσης.

Σε ότι αφορά τα αγροτικά οικοσυστήματα (βλέπε: ***B. Estimating productivity, detecting biotic disturbances, and assessing the health state of traditional olive groves, using non–destructive phenotypic techniques***), δημιουργήθηκε ένα ολοκληρωμένο μεθοδολογικό πλαίσιο για την εκτίμηση της κατάστασης της υγείας του παραδοσιακού ελαιώνα της Λέσβου, λαμβάνοντας υπόψη τα θεμελιώδη φαινοτυπικά, φασματικά και θερμικά χαρακτηριστικά των ελαιόδεντρων. Βάσει τετραετούς παρακολούθησης 80 ελαιόδεντρων, δημιουργήθηκαν γραμμικά και λογιστικά μοντέλα που επεξηγούν την παραγωγικότητά τους και την παρουσία του πιο σημαντικού μύκητα (κυκλοκόνειο) που διαταράσσει την υγεία τους. Βάσει των αποτελεσμάτων των μοντέλων τα ελαιόδεντρα ταξινομήθηκαν σε τρεις διαφορετικές καταστάσεις που περιγράφουν την υγεία τους.

Σε ότι αφορά τα δασικά συστήματα (βλέπε: ***C. Investigating the effect of resin collection and detecting fungal infection in resin-tapped and non-tapped pine trees, using minimally invasive and non-invasive diagnostics***), διερευνήθηκε η υγεία 496 πεύκων, σε 20 δειγματοληπτικές επιφάνειες στο κεντρικό πευκοδάσος της Λέσβου, τα οποία ρητινεύονταν συστηματικά στα μέσα του προηγούμενου αιώνα. Συγκεκριμένα, εξετάσθηκε η επίδραση της ρητίνευσης στην αύξησή τους ταυτόχρονα με την ανίχνευση της παρουσίας ξυλοσηπτικών μυκήτων στους κορμούς τους. Σε κάθε επιφάνεια, εξήχθησαν πυρήνες δέντρων από το 34% του συνόλου κάθε συστάδας, ενώ η παρουσία μυκήτων επιβεβαιώθηκε (α) από τον αποχρωματισμό και τα μοτίβα αποσύνθεσης στους πυρήνες των δέντρων, (β) από εξωτερικούς δείκτες αποσύνθεσης, όπως καρποφόρα σώματα, και (γ) από την ξαφνική αλλαγή στην αντίσταση διάτρησης κατά την εξαγωγή των πυρήνων των δέντρων. Αναπτύχθηκαν γραμμικά και λογιστικά μοντέλα τα οποία περιγράφουν με σαφήνεια την κατάσταση της υγείας των μελετώμενων δασικών συστημάτων.

A. Detecting, quantifying and mapping urban trees' structural defects using non–destructive diagnostics: implications for tree hazard assessment and management

Abstract

Urban trees are a fundamental and key component of urban green areas, however, are subject to several stresses which they can compromise their mechanical integrity through the development of structural defects. In this study, we evaluated the state of arboreal vegetation in four urban parks in the city of Mytilene, Greece, by taking into account structural and functional traits of the urban trees, their temperature distribution as illustrated through infrared thermography, and spatial statistics both in a single–tree level and in park level. We developed thermal indices by analyzing tree trunks' temperature data, and we estimated temperature spatial dependence across each tree's trunk using Moran's I index, while statistically significant spatial clusters were assessed using local spatial autocorrelation statistics. Relationships between tree stability, thermal, and spatial indices were established using linear and logistic regression models. Finally, we used the Getis–Ord Gi* statistic for the recognition of hazardous tree hotspots in the urban parks, and we applied the kriging geostatistical procedure for mapping their spatial extension. The results have shown that the thermal and spatial indices can sufficiently explain decay severity, identify hazardous trees, and contribute to tree health assessment for specialized park management.

Keywords

Arboreal vegetation; decayed wood; hazardous trees; infrared thermography; spatial statistics

A. List of Tables

A. List of Figures

A.1 Introduction

Urban green areas are complex dynamic ecosystems created by the interaction between anthropogenic and natural processes. They range from small patches of bushes, herbaceous plants, or lawns (Morgenroth and Östberg, 2017) to rather extensive urban forests of a primarily natural origin (Konijnendijk, 1997). They are widely recognised as playing an important role both for their aesthetic and amenity values (Bolund and Hunhammar, 1999) as well as for the provision of a wide range of ecosystem services (Livesley *et al.*, 2016; Gómez–Baggethun and Barton, 2013). Nowadays, urban green areas' multifunctional value is taken into account as a factor of sustainable development (Kabisch *et al.*, 2015; Su *et al.*, 2010), and their values are recognized and are part of the United Nations Sustainable Development Goals (Turner–Skoff and Cavender, 2019) well as of the 2030 biodiversity strategy, established in the European Union, which motivates cities to develop 'urban greening plans' including urban forests, parks, gardens, and tree–lined streets (European Commission, 2020).

Trees are a fundamental and key component of urban green areas, of great importance in urban planning (Cavender and Donnelly, 2019) as, beyond their ecosystem services to a city's inhabitants, they provide a variety of different habitat types and sizes especially for species being threatened by urban expansion (Russo and Ancillotto, 2015) as well as for animals and plants facilitating the necessary ecological processes (Lutz *et al.*, 2018; Lindenmayer and Laurance, 2017) for a sustainable city. Compared to trees in natural settings, urban trees are subject to several additional stresses. In particular, anthropogenic pressures such as undesirable tree site conditions (Scharenbroch *et al.*, 2017; Mullaney, 2015), gaseous air and particulate pollution (Rashidi *et al.*, 2012), increased road traffic density and intensity (Samecka–Cymerman *et al.*, 2009), and urban pollutants as indicated by heavy metal concentrations in urban tree rings (Chen *et al.*, 2011), could impose additional burden upon urban trees having already had setbacks due to the requirements for canopy and root space (Dahlhausen *et al.*, 2016; Mullaney, 2015), light availability limitations (Lüttge and Buckeridge, 2020), limitation of soil nutrient content (Ghosh *et al.*, 2016), and water stress (Savi *et al.*, 2015). At the same time, the increasing frequency and severity of extreme weather events (Hilbert *et al.*, 2019), as a result of climate change, contribute to reducing tree vigour and life span (Zhang and Brack, 2021), making tree growth and survival in urban environments more challenging, such as by increasing their susceptibility to fungi and other plant pathogens (Boa, 2003), as well as compromising their mechanical integrity and stability. All the above factors can increase the vulnerability of urban trees (Escobedo *et al.*, 2016) by creating mechanical weakness, especially through the development of structural defects, such as decayed wood, cracks, cankers, burls, and rotten tissue (Klein *et al.*, 2019; Miesbauer *et al.*, 2014). Urban trees' structural defects have a significant effect on their mechanical behaviour (Geitmann and Gril, 2018; Gardiner *et al.*, 2016; Miesbauer *et al.*, 2014), resulting in their structural instability and reduced strength (Escobedo *et al.*, 2016), and may lead to their failure (Kim *et al.*, 2020, 2021; Lonsdale, 2007; Kane and Ryan, 2004; Smiley and Fraedrich, 1992).

Unlike trees in a natural forest, trees developing structural defects in urban areas have to be removed for reasons of human safety and risk of damage to properties and infrastructures. Since trees take a long time to grow to mature size, deciding on the removal of urban trees cannot be taken lightly and must be based on the best possible assessment of the risks involved. Tree stability can be estimated via various strength loss equations (Mattheck and Breloer, 1994; Smiley and Fraedrich, 1992; Coder, 1989; Wagener, 1963) with a given threshold value, in order for the tree risk managers to decide in removing the potentially hazardous trees. In supporting decision–making for developing effective management plans to protect and conserve the trees from possible failing issues, several methodologies, characterized as either destructive or non–destructive, and a variety of tools, classified according to their measurement speed, resolution, and accuracy, are presented in the international scientific literature (Vidal and Pitarma, 2019; Leong *et al.*, 2012). Destructive

methods focus on the initial inspection of the trees visually (Mattheck and Breloer, 1994), in order to assess the presence of external indications of structural defects, and subsequently the tree bark is removed and holes are drilled into the trunk, using a variety of different tools (e.g., increment borer, decay detecting drill) and techniques, such as radiographic ones to measure the attenuation of X–rays and/or gamma rays of destructively obtained wood samples (cross–sections or cores) (Ouis, 2003), to detect and quantify the intensity of the structural defect (Goh *et al.*, 2018). A major drawback of these methods is that the wound caused in obtaining the samples creates conditions that lead to the gradual colonisation of internal functional or non–functional tissues by fungal communities (compartmentalized infection) (Boddy, 2001; Shigo and Marx, 1977). The latter constitutes a serious threat regarding standing vigorous urban trees, being among the leading causes of their mortality, and contributes greatly to their degradation (Deflorio *et al.*, 2008). On the contrary, proposed non–destructive methods, such as static bending and transverse vibration techniques (Allison and Wang, 2015), ground penetrating radar methods (Giannakis *et al.*, 2020; Nicolotti *et al.*, 2003), sonic/ultrasonic tomography (Espinosa *et al.*, 2019; Lin *et al.*, 2016), electrical resistivity tomography (Soge *et al.*, 2019), nuclear magnetic resonance (Zakaria *et al.*, 2013), microwave imaging (Martin *et al.*, 1987), and remote sensing imaging (Vidal and Pitarma, 2019; Catena and Catena, 2008), are considered more appropriate and efficient in detecting structural defects when assessing standing trees in the urban environment. However, even these non–invasive methods have drawbacks, when used in large scale tree inventories, in terms of sensitivity, accuracy, cost, time required, and operation easiness (Pitarma *et al.*, 2019).

Among these non–destructive methods, a relatively new technique, belonging to the broader field of remote sensing methods, is infrared thermography (IRT) (Bellett–Travers and Morris, 2010; Catena and Catena, 2008; Catena *et al.*, 2002). IRT is a non–destructive, non–contact, and non–invasive method for monitoring, among others, plant health state, as it can accurately estimate disturbances that may compromise their resilience; the infrared images can be obtained in real–time and the inspected trees can be examined as a whole, in contrast to other non–invasive methods (Pitarma *et al.*, 2019). The extracted temperature data from the trees' surface (e.g., bark, branches), in combination with visual examination for characteristic symptoms of fungal infections, can indicate possible structural defects (Terho, 2009) and can identify possible hazardous trees. In particular, a homogeneous temperature distribution on tree stems and branches is considered a health state indicator, as deterioration, voids, decay, and structural defects in general which may occur within their trunks, interrupt energy flow and cause temperature abnormalities on their surface (Catena and Catena, 2008; Hunt *et al.*, 2008). After all, structurally defected areas result from an internal long–term interaction between fungi and tree that leads to the disruption of energy flow, temperature abnormalities on the tree's surface, and possible tree mortality (Pokorny, 2003).

Despite the extensive use of IRT in various fields of natural sciences (Still *et al.*, 2019; Matese *et al.*, 2018; Ouledali *et al.*, 2018; Dragavtsev and Nartov, 2015; Ishimwe *et al.*, 2014; Ribeiro da Luz, 2006), its current use in assessing urban tree structural defects and their overall health is limited (Pitarma *et al.*, 2019; Bellett–Travers and Morris, 2010; Catena and Catena, 2008); it is therefore essential to advance further research efforts on its large scale use in urban trees, highlighting, beyond its importance as a rapid diagnostic method, its contribution when combined with data related to trees' strength loss. Thus, the main aim of our research was to detect and quantify urban tree structural defects with the use of IRT and to identify hazardous tree hotspots in an urban setting. For this, we obtained thermal data from the three main species of arboreal vegetation (*Robinia pseudoacacia, Morus alba, Melia azedarach*) in four urban parks of the city of Mytilene (Greece) and we combined these data, with trees' structural and functional traits, and spatial indices to investigate the following objectives: (a) to examine trees' thermal pattern differences both within tree species and among the recorded structural defects, (b) to quantify the effect of traits and indices on tree's trunk surface

thermal data, and (c) to explain the presence of trees' structural defects and to identify hazardous tree hotspots in the study area.

A.2 Materials and methods

A2.1 Study area

The city of Mytilene is the capital of the Greek island of Lesvos, in the NE Aegean Sea. The city has an area of 107.46 km² with 29,656 inhabitants according to the 2014 census of the Hellenic Statistical Authority, and has four main urban parks (**Figure A1**), with a total area of approximately 27,000 m^2, and many small urban green spaces, scattered within its boundaries. The climate of the area is mild Mediterranean–type with cool and moist winters, and warm and dry summers.

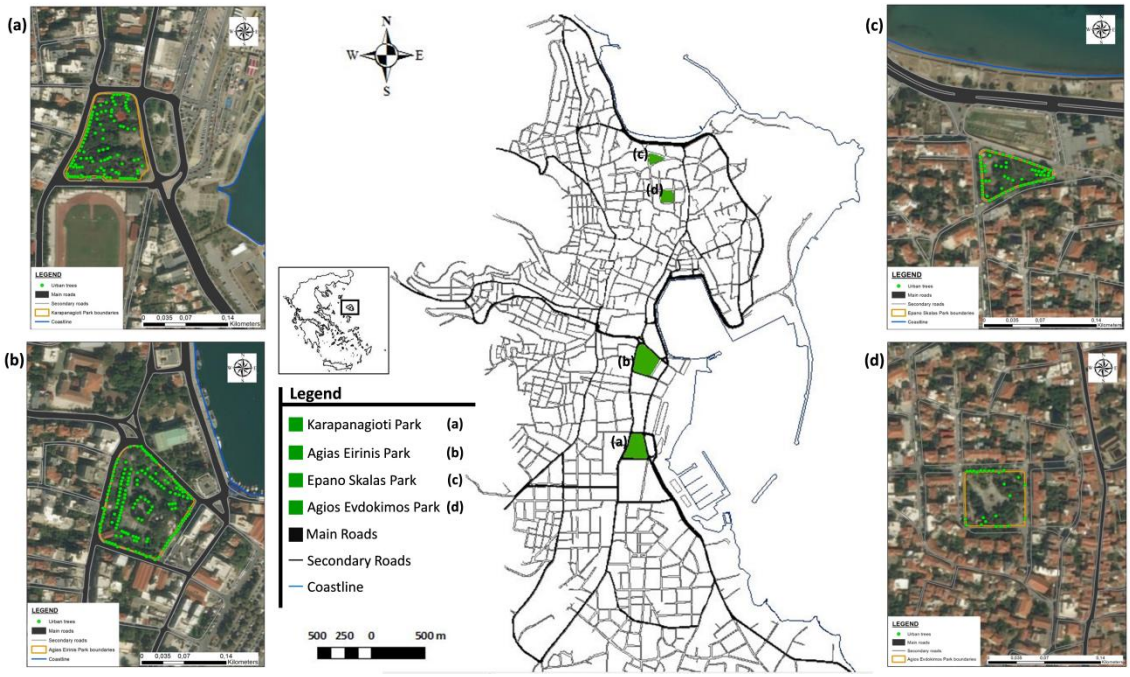

Figure A1: Location of the studied urban parks and urban trees in the city of Mytilene, Lesvos Island, Greece: (a) Karapanagioti Park, (b) Agias Eirinis Park, (c) Epano Skalas Park, and (d) Agios Evdokimos Park. The green dots represent the investigated urban trees.

A2.2 Tree selection and recording of structural and functional traits

A necessary first step, before proceeding to sampling trees, was to conduct a full woody vegetation inventory of the four urban parks (**Figure A1**), between September and November 2017. We collected a comprehensive set of qualitative and quantitative information for both arboreal and shrub vegetation regarding the species and the proportion of native and non–native species, as well as their structural and functional traits. In cases where species identification was uncertain, we collected leaf samples and keyed them in the laboratory using common identification keys. All data were recorded on an inventory form, which was designed and pilot–tested before its final use.

For each tree we measured the main structural and functional traits: tree height (H—m), diameter at breast height (DBH—cm), and height at the crown base (HC—m). Based on these metrics, we calculated the vertical dimensions of the crown (Assmann, 1970): the crown length (CL—m), and the crown ratio (CR). CL results from the subtraction of H from HC, while CR is the ratio of CL to H. Due to the strict annual pruning of most of these trees at the top of the trunk (pollarding) we considered it appropriate not to calculate the horizontal dimensions of the crown, as these measurements would not be representative of a tree's crown area.

Regarding tree structural defects, we estimated the number of external indications and the type of such defects (cavities, decayed wood, cracks, cankers, burls, rotten bark), by ground–based observation, on each tree. We especially paid attention to decayed parts on tree trunks since the decay of wood within a tree trunk has been widely reported as the principal cause of tree failures (Soge *et al.*, 2019; Johnstone *et al.*, 2010). In addition, in cases where cavities were present, we recorded their dimensions: the entrance vertical diameter (VCD—cm), the entrance horizontal diameter (HCD—cm), and the internal cavity diameter (ICD—cm). From these decay parameters, we estimated the decay proportion (DP), as a proxy of the defects' severity, as the ratio of the decay cross–sectional area to the total tree area at breast height (Frank *et al.*, 2018; Terho, 2009; Terho and Hallaksela, 2008; Kennard *et al.*, 1996; Smiley and Fraedrich, 1992).

Finally, to evaluate the trees' mechanical integrity, we applied a strength loss equation (SL) with a given threshold of 33% for hazardous trees as initially established by Smiley and Fraedrich ((Smiley and Fraedrich, 1992)), by taking into account variables related to the trees' and their defects diameter, and the ratio of cavity horizontal diameter to tree circumference (**Eq.**).

$$\textbf{Eq.:}\ SL = HCD^{\,3} + \left((R \times (DBH^{\,3} - HCD^{\,3})\right) * (100 \div DBH^{\,3}))$$

Where: SL = Strength loss (%), HCD = cavity diameter (cm), DBH = diameter of a healthy stem (cm), and R = ratio of the opening of the cavity to stem circumference.

A2.3 Collection and pre–processing of infrared images

We photographed the trunks of all the urban trees in the four parks restricting our attention to unique features which had made any of them potentially hazardous (**Figure A2**). This process was considerably easier in cases where we had an indication of an external defect.

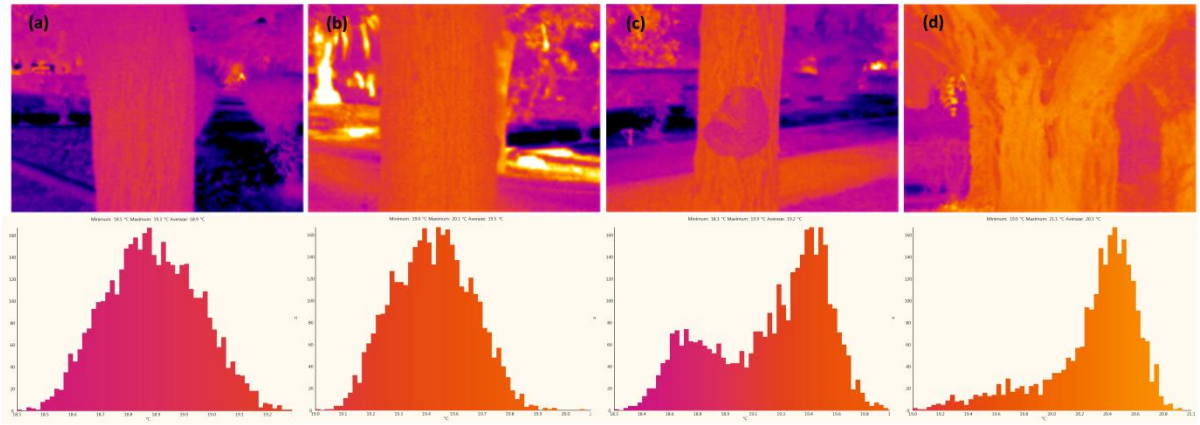

Figure A2: Sample thermal images of *R. pseudoacacia* (a) a healthy tree, (b) a tree with rotten bark, (c) a tree with a burl, (d) a tree with a cavity as well as their temperature histograms respectively, as extracted by the TESTO IRSoft® (v. 4.3) software.

In order to obtain accurate infrared images of the tree trunks, we followed a standard methodological protocol, which we designed so that the process of obtaining the images would be efficient and practical, both in terms of avoiding any serious inconvenience to the public as well as of taking full advantage of the camera potential. For this reason, we carried out IRT during days with light to no wind, no rain, and in the early morning hours, at a standard distance of 3.0 m from the trunk, and a height of 1.3 m, in order to capture the entire or as much as possible of the tree trunk. The consistent fair–weather conditions, in combination with taking the infrared photos in the early morning hours, help in minimising overestimation of the trees' surface temperature distribution,

due to the effect of atmospheric composition (Minkina and Dudzik, 2009) and the global radiation effect (Faye *et al.*, 2016; Minkina and Dudzik, 2009). We used a Testo 875–1i handheld infrared camera (Testo SE & Co. KGaA, Lenzkirch, Germany), with a thermal resolution of < .08 °C, thermal sensitivity of < 50 mK, and a resolution of 160 x 120 pixels, which we mounted on a tripod for both stabilization and accurate positioning at the required height and distance from each tree. The thermal camera was calibrated at the exact shooting moment in the field using ambient temperature, relative humidity, solar irradiance, collected with a portable meteorological station. Emissivity was set to have values (ε = .95) proposed by Briscoe *et al*. (Briscoe *et al.*, 2014), and corrected for the tree species under investigation.

A2.4 Extraction of the trunk surface temperatures from the infrared images

We processed the collected infrared images using the TESTO IRSoft® (v. 4.3) software (**Figure A2**) and afterward, we extracted, to a text file, the tree trunk temperatures, which we analysed using the ArcGIS 10.2 software (ESRI Inc., Redlands, CA, USA). For each infrared image, we created a polygon, in a shapefile format, which encircled each trunk, and then we extracted the trunk temperature values and calculated a set of thermal variables based on the tree trunk histogram; the T_{min}, the T_{max}, and the T_{mean}. However, assessing the state of individual traits appearing on tree trunks, which are directly related to their stability (e.g. signs of decomposition), requires the study of extreme temperature values. Contrarily, extreme temperature values on the trunk surface may be due to the presence of Bryophytes or any non–vascular plant that may settle on the trunk surface and occupy even one pixel in the infrared image to change the thermal pattern of a trunk drastically. With this purpose in mind, we also calculated the interquartile range (T_{IQR}) of the temperature distribution, on the surface of each tree.

A2.5 Spatial autocorrelation of the urban trees' trunks temperature

In order to examine the spatial clustering of the trunk temperatures we implemented several spatial statistical tools in GIS environment. To assess temperatures' spatial dependence, the overall degree of spatial autocorrelation across trees' bark texture, was estimated using Moran's I index (Moran, 1950). To identify statistically significant spatial clusters of high and low values, two local indicators of the spatial association were used, the Anselin Local Moran's I (Anselin, 1995) and the Getis–Ord Gi* (Getis and Ord, 1992). The procedure was as follows: first, we imported each infrared image as a text file and we then imported the .txt file to a raster dataset. Thereafter, we (a) converted the extracted raster dataset to point features, (b) we performed the Cluster and Outlier Analysis (Anselin Local Moran's I) to identify patches on the tree trunk (groups) of similar temperatures (clusters), and (c) we visualised those clusters in four major groups of high and low values (two were for clusters and the other two for outliers). Subsequently, we extracted a spatial autocorrelation report, for each tree, based on feature locations and attribute values, using the Global Moran's I statistic. Lastly, to delineate the temperatures spatial clustering, we carried out hotspot analysis, by using Getis–Ord G* (**Figure A4**).

A2.6 Statistical analysis

It is well known that a homogeneous temperature distribution on tree trunks is considered a health state indicator, thus, we considered it important to estimate this distribution by using the extracted thermal variables. However, due to the fact that the water supply conditions and the anatomical characteristics of each trunk (López–Bernal *et al.*, 2010) which causes the fluctuation of its surface temperature (Burcham *et al.*, 2012) are species and/or individual specific (Vidal and Pitarma, 2019), we initially examined thermal pattern differences both within tree species and among the recorded

structural defects, by using one–way analysis of variance (ANOVA), followed by Hochberg's GT2 test for multiple comparisons.

For investigating the association of trees' structural and functional traits, thermal variables, and Moran's I index, we used scatterplots and correlation statistics. In order to examine the effect of structural and functional traits, and Moran's I index, on T_{IQR}, we used multiple linear regression analysis, with a backward elimination procedure, based on the dependence between the observed correlations. The T_{IQR} of the tree's trunk surface was chosen as the dependent variable, while variables of the tree's traits as the independent ones. We performed this analysis on both the three main tree species and for all the recorded trees.

For examining the probability of structural and functional traits, thermal variables, and the spatial index to explain individually or in combination with the presence or absence of structural defects, as well as hazardous trees (trees were designated as hazardous if their estimated strength loss was more than 33%), we developed binary logistic regression models. We computed a classification table of observed and predicted values for each model which we evaluated with the receiver operating characteristic (ROC) curve analysis. The predictor variables were evaluated through a backward stepwise procedure in order to maintain the optimal model; we used the Hosmer & Lemeshow goodness of fit test for assessing the overall significance of the models, and Nagelkerke's R^2 as an explanatory index of the models' variation.

Finally, we used the Getis–Ord Gi* spatial autocorrelation method to recognize hazardous tree hotspots in each urban park and we applied the kriging geostatistical procedure, as an interpolation technique, for mapping the hotspots' spatial extension.

All statistical analysis was carried out using SPSS software (v. 25.0. Armonk, NY: IBM Corp.). Data are expressed as means ± standard deviation (SD) and statistical significance was assumed at the 5% level.

A.3 Results

A3.1 Descriptive statistics of the urban tree survey

We recorded a total of 334 trees from 9 different species (**Table A1**) and 1107 shrubs from 31 species, of which 63.63% concerned non–native species, in the four urban parks of the city of Mytilene. The predominant tree species was the black locust (*Robinia pseudoacacia*, 52.1%), followed by the white mulberry (*Morus alba*, 19.5%) and the chinaberry tree (*Melia azedarach*, 14.4%). Regarding shrubs, the majority belonged to species commonly used for hedging (e.g. *Laurus nobilis*, *Ligustrum japonicum*, *Nerium oleander*, *Pittosporum tobira*) and used in almost all the urban parks across Europe (Blanusa *et al.*, 2019; Gratani and Varone, 2013). Most of the studied trees were located in the Agias Eirinis Park (45.8%), followed by Karapanagioti Park (29.3%), Epano Skalas Park (17.7 %), and Agios Evdokimos Park (7.2%).

Table A1. Descriptive statistics of the recorded urban trees (N = 334).

Tree species	Individuals (n)	Percentage (%)	Classification	Functional form
Robinia pseudoacacia	174	52.1	Non – Native	Broad–leaved deciduous
Morus alba	65	19.5	Non – Native	Broad–leaved deciduous
Melia azedarach	48	14.4	Non – Native	Broad–leaved deciduous
Casuarina equisetifolia	16	4.8	Non – Native	Conifer evergreen
Cercis siliquastrum	16	4.8	Native	Broad–leaved deciduous
Cupressus sempervirens	8	2.4	Native	Conifer evergreen
Pinus brutia	3	.9	Native	Conifer evergreen
Koelreuteria paniculata	2	.6	Non – Native	Broad–leaved deciduous
Olea europaea	2	.6	Native	Broad–leaved evergreen

The sampled urban trees had a mean height of 7.94 ± 5.00 m, mean diameter of 39.41 ± 12.16 cm, and mean crown length of 5.80 ± 4.42 m. The recorded types of structural defects were cavities, burls, rotten bark, and a combination of two or more different structural defects. Of the 334 surveyed trees, 129 did not show any kind of structural defect, while from the remaining 205 trees the 44.6% presented cavities, 11.7% burls, 13.2% rotten bark, and 3.9% had both cavities and burls. The trees with structural defects had a mean number of 1.6 ± 3.23, while those with cavities had a VCD of 28.59 ± 37.92 cm, an HCD of 12.16 ± 12.39 cm, an ICD of 11.37 ± 13.26 cm. These trees also showed a mean DP of .14 ± .25 and an SL of 19.47 ± 33.71%. Among all woody plant species, we focused on the three commonest tree species (*R. pseudoacacia, M. alba, M. azedarach*). Their recorded traits are presented in **Table A2**.

Table A2. Structural and functional traits of the commonest urban tree species (N = 287).

Traits	***Robinia pseudoacacia*** (N =174)		***Morus alba*** (N = 65)		***Melia azedarach*** (N = 48)	
	Mean	**SD**	**Mean**	**SD**	**Mean**	**SD**
H (m)	6.15	1.65	7.57	3.06	8.22	3.12
DBH (cm)	41.01	9.70	40.23	11.33	28.68	10.67
HC (m)	1.90	.34	1.84	.36	2.01	.44
CL (m)	4.25	1.66	5.73	2.54	6.20	3.02
CR	.66	.12	.74	.08	.71	.12
Structural Defects (n)	2.02	3.50	1.26	2.00	.41	.61
VCD (cm)	37.91	44.56	21.84	22.59	21.12	30.48
HCD (cm)	15.14	13.38	13.41	11.16	6.82	8.50
ICD (cm)	14.25	13.89	13.00	13.82	6.87	9.77

SL (%)	18.99	27.65	29.83	42.95	24.48	47.10
DP	.15	.23	.21	.33	.16	.27

A3.2 Thermal patterns of trees' structural defects

We first calibrated the thermal images, required for a reliable examination of thermal patterns.. Thus, by taking into account the temperature, humidity, and solar radiation conditions measured under the crown of each examined tree, we found that the microclimate of the urban parks, during the field study, displayed an average temperature of 16.72 ± 1.76 °C, relative humidity 65.2 ± 4.04%, and solar intensity of 325.35 ± 105.66 W/m^2. The exported thermal statistical variables resulting from the trees' surface temperature presented a T_{mean} of 16.48 ± 2.37 °C, a T_{min} of 15.75 ± 2.37 °C, a T_{max} of 17.23 ± 2.41 °C, and a T_{IQR} of .43 ± .24.

Regarding the recorded structural defects, one–way ANOVA gave statistically significant differences when comparing them with the trunk temperature distribution as described by the T_{IQR} [F (4, 329) = 39.276, p = .001]. In particular, using Hochberg's GT2 test for multiple comparisons we found that the mean value of T_{IQR} was significantly different between trees with cavities (T_{IQR} = .58 ± .25) and (a) trees with burls (T_{IQR} = .33 ± .12) (p = .001, 95% C.I. = .15, .35), (b) trees with rotten bark (T_{IQR} = .31 ± .11) (p = .001, 95% C.I. = .17, .36), and (c) trees with no sigh of defects (T_{IQR} = .29 ± .13) (p = .001, 95% C.I. = .22, .36). We also found significant differences between trees with a combination of structural defects (T_{IQR} = .46 ± .22) with trees considered healthy (p = .036, 95% C.I. = .01, .33). We did not find any differences regarding the comparison of trees with burls and trees with rotten bark nor with trees with a combination of structural defects, or with healthy trees. In correspondence to the above we did not found any differences regarding trees with rotten bark and trees with a combination of structural defects, nor between trees absent of defects.

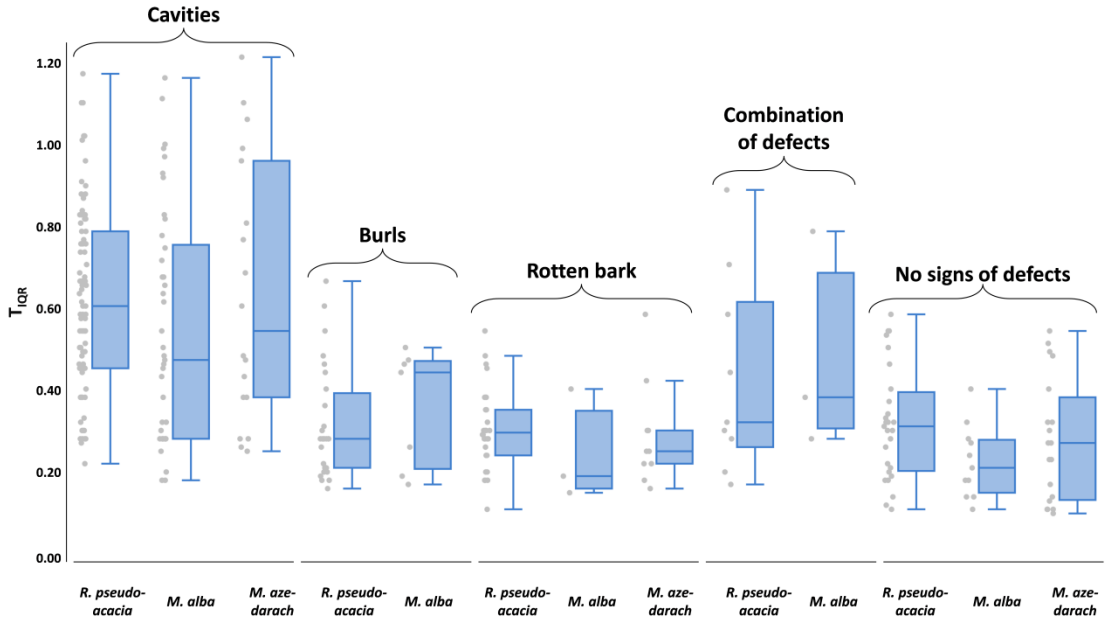

Figure A3: Box plot showing the T_{IQR} values regarding the three tree species structural defects as well as cases of trees with no signs of defects. Horizontal lines: medians; boxes: interquartile ranges (25–75%); whiskers: data ranges.

The thermal pattern showed uniformity among species for different structural defects (**Figure A3**). In particular, differences were not statistically significant comparing T_{IQR} of trees of *Robinia*

pseudoacacia, Morus alba, and *Melia azedarach*with (a) cavities (p = .252), (b) burls (p = .784), (c) rotten bark (p = .664), (d) combination of defects (p = .768), and (e) no signs of defects (p = .155).

A3.3 Detection of structural defects using spatial statistics

Based on the infrared images, we used the Getis–Ord Gi* statistic to detect spots of structural defects on the trees' trunk surface, while the Anselin Local Moran's I was used to verify and complement the hot spot analysis. We also determined whether the trunk temperature values are spatially dispersed, random, or clustered (ESRI, 2021) using the Global Moran's I and its corresponding z–score, an index which varies from –1 (highly dispersed) to +1 (highly correlated). In particular, we found significant spatial autocorrelation ($p < .05$) for trees with defects but low or no autocorrelation in trees with the absence of defects. Among the total of 334 trees examined this spatial index presented a significantly clustered pattern in trees with cavities ($\bar{x} = .76 \pm .12$; $p < .001$; z–score > 2.58), followed by trees that combine cavities and burls ($\bar{x} = .71 \pm .10$; $p < .001$; z–score > 2.58), and lastly by trees with burls ($\bar{x} = .62 \pm .07$; $p < .05$; z – score ≥ 1.96). In contrast, trees exhibiting rotten bark ($\bar{x} = .59 \pm .05$; $p \neq .05$; – 1.65 < z–score < 1.65) and with no signs of defects ($\bar{x} = .59 \pm .07$; $p \neq .05$; -1.65 < z–score < 1.65), presented almost similar values. Moreover, we observed significant clusters with high (hot spots) and low (cold spots) temperatures, as calculated by the Getis–Ord Gi* tool. The cluster and outlier analysis confirmed, for each tree, the areas where the temperature anomalies occurred (**Figure A4**).

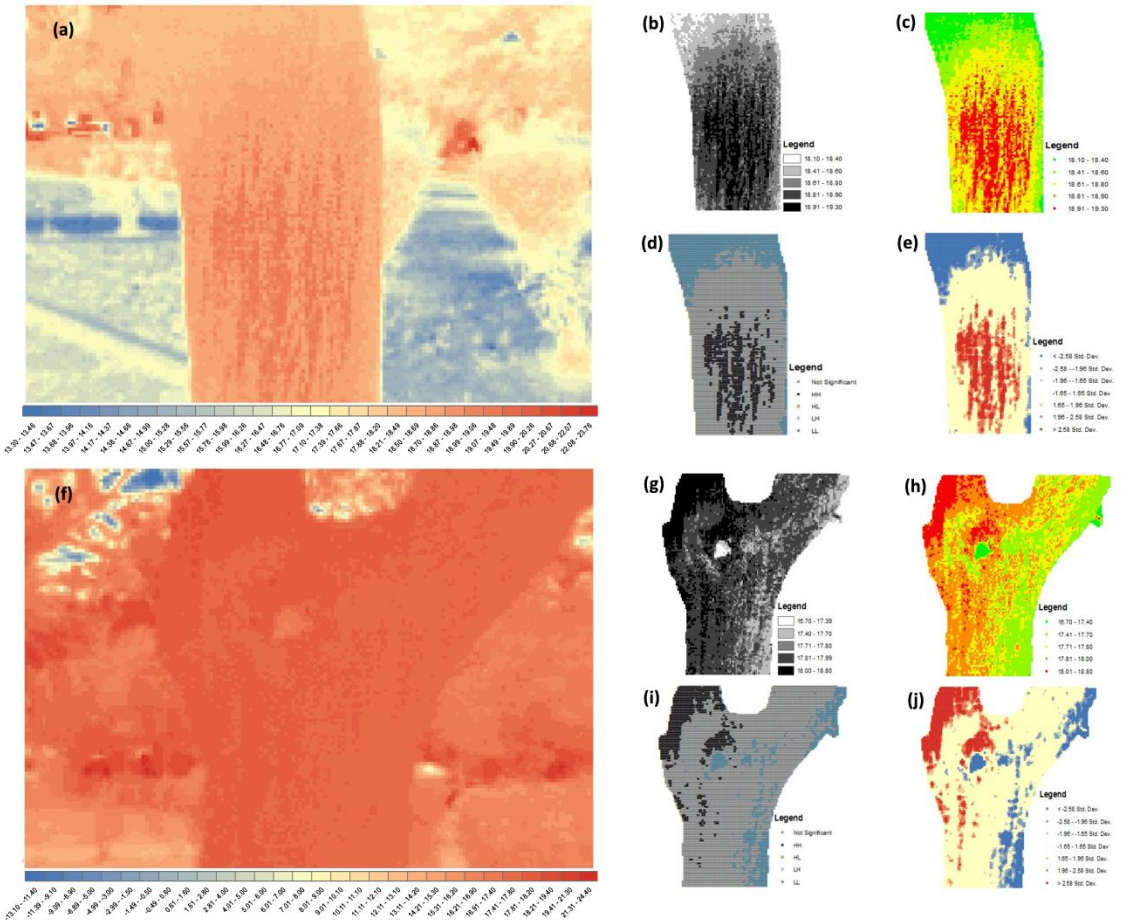

Figure A4: Step by step analysis, using ArcToolbox, of a sample of two individuals of the species Robinia pseudoacacia without a decay (a–e) and with a wood decay (f–j) analysis: (a, f) the initial thermal image as a file with .txt extension (feature class was created based on coordinates given in a text file); (b, g) conversion of

the txt. file to a raster dataset; (c, h) conversion of a raster dataset to point features; (d, i) Cluster and Outlier Analysis (Anselin Local Moran's I); (e, j) Hot Spot Analysis (Getis–Ord Gi*).

A3.4 Relationships among trees' traits, thermal variables, and spatial index

The correlation analysis of the three species under study revealed significant associations, either direct or inverse, among their structural and functional traits, the thermal variables, and the Moran's I index (**Figure A5**). Regarding the correlation between trees' physical characteristics (H, DBH, HC) and their canopy variables (CL, CR) statistically significant positive relations were observed except for DBH, an expected result since these variables are interdependent. Examining the relationships of these variables to the structural defects, the cavities dimensions, the stability index, the thermal variables, and the spatial index, did not exhibit any significant correlations. In contrast to these results, relationships between the number of structural defects, the dimensions of the cavities, trees' strength loss, and decay proportion were moderately to strongly positive statistically significant. In particular, (a) the structural defects exhibited positive significant relations with the VCD ($r = .32$; $p = .001$), HCD ($r = .46$; $p = .001$), ICD ($r = .60$; $p = .001$), SL ($r = .80$; $p = .001$), DP ($r = .74$; $p = .001$), (b) the cavities dimensions showed significant positive relations between them ($.75 < r < .48$; $p = .001$), (c) the SL displayed significant positive relations both with the cavities dimensions ($.74 < r < .29$; $p = .001$) and the decay proportion ($r = .90$; $p = .001$), and (d) the DP demonstrated significant positive relations with the cavities dimension, respectively. Focusing on the thermal variables, it was observed that the central tendency measures of the tree trunks, as described by the T_{min}, the T_{max}, and the T_{mean}, did not show any statistically significant correlation with the other variables. However, examination of the trunks' temperature variability measures (T_{IQR}), showed significant positive relations which ranged between .35 to .67 regarding the number of defects and the cavities dimensions, while for the SL, DP, and the spatial index, these relations heightened to a range between .72 to .74. Finally, the Moran's index followed the same pattern with T_{IQR} showing positive correlation with the structural defects ($r = .58$; $p = .001$), the cavities' dimensions ($.44 < r < .74$; $p = .001$), the SL ($r = .70$; $p = .001$), and the DP ($r = .72$; $p = .001$).

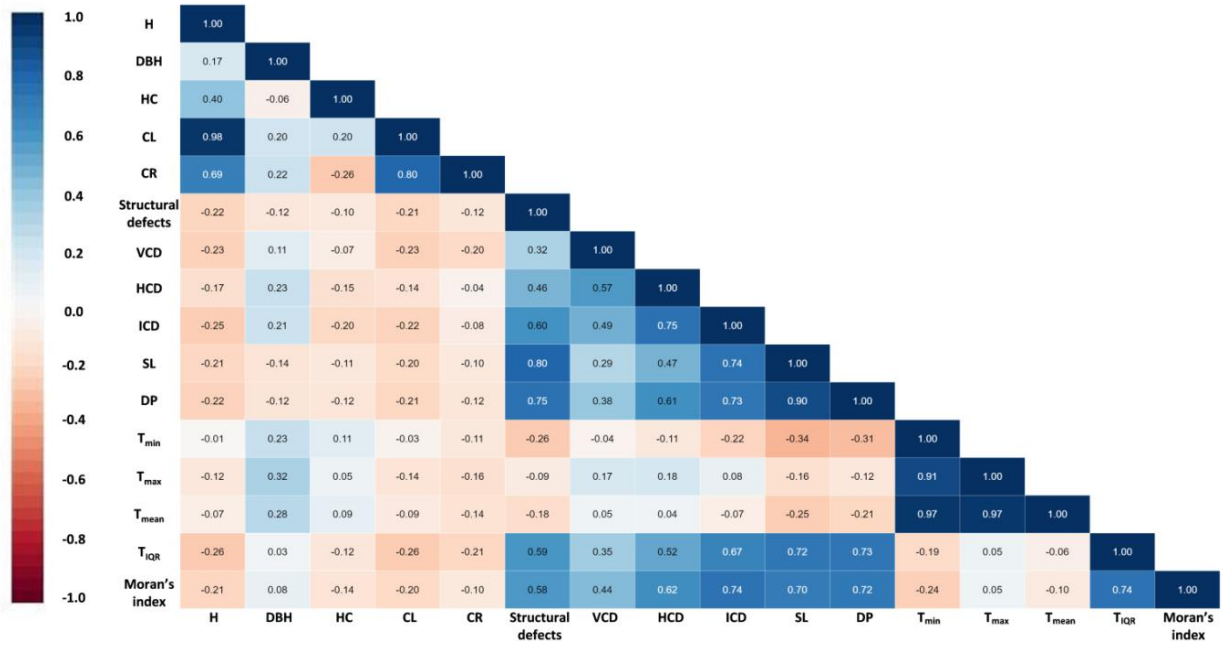

Figure A5: Correlation matrix showing the relationships between urban trees' structural and functional traits, thermal variables, and the spatial index. Red and blue colours indicate positive and negative correlations

respectively, while intensity of colour indicates the strength of the relationship. All correlation coefficients above .29 or below –.29 are statistically significant ($p < .05$).

A3.5 Effect of trees' traits and Moran's index on T_{IQR}

To test dependence of tree trunk surface temperature from the recorded traits, as well as the spatial index of the examined trees, we used multiple regression analysis with backward elimination. We carried out the analysis both for the three species of interest combined as well as for each species separately, bearing in mind the differentiation of their structural and functional traits (**Table A2**) and of their bark texture (*R. pseudoacacia* has a fibrous, heavily ridged and furrowed bark, *M. alba* has a coarse bark with curving deep furrows, and *M. azedarach* has a narrowly furrowed bark). We did not use the DBH and the HCD as independent variables because these traits are the main components for the SL estimation.

The models for predicting the T_{IQR} were statistically significant in all four cases, i.e., for the three species combined: $F (3, 282) = 165.43$, $p < .001$, $R^2_{adj} = .634$, for *R. pseudoacacia*: $F (2, 171) = 142.82$, $p < .001$, $R^2_{adj} = .621$, for *M. alba*: $F (2, 62) = 55.34$, $p < .001$, $R^2_{adj} = .629$, and for *M. azedarach*: $F (2, 45) = 56.050$, $p < .001$, $R^2_{adj} = .701$ (**Table A3**). In all models the predictor variables had quite similar explanatory power, explaining an important proportion of the total variance.

Table A3. Final models obtained from multiple linear regression analyses for estimating T_{IQR}. All multiple regression models were statistically significant ($p < .05$).

Tree species	Response variable	Predictor variables	B	SE B	β	t	p	$R^2_{adj.}$	F
3 species (N = 287)	T_{IQR}	(constant)	-.165	.063		-2.604	.010	.634	165.43
		SL	.002	.001	.238	2.872	.004		
		DP	.198	.079	.211	2.507	.013		
		Moran's index	.799	.099	.422	8.059	.001		
R. pseudoacacia (N = 174)	T_{IQR}	(constant)	-.157	.077		-2.046	.042	.621	142.85
		SL	.004	.001	.427	6.613	.000		
		Moran's index	.798	.119	.434	6.736	.000		
M. alba (N = 65)	T_{IQR}	(constant)	-.034	.143		-.241	.810	.629	55.34
		ICD	.011	.002	.572	4.537	.000		
		Moran's index	.498	.236	.266	2.110	.039		
M. azedarach (N = 48)	T_{IQR}	(constant)	-.361	.176		-2.051	.046	.702	56.050
		Structural defects	.075	.026	.384	2.872	.006		
		Moran's index	1.10	.292	.506	3.786	.000		

The Moran's index was found to be the most important predictor of T_{IQR} in three out of the four models, while its individual importance, controlling for the effect of the other predictors, expressed: (a) 8.35% of the 3 species model's total variance, (b) 9.92% in the *R. pseudoacacia* model, (c) 2.59% in the *M. alba* model, and (d) 9.12% in the *M. azedarach* model. The combined prediction of the SL, DP, and Moran's index, for the three species model, corresponds to 53.17% of variance with respect to T_{IQR}. The SL and the Moran's index in combination, predicted 42.62% in the *R. pseudoacacia* model, the ICD and the Moran's index predicted 40.05% of the *M. alba* model, and the Structural defects and the Moran's index had a combined effect accounting for 55.73% of the *M. azedarach* model.

A3.6 Logistic regression models for the classification of structural defects and hazardous trees

We conducted a series of logistic regression analyses to test not only for the effect of the presence of structural defects but also for the effect of every subclass of this variable. Thus, we tested if the tree traits, thermal variables, and the spatial index can explain the presence probability of cavities, burls, rotten bark, and the combined defects. We ran this analysis for the three species combined and for each one separately while we also tested the presence probability of hazardous trees, keeping in mind that, trees were designated as hazardous if their strength loss was more than 33% (Smiley and Fraedrich, 1992). We evaluated the discrimination ability of each model by ROC curve analysis.

In all cases, the logistic regression models identified the T_{IQR} and the Moran's index, either separately or together, as the most important factors which best distinguish the presence or absence of the examined defects. In particular, regarding the presence of structural defects, the model correctly classified trees with and without defects in 72.1% of cases. The accuracy of the model was moderate for trees with defects (69.9%) but quite better (80.3%) for those without defects. The Nagelkerke R^2 value indicated that the model explained 27.6% of the total variance of the structural defects, and the Hosmer—Lemeshow test had a chi–square value of 7.567 ($p > .05$) which estimates that the model fits the data at an acceptable level (**Table A4a**).

Regarding the occurrence of cavities, the model had a much better fit [χ^2 (2, N = 287) = 113.21; $p < .0001$; **Table A4b**) with an overall classification accuracy of 87.3% (Nagelkerke R^2 = .625, Hosmer – Lemeshow = 14.054; $p > .05$), 85.7% for trees with cavities and 91.2% for those without, as estimated by the area under the ROC curve (AUC = .922; S.E. =.020; 95% CI .883 – .961; p = .0001). The models obtained for burls and rotten bark did not sufficiently explain their presence probability. The classification accuracy for these models was particularly low (burls = 64.6%; rotten bark = 58.7%). In contrast, the classification accuracy of the model for the combination of different structural defects was much higher (83.3% for presence, 89.5% for absence, 88.4% in total). In this case, the AUC was .928 (S.E. =.034, 95% CI .861 – .995; $p < .0001$), the Nagelkerke R^2 was .477, and the Hosmer – Lemeshow test was 4.461 ($p > .05$) (**Table A4c**).

Table A4. Logistic regression models for the prediction of the presence of structural defects in the total trees of the three species under study (N = 287). B = logistic coefficient; S.E. = standard error of estimate; Wald = Wald chi–square; df = degree of freedom; p – value = significance.

Structural defects					
Predictor	**B**	**S.E.**	**Wald's χ^2**	**df**	**p – value**
T_{IQR}	-2.642	1.218	4.707	1	.030
Moran's index	-8.569	2.366	13.119	1	.001
Constant	5.178	1.331	15.124	1	.001
Cavities					
T_{IQR}	4.896	1.638	8.936	1	.003
Moran's index	16.394	3.481	22.178	1	.0001
Constant	-11.658	2.124	30.129	1	.0001
Combination of defects					
Moran's index	-18.182	4.780	14.467	1	.0001
Constant	13.083	3.092	17.903	1	.0001

The results for each tree species were similar to those obtained for the three species combined. Due to smaller sample sizes and the consequent lower explanatory capacity of the individual species models, we restricted the analysis to predicting presence of cavities (**Table A5)**. For *R. pseudoacacia*, the model identified T_{IQR} and the Moran's index as the factors which can discriminates trees with or

without cavities [χ^2 (2, N = 108) = 60.63; p < .0001], with a predicted classification accuracy of 81.4% for presence and 93.3% for absence. The AUC was .923 ± .20 (95% CI .885 – .961; p = .0001), the Nagelkerke R^2 was .636, and the Hosmer – Lemeshow test was 21.873 (p > .05). For *M. alba*, the model identified only the Moran's index as the only predictor to effectively separate trees with (89.9%) and without (91.3%) cavities [χ^2 (1, N = 52) = 18.57; p < .0001; Nagelkerke R^2 = .467; Hosmer – Lemeshow = 7.496, p > .05; AUC = .897, S.E. =.024, 95% CI .850 – .944, p = .0001; **Table A5**]. Lastly, for *M. azedarach*, the model also identifies the Moran's index as the most significant factor to separate the presence (85.2%) and the absence (92.1%) of cavities [χ^2 (1, N = 37) = 27.84; p < .0001; Nagelkerke R^2 = .705; Hosmer – Lemeshow = 7.849, p > .05; AUC = .897, S.E. =.023, 95% CI .850 – .942, p = .0001; **Table A5**].

Table A5. Logistic regression models for the prediction of the presence of cavities in the three species under study. B = logistic coefficient; S.E. = standard error of estimate; Wald = Wald chi–square; df = degree of freedom; p – value = significance.

R. pseudoacacia					
Predictor	**B**	**S.E.**	**Wald's χ^2**	**df**	**p – value**
T_{IQR}	5.682	2.443	5.412	1	.020
Moran's index	15.023	4.451	11.391	1	.001
Constant	-11.324	2.736	17.132	1	.000
M. alba					
Moran's index	19.473	8.043	5.862	1	.015
Constant	–10.947	4.724	5.370	1	.020
M. azedarach					
Moran's index	24.019	7.781	9.529	1	.002
Constant	-15.557	4.854	10.273	1	.001

Lastly, we examined all the trees for which the SL index was obtained, as it is this set that will produce the maps of the hazardous trees hotspots. The binary logistic model examining the presence probability of hazardous trees, classified correctly 89.9% of cases; 91% for hazardous and 89.3% for non–hazardous trees [χ^2 (2, N = 237) = 174.71; p < .0001; Nagelkerke R^2 = .726; Hosmer – Lemeshow = 13.040, p > .05; AUC = .953, S.E. =.012, 95% CI .930 – .977, p = .0001; **Table A6**].

Table A6. Logistic regression models for hazardous trees classification. B = logistic coefficient; S.E. = standard error of estimate; Wald = Wald chi–square; df = degree of freedom; p – value = significance.

Predictor	**B**	**S.E.**	**Wald's χ^2**	**df**	**p – value**
T_{IQR}	-6.501	1.311	24.584	1	.0001
Moran's index	-10.699	2.187	23.931	1	.0001
Constant	11.992	1.661	52.135	1	.0001

A3.7 Hazardous tree hotspots

The output of Getis–Ord Gi* tool provides a GIZScore map that indicates the hot and cold spots in the urban parks. The GiZScore tool generates a z-score value for each tree and helps in indicating the statistical significance of feature clusters and eventually the hot and cold spots. In our case, hotspot analysis revealed significant clusters of hazardous and non–hazardous urban trees, presented for each of the four parks examined in **Figure A6** (a–d). The Gi* statistic, z-score represented by the red dot (hotspots) and blue (coldspots) indicates the statistical significance of clusters. Z–scores of > 1.96 indicates statistically significant hotspot clusters (p < .05), while z-scores lower than −1.96 indicates significant coldspot clusters (p < .05). In correspondence to the hotspots, the coldspots, in each urban park, represent healthy urban trees. We also applied the Kriging geostatistical procedure to the resulting hotspot map, for each urban park (**Figure A6** e–h), which was generated based on the

Getis–Ord Gi* analysis for the visualization of hotspots. The resulting smooth continuous surface is classified into nine different classes of hotspots, which clearly illustrated priority locations for mitigation activities regarding hazardous urban trees.

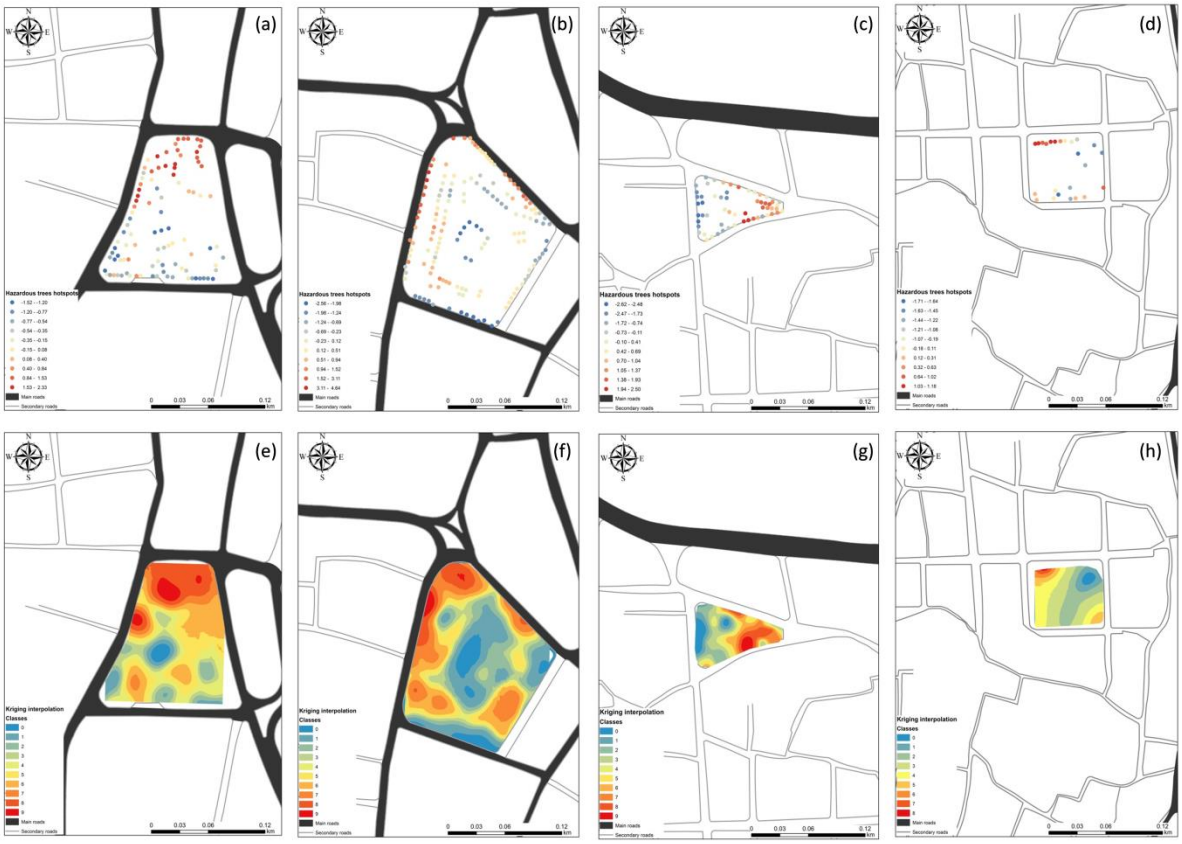

Figure A6: Locations of urban trees' hotspots and coldspots in the four urban parks: (a) Karapanagioti Park, (b) Agias Eirinis Park, (c) Epano Skalas Park, and (d) Agios Evdokimos Park, Mytilene, Greece. Values represent z–scores from the Getis Ord Gi* analysis; 1.65 corresponds to $p < .10$, 1.96 corresponds to $p < .05$, 2.58 corresponds to $p < .01$. Negative z–scores indicate cold spots, while positive z–scores indicate hot spots. Maps (e–h) effectively visualize the results of a hot spot analysis, by creating an interpolated surface, using kriging geostatistical procedure, for mapping the hotspots' spatial extension.

A.4 Discussion

Our study represents an attempt to explore an important concept regarding tree health assessment in urban environments; the detection and quantification of trees' structural defects as well as the identification of hazardous tree hotspots is important in order to obtain effective and precise management strategies concerning the protection of the environmental and social benefits of urban green areas. In this context, we chose to focus on the four urban parks of the city of Mytilene because they are not only areas of interest for the city's inhabitants but also areas including a variety of different species of arboreal vegetation. The full woody vegetation inventory and especially the arboreal vegetation inventory, which we initially conducted, is a valuable data source for studying the environmental, social, and economic services provided by the urban trees (Nielsen *et al.*, 2014), in our study area. At the same time, the diversity of vegetation species, their different structural and functional traits, and their spatial distribution in the urban parks, enabled us to examine holistically, to some extent, their state, by combining We attempted to combine different methodological approaches, based on (a) the typical information about the main structural and functional traits of the urban trees, (b) the IRT and the thermal variables derived from it, describing tree thermal patterns, and (c) the spatial statistics both at tree trunk and at park level. All this information can promote urban tree management and planning, responding to different goals of the administration such as species planting, arboricultural management, hazard control, and people and traffic safety (Östberg *et al.*, 2018). After all, the arboreal vegetation which is present in the studied urban parks, consists of the typical very fast–growing species usually used in European cities (Bayer *et al.*, 2018; Pauleit *et al.*, 2002) and, thus, we believe that our study has a wider applicability without the need for major re-adjustments..

The examination of urban trees through IRT showed that this non–destructive method can be used as a rapid diagnostic tool to illustrate their thermal patterns and to explain the presence of defects. Among various alternative thermal variables, we selected the T_{IQR} which has been found to be one of the most important indicators when examining a tree as a whole and for estimating its thermal profile (Zevgolis *et al.*, 2022). The observed differences of this index regarding the different types of structural defects, both in absolute numbers and in statistical significance, confirms the healthy tree concept, originally presented by Catena and Catena (Catena and Catena, 2008); a healthy tree is considered the one whose trunk temperature is homogeneously distributed, while an unhealthy tree is the one which presents temperature abnormalities. Based on the results obtained from the thermal profile of the examined trees (**Figure A3**), it is understood that trees with cavities exhibited the highest deviation from the value which describes a healthy tree (.29 ± .13), followed by trees with a combination of structural defects, burls, and rotten bark. Based on the available data we could not determine the types of the trees' structural damages (Wong *et al.*, 2020), but we noticed that, in our case, this particular thermal index can, to some degree, be used to classify them. It is worth mentioning that while IRT can distinguish the basic types of structural defects with high sensitivity, it is nevertheless difficult to distinguish trees with rotten bark (.31 ± .11) from healthy trees (.29 ± .13). This is likely due to the trees' outer bark being highly influenced by external weathering conditions (Whitmore, 1962) and tangential strain to produce the fissures and ridges of the surface, and/or by there being a small gap between the phloem and the sapwood where the air enters and cools or heats homogeneously the trunk surface. Moreover, trees of similar or different species, with the same type of structural defects, displayed slightly different thermal patterns as already discussed by Vidal and Pitarna (Vidal and Pitarma, 2019), and consequently, must be examined on an individual species basis (Catena and Catena, 2008). However, the absence of significant differences in the thermal patterns of different tree species, measured by T_{IQR}, with the same type of defects, indicates that IRT can be used in a wide context, for estimating trees' health state regardless of the species, the trunk texture, or other structural and functional species–specific traits.

Further analysis of trees' structural defects using spatial statistical methods gave us the opportunity to test the precision and applicability of spatial indices in the context of tree health assessment. To the extent of our knowledge, there is no other relevant study to use indicators of spatial association in gaining more detailed information about detecting structural defects on trees' trunk surface. Furthermore, in order to differentiate our analysis from the thermal index that we used to investigate trees' thermal patterns (T_{IQR}), when we imported the infrared images to ArcGIS, we chose to run the analysis by using the actual temperature value of every pixel of the infrared image. The Getis–Ord Gi∗ statistic and the Anselin Local Moran's I despite being widely applied in hot spot identification in different research areas (Li *et al.*, 2017), have nevertheless not been used to detect structural defects on trees' trunk surface. We did not use this statistic to find the exact area of the structural defects, as we had already measured it in the field, but only to visualize them, providing a better understanding of their spatial distribution along the surface of the tree trunk (**Figure A4**). We focused on the Global Moran's I statistic as it is a normalized index, analogous to the conventional correlation coefficient (Sokal and Oden, 1978). In theory, we would expect a tree with a large cavity to show a well–defined non–uniform distribution of the surface temperature of the trunk and consequently to provide a significant clustered pattern of its temperature distribution. The Global Moran's I index on which we focused provided precise information describing the tree trunk's surface temperature patterns, amplifying the existing information resulting from the thermal index. In fact, the observed spatial clustering follows the same pattern as the thermal index, for the whole arboreal vegetation inventory; the highest clustering is illustrated in trees with cavities, while the lowest in trees with rotten bark and with no signs of defects. To enhance the importance of the Global Moran's I index, in correspondence to the differences that appeared between the trees' structural defects described by the T_{IQR}, we examined possible differences of the structural defect types when comparing them with the trees' clustered pattern. An analysis of variance showed that the effect of structural defects types on Global Moran's I index was significant [$F(4, 282) = 55.099$, $p = .0001$]. Hochberg's GT2 test for multiple comparisons found that the mean value of the spatial index was differentiated between trees with cavities and (a) trees with burls ($p = .0001$, 95% C.I. = .09, .19), (b) trees with rotten bark ($p = .0001$, 95% C.I. = .12, .22), and (c) trees with no signs of defects ($p = .0001$, 95% C.I. = .14, .23). Moreover, Global Moran's I index was significantly different between trees having a combination of structural defects with (a) trees with burls ($p = .046$, 95% C.I. = .00, .18), (b) trees with rotten bark ($p = .001$, 95% C.I. = .03, .21), and (c) healthy trees ($p = .0001$, 95% C.I. = .05, .23). In accordance to differences, which were absent, regarding T_{IQR} between tree species, we did not observe any significant differences when examining the spatial index [$F(2, 284) = 2.409$, $p = .092$]. However, in the three species under study, the spatial index presented a significant clustered pattern (*R. pseudoacacia*: .69 ± .12; *M. alba*: .70 ± .14; *M. azedarach*: .65 ± .12).

Investigating the relationship among thermal variables, Moran's I index, and the structural and functional traits of the examined trees (**Figure A5**), revealed significant findings in linking these variables to urban trees' health state. The absence of any correlation between trees' structural and canopy traits with the variables concerning their structural defects, as these may be described by their dimensions, stability index, thermal variables, and spatial index, justifies the omission of these measurements from such an analysis, allowing one to focus on other the important parameters. These parameters (Structural Defects, VCD, HCD, ICD, SL, DP, T_{IQR}, Moran's index), especially the ones with strong correlations between them (e.g., SL, DP, T_{IQR}, Moran's index), can be considered as ideal indices in describing and quantifying hazardous trees. After all, we consider that the connection between an index that describes tree strength loss, a thermal index and a spatial index, which is not established elsewhere, will be exceptionally helpful in cases where administration authorities do not have the available resources for a full tree health assessment. Tree structural and canopy traits would matter if we measured the stability of larger and taller tree species with larger and/or asymmetric canopies, as the taller the tree, the greater the chance of failure (Kontogianni *et al.*,

2011). Moreover, if tree canopies grow unevenly, their loading patterns would not be enough to respond to strong winds (Kontogianni *et al.*, 2011; James *et al.*, 2006). Besides, it is well known that tree stability decreases with the increase of height, slenderness index, crown area, crown roundness, and crown asymmetry (Stăncioiu *et al.*, 2021; Cullen, 2002).

Although it is well known that IRT is considered an important method providing precise information about the types of trees' structural defects and tree health in general (Zevgolis *et al.*, 2022; Vidal and Pitarma, 2019; Catena and Catena, 2008), its application in examining tree health state has some limitations as it is affected by a variety of different factors such as (a) the environmental conditions of the study area (Faye *et al.*, 2016; Nunak *et al.*, 2015; Minkina and Dudzik, 2009), (b) the contrast between tree trunk and the environment (Catena, 1990), (c) the possible tree trunk cover of epiphytic vegetation (Catena and Catena, 2008), and (d) the tree bark texture (Pitarma *et al.*, 2019). However, the dependence of IRT traits from particular tree traits has not yet been recognized. Therefore, this relationship required further analysis, based on tree structural and functional traits and their stability and spatial indices. In this context, we have illustrated a set of variables (**Table A3**) which can explain this dependence. The high explanatory nature of the linear regression models, consistently with the same predictor variables for the three examined species, either combined or separately, indicated a strong dependence of T_{IQR} on strength loss index, cavity dimensions, defect severity, and Global Moran's I index. The explanatory power of these models, varying from .621 to .702, showed that with the use of T_{IQR} as a product extracted from an infrared image describing the surface temperature of the tree trunk it is possible to make a relatively secure prediction of the state of a tree. Moreover, the similar explanatory power observed for the three tree species suggests that this thermal index can be of universal applicability. This finding reinforces not only the use of IRT as an essential diagnostic tool for assessing the state of urban trees, but also the variables that explain it, especially those that can be easily measured in field conditions using just a measuring tape (e.g., SL, DP). On the other hand, the existence of a spatial statistical index which was the most important predictor of the variation of T_{IQR}, enhances the already quite high (owing to the infrared camera) accuracy, both in terms of the extent of structural defects and in terms of the intensity of those defects.

Regardless of the fact that the tree species under study (*R. pseudoacacia*, *M. alba*, *M. azedarach*) are considered useful in urban green areas due to their low sensitivity to most abiotic stressors (Liu *et al.*, 2019; Dias *et al.*, 2014; Borowski and Latocha, 2006), and, as non–native species, to low susceptibility to diseases and pests (Cierjacks *et al.*, 2013), 61.37% presented structural defects. Even though the logistic regression models had a low discriminatory performance regarding the total of defected trees both in terms of the classification accuracy (72.1%) and the degree of the explanatory power of the model (27.6%) when focusing on trees with cavities or in trees with a combination of different structural defects, the classification accuracy increased significantly to 87.3% and 88.4%, respectively. Although the discrimination ability of the models for trees with burls and rotten bark was much lower, it might still be considered sufficient enough in cases of a rapid urban tree health assessment.

We investigated the presence of tree cavities and not on any other defect as cavities in tree stems, forming via the decay of wood by natural age, rot, and fungi (Gibbons and Lindenmayer, 2002) are considered a primary cause of tree failure (Soge *et al.*, 2019; Johnstone *et al.*, 2010). At the same time, cavity formation is a substantial factor for cavity–nesting and/or roosting animal communities (Cockle *et al.*, 2011), and, thus, the ability for rapid detection of tree cavities is of high importance. We estimated tree cavities by ground–based observation, even though we are aware that this method can lead to misleading results for complete cavity inventories (Cockle *et al.*, 2010; Blakely and Didham, 2008) but we deemed this was sufficient for our purpose. The logistic regression models had a high classification accuracy for the three examined tree species and were quite

informative regarding the predictors ($T_{IQR,}$ Moran's index) which explain cavity presence probability (**Table A5**). Moreover, focusing on the presence or the absence probability of hazardous trees, based on the strength loss criterion of Smiley and Fraedrich (Smiley and Fraedrich, 1992), it is noted that the model had exceptionally high classification accuracy (89.9% in all cases) with the highest degree of explanatory power (72.6%) of all models (**Table A6**). Keeping in mind the importance of T_{IQR} and Moran's index, described previously, it is apparent that they can also provide an accurate prediction of cavities' presence and can be considered as reliable indicators of urban trees' health state.

The use of the SL index in combination with IRT and spatial indices led to the extraction of the hazardous trees hotspots in the studied urban parks. A reliable map image of the exact locations of hazardous trees is obviously extremely useful offering valuable data for specialized park management and allowing the prioritization of those locations for mitigation activities aimed to reduce accidents. The interpolation of these hotspots by using the kriging geostatistical procedure (**Figure A6**) showed that urban parks could be organized in different 'thermal' zones, based on the proposed analysis, implying variance in their structural quality and health.

In conclusion, the main contribution of this research work is the promotion of the use of thermal and spatial indices for tree hazard assessment in urban areas. This can be accomplished by creating a combinatory methodology and by taking into account the structural and functional traits of trees, their trunk temperature distribution obtained using the relatively new non–destructive method of IRT, and with the introduction of spatial statistics both at the single tree level and the park level. We showed that it is possible to detect, quantify, and map urban trees' structural defects and to distinguish them into different categories, bearing in mind their individuality according to the type of their defects. We also demonstrated the importance of T_{IQR} and Moran's index; they can be used in estimating the health state of different tree species especially when examining the presence of cavities. Finally, these indices along with the long established methods for tree hazard assessment, describing tree strength loss, can contribute to a rapid but reliable assessment of tree health state and may be used to map hazardous trees in an urban setting.

References

1. Morgenroth, J.; Östberg, J. *Routledge Handbook of Urban Forestry*; Ferrini, F., Konijnendijk van den Bosch, C.C., Fini, A., Eds.; Routledge: London ; New York : Routledge, 2017., 2017; ISBN 9781315627106.
2. Konijnendijk, C. A Short History of Urban Forestry in Europe. *J. Arboric.* **1997**, *23*, 31–39.
3. Bolund, P.; Hunhammar, S. Ecosystem services in urban areas. *Ecol. Econ.* **1999**, *29*, 293–301, doi:10.1016/S0921-8009(99)00013-0.
4. Gómez-Baggethun, E.; Barton, D.N. Classifying and valuing ecosystem services for urban planning. *Ecol. Econ.* **2013**, *86*, 235–245, doi:10.1016/j.ecolecon.2012.08.019.
5. Livesley, S.J.; McPherson, E.G.; Calfapietra, C. The Urban Forest and Ecosystem Services: Impacts on Urban Water, Heat, and Pollution Cycles at the Tree, Street, and City Scale. *J. Environ. Qual.* **2016**, *45*, 119–124, doi:10.2134/jeq2015.11.0567.
6. Kabisch, N.; Qureshi, S.; Haase, D. Human-environment interactions in urban green spaces - A systematic review of contemporary issues and prospects for future research. *Environ. Impact Assess. Rev.* **2015**, *50*, 25–34, doi:10.1016/j.eiar.2014.08.007.
7. Su, M.; Fath, B.D.; Yang, Z. Urban ecosystem health assessment: A review. *Sci. Total Environ.* **2010**, *408*, 2425–2434, doi:10.1016/j.scitotenv.2010.03.009.
8. Turner-Skoff, J.B.; Cavender, N. The benefits of trees for livable and sustainable communities. *Plants People Planet* **2019**, *1*, 323–335, doi:10.1002/ppp3.39.
9. European Commission *EU Biodiversity Strategy, Bringing Nature back into Our Lives*; EC COM(2020) 380 Final, 2020;
10. Cavender, N.; Donnelly, G. Intersecting urban forestry and botanical gardens to address big challenges for healthier trees, people, and cities. *Plants People Planet* **2019**, *1*, 315–322, doi:10.1002/ppp3.38.
11. Russo, D.; Ancillotto, L. Sensitivity of bats to urbanization: A review. *Mamm. Biol.* **2015**, *80*, 205–212, doi:10.1016/j.mambio.2014.10.003.
12. Lindenmayer, D.B.; Laurance, W.F. The ecology, distribution, conservation and management of large old trees. *Biol. Rev.* **2017**, *92*, 1434–1458, doi:10.1111/brv.12290.
13. Lutz, J.A.; Furniss, T.J.; Johnson, D.J.; Davies, S.J.; Allen, D.; Alonso, A.; Anderson-Teixeira, K.J.; Andrade, A.; Baltzer, J.; Becker, K.M.L.; *et al*. Global importance of large-diameter trees. *Glob. Ecol. Biogeogr.* **2018**, *27*, 849–864, doi:10.1111/geb.12747.
14. Mullaney, J. *Using Permeable Pavements to Promote Street Tree Growth*; 2015; ISBN 1312698837.
15. Scharenbroch, B.C.; Carter, D.; Bialecki, M.; Fahey, R.; Scheberl, L.; Catania, M.; Roman, L.A.; Bassuk, N.; Harper, R.W.; Werner, L.; *et al*. A rapid urban site index for assessing the quality of street tree planting sites. *Urban For. Urban Green.* **2017**, *27*, 279–286, doi:10.1016/j.ufug.2017.08.017.
16. Rashidi, F.; Jalili, A.; Kafaki, S.B.; Sagheb-Talebi, K.; Hodgson, J. Anatomical responses of leaves of Black Locust (Robinia pseudoacacia L.) to urban pollutant gases and climatic factors. *Trees - Struct. Funct.* **2012**, *26*, 363–375, doi:10.1007/s00468-011-0598-y.
17. Samecka-Cymerman, A.; Kolon, K.; Kempers, A.J. Short shoots of Betula pendula Roth. as bioindicators of urban environmental pollution in Wrocław (Poland). *Trees - Struct. Funct.* **2009**, *23*, 923–929, doi:10.1007/s00468-009-0334-z.
18. Chen, Z.; He, X.; Cui, M.; Davi, N.; Zhang, X.; Chen, W.; Sun, Y. The effect of anthropogenic activities on the reduction of urban tree sensitivity to climatic change: Dendrochronological evidence from Chinese pine in Shenyang city. *Trees - Struct. Funct.* **2011**, *25*, 393–405, doi:10.1007/s00468-010-0514-x.
19. Dahlhausen, J.; Biber, P.; Rötzer, T.; Uhl, E.; Pretzsch, H. Tree species and their space requirements in six urban environments worldwide. *Forests* **2016**, *7*, doi:10.3390/f7060111.
20. Lüttge, U.; Buckeridge, M. Trees: structure and function and the challenges of urbanization.

Trees - Struct. Funct. **2020**, doi:10.1007/s00468-020-01964-1.
21. Ghosh, S.; Scharenbroch, B.C.; Burcham, D.; Ow, L.F.; Shenbagavalli, S.; Mahimairaja, S. Influence of soil properties on street tree attributes in Singapore. *Urban Ecosyst.* **2016**, *19*, 949–967, doi:10.1007/s11252-016-0530-8.
22. Savi, T.; Bertuzzi, S.; Branca, S.; Tretiach, M.; Nardini, A. Drought-induced xylem cavitation and hydraulic deterioration: Risk factors for urban trees under climate change? *New Phytol.* **2015**, *205*, 1106–1116, doi:10.1111/nph.13112.
23. Hilbert, D.R.; Roman, L.A.; Koeser, A.K.; Vogt, J.; van Doorn, N.S. Urban tree mortality: A literature review. *Arboric. Urban For.* **2019**, *45*, 167–200, doi:10.48044/jauf.2019.015.
24. Zhang, B.; Brack, C.L. Urban forest responses to climate change: A case study in Canberra. *Urban For. Urban Green.* **2021**, *57*, 126910, doi:10.1016/j.ufug.2020.126910.
25. Boa, E. *An illustrated guide to the state of health of trees Recognition and interpretation*; FAO, Ed.; CABI Bioscience, London, UK., 2003; ISBN 9251050201.
26. Escobedo, F.J.; Palmas-Perez, S.; Dobbs, C.; Gezan, S.; Hernandez, J. Spatio-temporal changes in structure for a mediterranean urban forest: Santiago, Chile 2002 to 2014. *Forests* **2016**, *7*, 1–14, doi:10.3390/f7060121.
27. Klein, R.W.; Koeser, A.K.; Hauer, R.J.; Hansen, G.; Escobedo, F.J. Risk assessment and risk perception of trees: A review of literature relating to arboriculture and urban forestry. *Arboric. Urban For.* **2019**, *45*, 26–38, doi:10.48044/jauf.2019.003.
28. Miesbauer, J.W.; Gilman, E.F.; Masters, F.J.; Nitesh, S. Impact of branch reorientation on breaking stress in Liriodendron tulipifera L. *Urban For. Urban Green.* **2014**, *13*, 526–533, doi:10.1016/j.ufug.2014.05.002.
29. Geitmann, A.; Gril, J. *Plant Biomechanics: From Structure to Function at Multiple Scales*; 2018; ISBN 9783319790992.
30. Gardiner, B.; Berry, P.; Moulia, B. Review: Wind impacts on plant growth, mechanics and damage. *Plant Sci.* 2016, *245*, 94–118.
31. Smiley, E.T.; Fraedrich, B.R. Determining strength loss from decay. *J. Arboric.* **1992**, *18*, 201–204.
32. Kane, B.C.P.; Ryan, H.D.P. The accuracy of formulas used to assess strength loss due to decay in trees. *J. Arboric.* **2004**, *30*, 347–356.
33. Lonsdale, D. Current issues in arboricultural risk assessment and management. *Arboric. J.* **2007**, *30*, 163–174, doi:10.1080/03071375.2007.9747490.
34. Kim, Y.; Rahardjo, H.; Tsen-Tieng, D.L. Stability analysis of laterally loaded trees based on tree-root-soil interaction. *Urban For. Urban Green.* **2020**, *49*, 126639, doi:10.1016/j.ufug.2020.126639.
35. Kim, Y.; Rahardjo, H.; Tsen-Tieng, D.L. Mechanical behavior of trees with structural defects under lateral load: A numerical modeling approach. *Urban For. Urban Green.* **2021**, *59*, 126987, doi:10.1016/j.ufug.2021.126987.
36. Wagener, W.W. *Judging Hazard From Native Trees in California Recreational Areas: A Guide for Professional Foresters*; 1963;
37. Coder, K.D. Should you or shouldn't you fill tree hollows? *Grounds Maint.* **1989**, *24*, 68–72.
38. Mattheck, C.; Breloer, H. Field guide for visual tree assessment (Vta). *Arboric. J.* **1994**, *18*, 1–23, doi:10.1080/03071375.1994.9746995.
39. Leong, E.C.; Burcham, D.C.; Fong, Y.K. A purposeful classification of tree decay detection tools. *Arboric. J.* **2012**, *34*, 91–115, doi:10.1080/03071375.2012.701430.
40. Vidal, D.; Pitarma, R. Infrared thermography applied to tree health assessment: A review. *Agric.* **2019**, *9*, doi:10.3390/agriculture9070156.
41. Ouis, D. Non Destructive Techniques for Detecting Decay in Standing Trees. *Arboric. J.* **2003**, *27*, 159–177, doi:10.1080/03071375.2003.9747371.
42. Goh, C.L.; Abdul Rahim, R.; Fazalul Rahiman, M.H.; Mohamad Talib, M.T.; Tee, Z.C. Sensing wood decay in standing trees: A review. *Sensors Actuators, A Phys.* **2018**, *269*, 276–282, doi:10.1016/j.sna.2017.11.038.

43. Boddy, L. Oikos Editorial Office Fungal Community Ecology and Wood Decomposition Processes in Angiosperms : From Standing Tree to Complete Decay of Coarse Woody Debris processes decomposition ecology and wood Fungal community coarse tree to in angiosperms : from st. *Ecol. Bull.* **2001**, 43–56.
44. Shigo, A.L.; Marx, H.G. *Compartmentalization of decay in trees.*; Department of Agriculture, Forest Service, 1977; Vol. 252;.
45. Deflorio, G.; Johnson, C.; Fink, S.; Schwarze, F.W.M.R. Decay development in living sapwood of coniferous and deciduous trees inoculated with six wood decay fungi. *For. Ecol. Manage.* **2008**, *255*, 2373–2383, doi:10.1016/j.foreco.2007.12.040.
46. Allison, R.B.; Wang, X. Chapter 7 Nondestructive Testing in the Urban Forest. *USDA For. Serv.* **2015**, *238*, 77–86.
47. Nicolotti, G.; Socco, L. V.; Martinis, R.; Godio, A.; Sambuelli, L. Application and comparison of three tomographic techiques for detection decay in trees. *J. Arboric.* **2003**, *29*, 66–78.
48. Giannakis, I.; Tosti, F.; Lantini, L.; Alani, A.M. Diagnosing Emerging Infectious Diseases of Trees Using Ground Penetrating Radar. *IEEE Trans. Geosci. Remote Sens.* **2020**, *58*, 1146–1155, doi:10.1109/TGRS.2019.2944070.
49. Lin, C.J.; Huang, Y.H.; Huang, G.S.; Wu, M.L. Detection of decay damage in iron-wood living trees by nondestructive techniques. *J. Wood Sci.* **2016**, *62*, 42–51, doi:10.1007/s10086-015-1520-9.
50. Espinosa, L.; Prieto, F.; Brancheriau, L.; Lasaygues, P. Ultrasonic imaging of standing trees: Factors influencing the decay detection. *2019 22nd Symp. Image, Signal Process. Artif. Vision, STSIVA 2019 - Conf. Proc.* **2019**, 1–5, doi:10.1109/STSIVA.2019.8730215.
51. Soge, A.O.; Popoola, O.I.; Adetoyinbo, A.A. A four-point electrical resistivity method for detecting wood decay and hollows in living trees. *Eur. J. Wood Wood Prod.* **2019**, *77*, 465–474, doi:10.1007/s00107-019-01402-1.
52. Zakaria, Z.; Mansor, M.S.B.; Rahim, R.A.; Balkhis, I.; Rahiman, M.H.F.; Rahim, H.A.; Yaacob, S. Magnetic Induction Tomography: A Review on the Potential Application in Agricultural Industry of Malaysia. *J. Agric. Sci.* **2013**, *5*, 78–82, doi:10.5539/jas.v5n9p78.
53. Martin, P.; Collet, R.; Barthelemy, P.; Roussy, G. Evaluation of wood characteristics: Internal scanning of the material by microwaves. *Wood Sci. Technol.* **1987**, *21*, 361–371, doi:10.1007/BF00380203.
54. Catena, A.; Catena, G. Overview of thermal imaging for tree assessment. *Arboric. J.* **2008**, *30*, 259–270, doi:10.1080/03071375.2008.9747505.
55. Pitarma, R.; Crisóstomo, J.; Ferreira, M.E. Contribution to trees health assessment using infrared thermography. *Agric.* **2019**, *9*, doi:10.3390/agriculture9080171.
56. Bellett-Travers, M.; Morris, S. The relationship between surface temperature and radial wood thickness of twelve trees harvested in nottinghamshire. *Arboric. J.* **2010**, *33*, 15–26, doi:10.1080/03071375.2010.9747589.
57. Catena, A.; Catena, G.; Lugaresi, D.; R., G. La Termografia rivela la presenza di danni anche nell'apparato radicale degli alberi. *Agric. Ric.* 2002, 81–100.
58. Terho, M. An assessment of decay among urban Tilia, Betula, and Acer trees felled as hazardous. *Urban For. Urban Green.* **2009**, *8*, 77–85, doi:10.1016/j.ufug.2009.02.004.
59. Hunt, J.F.; Gu, H.; Lebow, P.K. Theoretical thermal conductivity equation for uniform density wood cells. *Wood Fiber Sci.* **2008**, *40*, 167–180.
60. Pokorny, J.D. Urban tree risk management, a community guide to program design and implementation, USDA Forest Service Northeastern Area State and Private Forestry. **2003**.
61. Ribeiro da Luz, B. Attenuated total reflectance spectroscopy of plant leaves: A tool for ecological and botanical studies. *New Phytol.* **2006**, *172*, 305–318, doi:10.1111/j.1469-8137.2006.01823.x.
62. Ishimwe, R.; Abutaleb, K.; Ahmed, F. Applications of Thermal Imaging in Agriculture—A Review. *Adv. Remote Sens.* **2014**, *03*, 128–140, doi:10.4236/ars.2014.33011.
63. Dragavtsev, V.; Nartov, V.P. Application of Thermal Imaging in Agriculture and Forestry. *Eur. Agrophysical J.* **2015**, *2*, 15, doi:10.17830/j.eaj.2015.01.015.

64. Matese, A.; Baraldi, R.; Berton, A.; Cesaraccio, C.; Di Gennaro, S.F.; Duce, P.; Facini, O.; Mameli, M.G.; Piga, A.; Zaldei, A. Estimation of Water Stress in grapevines using proximal and remote sensing methods. *Remote Sens.* **2018**, *10*, 1–16, doi:10.3390/rs10010114.
65. Ouledali, S.; Ennajeh, M.; Zrig, A.; Gianinazzi, S.; Khemira, H. Estimating the contribution of arbuscular mycorrhizal fungi to drought tolerance of potted olive trees (Olea europaea). *Acta Physiol. Plant.* **2018**, *40*, 1–13, doi:10.1007/s11738-018-2656-1.
66. Still, C.; Powell, R.; Aubrecht, D.; Kim, Y.; Helliker, B.; Roberts, D.; Richardson, A.D.; Goulden, M. Thermal imaging in plant and ecosystem ecology: applications and challenges. *Ecosphere* **2019**, *10*, doi:10.1002/ecs2.2768.
67. Assmann, E. *The Principles of Forest Yield Study: Studies in the Organic Production, Structure, Increment and Yield of Forest Stands*; Oxford: Pergamon, 1970; ISBN 9781483150932.
68. Johnstone, D.; Moore, G.; Tausz, M.; Nicolas, M. The Measurement of Wood Decay in Landscape Trees. *Arboric. Urban For.* **2010**, *36*, 121–127, doi:10.48044/jauf.2010.016.
69. Kennard, D.K.; Putz, F.E.; Niederhofer, M. The predictability of tree decay based on visual assessments. *J. Arboric.* **1996**, *22*, 249–254.
70. Terho, M.; Hallaksela, A.M. Decay characteristics of hazardous Tilia, Betula, and Acer trees felled by municipal urban tree managers in the Helsinki City Area. *Forestry* **2008**, *81*, 151–159, doi:10.1093/forestry/cpn002.
71. Frank, J.; Castle, M.E.; Westfall, J.A.; Weiskittel, A.R.; Macfarlane, D.W.; Baral, S.K.; Radtke, P.J.; Pelletier, G. Variation in occurrence and extent of internal stem decay in standing trees across the eastern US and Canada: Evaluation of alternative modelling approaches and influential factors. *Forestry* **2018**, *91*, 382–399, doi:10.1093/forestry/cpx054.
72. Minkina, W.; Dudzik, S. Algorithm of Infrared Camera Measurement Processing Path. In *Infrared Thermography*; John Wiley & Sons, Ltd: Chichester, UK, 2009; pp. 41–60 ISBN 9780470747186.
73. Faye, E.; Dangles, O.; Pincebourde, S. Distance makes the difference in thermography for ecological studies. *J. Therm. Biol.* **2016**, *56*, 1–9, doi:10.1016/j.jtherbio.2015.11.011.
74. Briscoe, N.J.; Handasyde, K.A.; Griffiths, S.R.; Porter, W.P.; Krockenberger, A.; Kearney, M.R. Tree-hugging koalas demonstrate a novel thermoregulatory mechanism for arboreal mammals. *Biol. Lett.* **2014**, *10*, doi:10.1098/rsbl.2014.0235.
75. Moran, P. Notes on Continuous Stochastic Phenomena. *Biometrika* **1950**, *37*, 17–23.
76. Anselin, L. Local Indicators of Spatial Association—LISA. *Geogr. Anal.* **1995**, *27*, 93–115, doi:10.1111/j.1538-4632.1995.tb00338.x.
77. Getis, A.; Ord, J.K. The Analysis of Spatial Association by Use of Distance Statistics. *Geogr. Anal.* **1992**, *24*, 189–206, doi:10.1111/j.1538-4632.1992.tb00261.x.
78. López-Bernal, Á.; Alcántara, E.; Testi, L.; Villalobos, F.J. Spatial sap flow and xylem anatomical characteristics in olive trees under different irrigation regimes. *Tree Physiol.* **2010**, *30*, 1536–1544, doi:10.1093/treephys/tpq095.
79. Burcham, D.C.; Leong, E.C.; Fong, Y.K.; Tan, P.Y. An evaluation of internal defects and their effect on trunk surface temperature in casuarina equisetifolia L. (Casuarinaceae). *Arboric. Urban For.* **2012**, *38*, 277–286, doi:10.48044/jauf.2012.037.
80. Gratani, L.; Varone, L. Carbon sequestration and noise attenuation provided by hedges in Rome: The contribution of hedge traits in decreasing pollution levels. *Atmos. Pollut. Res.* **2013**, *4*, 315–322, doi:10.5094/APR.2013.035.
81. Blanusa, T.; Garratt, M.; Cathcart-James, M.; Hunt, L.; Cameron, R.W.F. Urban hedges: A review of plant species and cultivars for ecosystem service delivery in north-west Europe. *Urban For. Urban Green.* **2019**, *44*, 126391, doi:10.1016/j.ufug.2019.126391.
82. ESRI How Spatial Autocorrelation (Global Moran's I) works Available online: https://pro.arcgis.com/en/pro-app/tool-reference/spatial-statistics/h-how-spatial-autocorrelation-moran-s-i-spatial-st.htm. (accessed on Jun 21, 2021).
83. Nielsen, A.B.; Östberg, J.; Delshammar, T. Review of urban tree inventory methods used to collect data at single-tree level. *Arboric. Urban For.* **2014**, *40*, 96–111,

doi:10.48044/jauf.2014.011.
84. Östberg, J.; Wiström, B.; Randrup, T.B. The state and use of municipal tree inventories in Swedish municipalities – results from a national survey. *Urban Ecosyst.* **2018**, *21*, 467–477, doi:10.1007/s11252-018-0732-3.
85. Pauleit, S.; Jones, N.; Garcia-Martin, G.; Garcia-Valdecantos, J.L.; Rivière, L.M.; Vidal-Beaudet, L.; Bodson, M.; Randrup, T.B. Tree establishment practice in towns and cities - Results from a European survey. *Urban For. Urban Green.* **2002**, *1*, 83–96, doi:10.1078/1618-8667-00009.
86. Bayer, D.; Reischl, A.; Rötzer, T.; Pretzsch, H. Structural response of black locust (Robinia pseudoacacia L.) and small-leaved lime (Tilia cordata Mill.) to varying urban environments analyzed by terrestrial laser scanning: Implications for ecological functions and services. *Urban For. Urban Green.* **2018**, *35*, 129–138, doi:10.1016/j.ufug.2018.08.011.
87. Zevgolis, Y.G.; Kamatsos, E.; Akriotis, T.; Dimitrakopoulos, P.G.; Troumbis, A.Y. Estimating Productivity, Detecting Biotic Disturbances, and Assessing the Health State of Traditional Olive Groves, Using Nondestructive Phenotypic Techniques. *Sustainability* **2022**, *14*, 391, doi:10.3390/su14010391.
88. Wong, M.; Tang, H.; Lam, L. *Introduction to the Applications of Remote Sensing Techniques on the Tree Health Monitoring*; 2020;
89. Whitmore, T.C. Studies in Systematic Bark Morphology: I. Bark Morphology in Dipterocarpaceae. *New Phytol.* **1962**, *61*, 191–207, doi:10.1111/j.1469-8137.1962.tb06288.x.
90. Li, Y.; Zhang, L.; Yan, J.; Wang, P.; Hu, N.; Cheng, W.; Fu, B. Mapping the hotspots and coldspots of ecosystem services in conservation priority setting. *J. Geogr. Sci.* **2017**, *27*, 681–696, doi:10.1007/s11442-017-1400-x.
91. Sokal, R.R.; Oden, N.L. Sokal 1978. **1978**, 199–228.
92. Kontogianni, A.; Tsitsoni, T.; Goudelis, G. An index based on silvicultural knowledge for tree stability assessment and improved ecological function in urban ecosystems. *Ecol. Eng.* **2011**, *37*, 914–919, doi:10.1016/j.ecoleng.2011.01.015.
93. James, K.R.; Haritos, N.; Ades, P.K. Mechanical stability of trees under dynamic loads. *Am. J. Bot.* **2006**, *93*, 1522–1530, doi:10.3732/ajb.93.10.1522.
94. Cullen, S. Trees and wind: wind scales and speeds. *J. Arboric.* **2002**, *28*, 237–242.
95. Stăncioiu, P.T.; Șerbescu, A.A.; Dutcă, I. Live Crown Ratio as an Indicator for Tree Vigor and Stability of Turkey Oak (Quercus cerris L.): A Case Study. *Forests* **2021**, *12*, 1763, doi:10.3390/f12121763.
96. Nunak, T.; Nunak, N.; Tipsuwanporn, V.; Suesut, T. Surrounding effects on temperature and emissivity measurement of equipment in electrical distribution system. *Lect. Notes Eng. Comput. Sci.* **2015**, *2219*, 292–296.
97. Catena, G. A new application of thermography. *Atti della Fond. Giorgio Ronchi* 1990, *45*, 947–952.
98. Borowski, J.; Latocha, P. Dobór drzew i krzewów do warunków przyulicznych Warszawy i miast centralnej Polski. *Rocz. Dedrologiczny* **2006**, *54*, 83–93.
99. Dias, M.C.; Azevedo, C.; Costa, M.; Pinto, G.; Santos, C. Melia azedarach plants show tolerance properties to water shortage treatment: An ecophysiological study. *Plant Physiol. Biochem.* **2014**, *75*, 123–127, doi:10.1016/j.plaphy.2013.12.014.
100. Liu, Y.; Ji, D.; Turgeon, R.; Chen, J.; Lin, T.; Huang, J.; Luo, J.; Zhu, Y.; Zhang, C.; Lv, Z. Physiological and proteomic responses of mulberry trees (morus alba. L.) to combined salt and drought stress. *Int. J. Mol. Sci.* **2019**, *20*, doi:10.3390/ijms20102486.
101. Cierjacks, A.; Kowarik, I.; Joshi, J.; Hempel, S.; Ristow, M.; von der Lippe, M.; Weber, E. Biological flora of the british isles: Robinia pseudoacacia. *J. Ecol.* **2013**, *101*, 1623–1640, doi:10.1111/1365-2745.12162.
102. Gibbons, P.; Lindenmayer, D. *Tree hollows and wildlife conservation in Australia*; CSIRO publishing: Collingwood, Victoria, 2002;
103. Cockle, K.L.; Martin, K.; Wesołowski, T. Woodpeckers, decay, and the future of cavity-nesting

vertebrate communities worldwide. *Front. Ecol. Environ.* **2011**, *9*, 377–382, doi:10.1890/110013.
104. Blakely, T.J.; Didham, R.K. Tree holes in a mixed broad-leaf-podocarp rain forest, New Zealand. *N. Z. J. Ecol.* **2008**, *32*, 197–208.
105. Cockle, K.L.; Martin, K.; Drever, M.C. Supply of tree-holes limits nest density of cavity-nesting birds in primary and logged subtropical Atlantic forest. *Biol. Conserv.* **2010**, *143*, 2851–2857, doi:10.1016/j.biocon.2010.08.002.

B. Estimating productivity, detecting biotic disturbances, and assessing the health state of traditional olive groves, using non–destructive phenotypic techniques

Zevgolis Y.G., Kamatsos E., Akriotis T., Dimitrakopoulos P.G., Troumbis A.Y. (2022), *Sustainability*, 14(1), 391, https://doi.org/10.3390/su14010391

Abstract

Conservation of traditional olive groves through effective monitoring of their health state is crucial both at a tree and at a population level. In this study, we introduce a comprehensive methodological framework for estimating the traditional olive grove health state, by considering the fundamental phenotypic, spectral, and thermal traits of the olive trees. We obtained phenotypic information from olive trees on the Greek island of Lesvos by combining this with in situ measurement of spectral reflectance and thermal indices to investigate the effect of the olive tree traits on productivity, the presence of the olive leaf spot disease (OLS), and olive tree classification based on their health state. In this context, we identified a suite of important features, derived from linear and logistic regression models, which can explain productivity and accurately evaluate infected and non–infected trees. The results indicated that either specific traits or combinations of them are statistically significant predictors of productivity, while the occurrence of OLS symptoms can be identified by both the olives' vitality traits and by the thermal variables. Finally, the classification of olive trees into different health states possibly offers significant information to explain traditional olive grove dynamics for their sustainable management.

Keywords

Traditional agroecosystems; phenotypic traits; infrared thermography; Lesvos; Olea europaea var. pyriformis

B. List of Tables

B. List of Figures

B.1 Introduction

In agricultural landscapes, the continuous and complex co–evolutionary process among natural and agricultural production systems has led to the formation of traditional agroecosystems (Altieri, 2004). These are considered essential sanctuaries of agrobiodiversity (Achtak *et al*., 2010; Jarvis *et al*., 2008) of a high conservation value (Fischer *et al*., 2012). The values of traditional agroecosystems, along with the great variety of traditional practices implemented in these areas, are gradually recognized in the context of the European agro–environmental policies; they are referred to as "High Nature Value farmland areas" (hereafter HNVf) (Plieninger and Bieling, 2013; Beaufoy and Jones, 2012), and have contributed to enhancing the implementation and effectiveness of conservation actions (Lomba *et al*., 2014).

In the Mediterranean basin, a variety of traditional agroecosystems can be found, including traditional olive groves (Price, 2013; Solomou and Sfougaris, 2011; Loumou and Giourga, 2003), which are considered a type of HNVf in Europe (Pointereau *et al*., 2007). Traditional olive groves are characterized by the presence of old trees growing at low densities, absence of irrigation, non–regular pruning, grazing of semi–natural vegetation under and between the olive trees, low or no input of fertilizers and biocides (Keenleyside *et al*., 2014; Poláková *et al*., 2011), and infrastructures such as terraces and dry stone walls (Duarte *et al*., 2008) that contribute to preserving natural habitats and viable animal diversity populations of the highest conservation value (Plieninger and Bieling, 2013; Henle *et al*., 2008), supporting conservation and/or creating a stable and high–value agricultural ecosystem. In parallel, the ineffective European Union regulations and policies towards the intensification of olive and olive oil production of the past (Lefebvre *et al*., 2012; De Graaff *et al*., 2011; de Graaff *et al*., 2010) have changed and shifted towards sustainable practices, supporting traditional olive grove conservation and acknowledging the importance of traditional practices for alleviating biodiversity loss, soil erosion, and land degradation (Brunori *et al*., 2018; Brandolini, 2017; Modica *et al*., 2017).

Despite these positive steps, traditional olive groves of the Mediterranean basin, especially terraced ones, are progressively deteriorating due to the continuous intensification of agriculture (Fleskens, 2007; Hole *et al*., 2005; Benton *et al*., 2003), as well as land depopulation and abandonment (Modica *et al*., 2017; Kizos *et al*., 2010; Caraveli, 2000). Land abandonment, in particular, exerts additional indirect abiotic (e.g., hydrogeological instability, water stress, loss of soil organic matter, soil erosion) (Salvati and Ferrara, 2015; Dunjó *et al*., 2003) and pathogenic (fungi, bacteria, viruses) pressures on terraced olive trees. At the same time, gradual re–naturalization processes are an added factor directly influencing the dynamics of these ecosystems and can lead to terrace collapse (Stanchi *et al*., 2012) and microclimate alterations (e.g., humidity), resulting in increased incidence of airborne fungi, such as the olive leaf spot (International Olive Council., 2007), and a combined further degradation of these HNVf areas.

In order to sustain the conservation of terraced olive groves, European countries should (a) identify, characterize, and map the HNVf olive groves in their territory, (b) support their maintenance and their socioecological values, and (c) monitor the pressures and their overall state (Tartaglini and Calabrese, 2012; Beaufoy, 2009). In this regard, despite the effort that has been made both through legal instruments and through targeted research, monitoring the state and pressures exerted on traditional olive groves is still a challenge.

Recent advances in monitoring methodologies combine field data and multispectral sensors of various spatial resolutions (Zhang, 2010), enabling the rapid detection of land–use changes and ecosystem degradation (Eva *et al*., 2010; Hansen *et al*., 2008). This set of rapid and noninvasive plant phenotypic techniques (Huang *et al*., 2020) is mainly used towards agricultural productivity increase

and disease detection (Blekos *et al*., 2021; Castrignanò *et al*., 2021; Nisio *et al*., 2020), while it can also adequately support effective conservation strategies (Delgado and Berry, 2008; Berry *et al*., 2003, 2005). At individual tree level, a relevant nondestructive technique is infrared thermography (IRT) (Ouis, 2003), a fast–growing type of aerial and/or ground optical remote sensing technique (Still *et al*., 2019; Dragavtsev and Nartov, 2015; Ishimwe *et al*., 2014). To date, IRT is widely used in various agroecological systems (Ishimwe *et al*., 2014; Vadivambal and Jayas, 2011), in monitoring crop vegetation (Lenthe *et al*., 2007; Chaerle *et al*., 1999, 2001), in detecting water stress (Egea *et al*., 2017; Struthers *et al*., 2015; Agam *et al*., 2013) and fungal infestation (Ouledali *et al*., 2018; Oerke *et al*., 2011), and in assessing the health state of various woody vegetation species (Catena and Catena, 2008).

Along with IRT, plant phenotyping spectral reflectance indices related to plant photosynthetic status such as leaf and crown chlorophyll concentration (Li *et al*., 2019; Obeidat *et al*., 2018; Guo *et al*., 2016; Wang *et al*., 2015), obtained in situ and non–invasively, can reflect the health state of plants. After all, chlorophyll as a pivotal photosynthetic pigment on which plant growth and productivity depend (Li *et al*., 2019; Ali *et al*., 2017), is considered a hallmark index to plant health estimation (Almansoori *et al*., 2021; Pavlovic *et al*., 2014; Steele *et al*., 2008). Low chlorophyll content may mean exposure to biotic and/or abiotic stresses, diseases, and senescence (Sánchez–Reinoso *et al*., 2019; Mishra *et al*., 2016; Richardson *et al*., 2002), and provides significant information about plant photosynthetic potential and primary production.

The above non–invasive monitoring techniques can be further enhanced with the support of traditional methods of measuring plant structural and functional traits, such as height, diameter, leaf area and its related indices (e.g., leaf area index—LAI), and canopy architecture. Specifically, in terraced olive groves, as in any other agroecosystem, LAI is considered one of the fundamental biophysical traits and is directly associated, among others, with olive growth and productivity (Pelil, P., Biradar, P., Bhagawathi, A.U., Hejjigar, 2018; Villalobos *et al*., 2006). A combination of these traits can provide a variety of different composite indices and equations that describe the overall condition of trees in traditional olive groves.

Thus, the main aim of our research was to assess traditional olive grove health state, with the emphasis on estimating productivity, using nondestructive phenotypic techniques, in a typical Mediterranean environment. We obtained phenotypic information from olive trees on the Greek island of Lesvos by combining this with in situ measurement of spectral reflectance indices and collection of IRT images to investigate the following objectives: (a) to quantify the effect of the olive tree phenotypic traits and indices on productivity, (b) to examine if olive tree phenotypic parameters can explain the presence of one of the most common biotic stressors, the olive leaf spot disease (OLS), and (c) to examine whether olive trees can be classified into groups of different health state, based on the above information.

B.2 Materials and Methods

B2.1 Study Area and Sites Selection

Lesvos, the third largest island of Greece in the NE Aegean Sea, with an area of 1632.8 km^2, encompasses geographical, biogeographical, and ecological features that promote the existence of traditional olive groves (Loumou and Giourga, 2003). The climate of the island is typical Mediterranean with a mean monthly temperature of 10.4 °C in January and 26.1 °C in July at Mytilini Airport (Kosmas *et al*., 1998). Lesvos is one of the main olive–growing parts of Greece. Its olive groves cover approximately a quarter of its total area, 415.7 km^2 and 87.4% of its agricultural area, according to the 2019 report of the Hellenic Statistical Authority, while the number of olive trees is estimated at between eight and eleven million (Kizos *et al*., 2010), with most of them located on hilly or mountainous and lowland areas (Marathianou *et al*., 2000).

Study site selection was founded on two main criteria: (a) location within the officially delineated island's HNVf area, and (b) the existence of terraces and dry stone walls, essential elements associated with this particular type of HNVf. To meet the first criterion, we combined spatial data derived from the following sources: (a) the 2008 European HNVf dataset for Greece (Paracchini *et al*., 2008), (b) the CORINE Land Cover (CLC) dataset (European Environment Agency (EEA), 2012), and (c) the tree type and density data available in the Tree Cover Density (TCD) subset of the COPERNICUS high–resolution layers (European Environment Agency (EEA), 2015b, 2015a). To identify areas of HNVf olive groves, the olive groves cover was extracted, by intersecting the Broadleaves data of COPERNICUS with the agricultural areas layer of CLC, and then retaining the olive grove cells contained in the Lesvos HNVf dataset (**Figure B1**). Based on the above, we estimated that the total area of HNVf olive groves of the island is 130.06 km^2. The entire process was performed with ESRI ArcGIS software (v. 10.2). In order to meet the second criterion, we carried out an in situ inspection of HNVf sites extracted with the first criterion, focusing on the absence of cultivation practices such as severe pruning, irrigation, fertilization, ploughing of understory, chemical disease protection, and harvesting of understory grasses for at least five years.

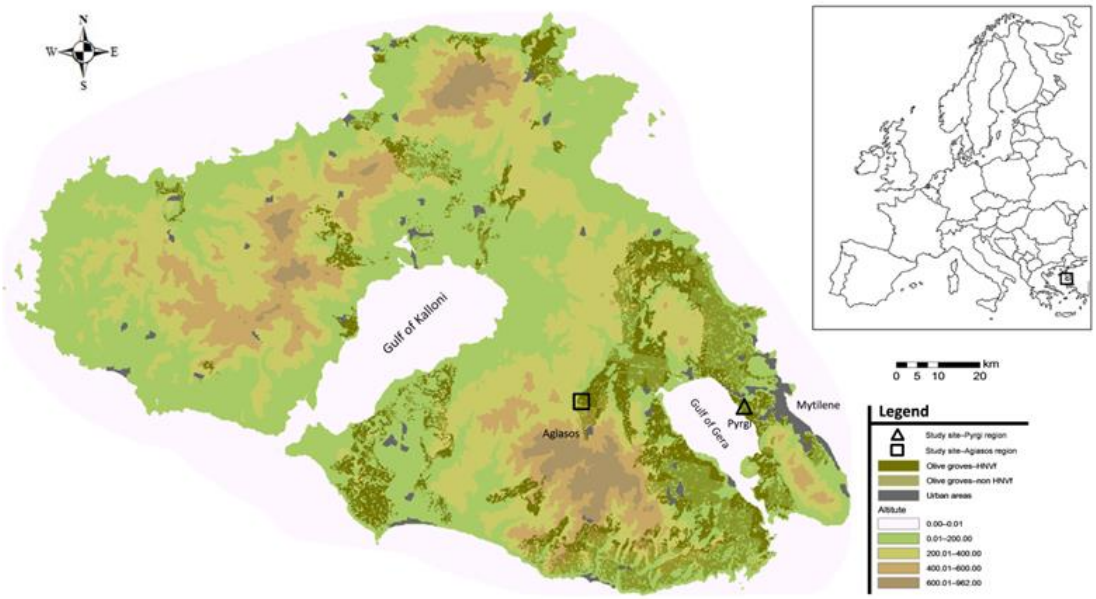

Figure B1. Map of the island of Lesvos showing the two study sites and the distribution of olive groves within and outside the island's HNVf.

Thus, we selected two terraced olive grove sites, one in the Pyrgi region (39°05’51.1’’N 26°30’48.2’’E, 10 m a.s.l.), with an area of 1.84 ha and an average slope of 18.6%, and one in the Agiasos region (39°06’28.9’’N 26°21’48.5’’E, 230 m a.s.l.), having an area of 1.41 ha and a slope of 31.7% (Figure 1). At these sites, the two main varieties of the island’s olive trees can be found, the variety “Kolovi” (Olea europaea var. pyriformis), which covers 85% of the two sites, while the remaining 15% is of the variety named “Adramytini” (Olea europaea var med. subrotunda). Tree density was 102 trees per ha at Pyrgi and 107 trees per ha at Agiasos.

B2.2 Metrics of Olive Trees’ Architecture and Vitality Traits

The two study sites were monitored from 2017 to 2020 during four olive harvest seasons. At each site, we randomly selected 40 olive trees (80 in total); for uniformity, all were the commoner “Kolovi” variety, and we measured a set of typical phenotypic traits related to their architecture and vitality. In order to estimate annual crop productivity (Pr—kg), the most essential metric for our study, we collected the olives from each tree during the harvest period (November–December) of each year. We weighed the olives in situ, using a field precision scale. We calculated the mean productivity of each tree (Prmean) as the mean of productivity values for all four years.

During the first harvest season, we recorded traits directly related to the trees’ architecture: (a) height (H—m), (b) diameter at breast height (DBH—cm), and (c) crown area (CA—m^2), using a clinometer, measuring tapes, and the vertical sighting method, respectively (Pretzsch *et al*., 2015). Regarding tree vitality, we recorded, by visual examination and an olive tree expert’s judgement, three additional phenotypic traits for each olive tree: (a) the number of productive shoots (medium–sized current year shoots, with high flowering and fruit set, about 25 cm long—PS), (b) the number of unproductive shoots (strong vertical branches in the inner part of the crown—US), and (c) the number of structural defects (external indications of rotten wood, missing bark, cavities, and hollows). We used the ratio of this number to the tree’s estimated age (SDV) instead of the absolute number to avoid any bias, given that structural defects accumulate with age. SDV is a critical parameter for olive trees as they develop deep grooves and cavities; this affects their health state and their productivity as they age. From the first two vitality traits, we extracted the tree shoots ratio (SR) variable (SR = PS/(PS + US)) as another proxy of tree productivity, while we measured PS, US, and SR at each harvest season.

Another factor of great significance, directly related both to tree health and productivity, is ageing (Ryan *et al*., 1997). Olive tree senescence is associated with processes typical of tree ageing, such as a decrease in vegetative activity and the expansion of the root system, with a concomitant increase in susceptibility to diseases (Fabbri *et al*., 2004). As olive tree age estimation by annual growth ring measurement is problematic, due to the inner part of the tree trunk having cavities and rotten tissues (Arnan *et al*., 2012; Cherubini *et al*., 2003), we resorted to an allometric equation described by Arnan *et al*. (Arnan *et al*., 2012) (Age = 2.11 × Diameter (cm) + 88.93; R^2 = .80), for its estimation.

Thereafter, we estimated the mean LAI (LAI_{mean}) of each olive tree using the SunScan plant canopy analyzer (Delta–T Devices, Cambridge, UK), by averaging five measurements taken from a height of 1.3 m from the ground, at equal distances below the crown of each tree. We also calculated the range of LAI values for each tree (LAI_{range}) from the same LAI measurements, as another indirect metric of tree health state; greater LAI_{range} shows greater non–uniformity of the tree crown indicative of lower productivity. LAI measurements were taken at the end of November when all shoot growth had stopped. Since our approach was to rely on fast and accurate field measurements, we did not include other ecophysiological parameters, such as stomatal conductance, that would require repeated measurements over a long time period.

B2.3 Estimation of Olives' Chlorophyll Concentration

As a further metric of tree vitality, we estimated chlorophyll concentration in olive tree leaves as an index of photosynthetic capacity, using a handheld chlorophyll meter (CCM—200 plus, OPTI–Sciences, Inc., Hudson, NH, USA). This optical device estimates chlorophyll concentration by extracting a spectral index, termed the chlorophyll content index (CCI), of leaf light absorbance and/or reflectance in the visible and near–infrared regions, as a ratio of transmittance percentages at 931 nm to 653 nm (Richardson *et al*., 2002). This index is strongly related to the actual amount of chlorophyll (Parry *et al*., 2014).

To measure CCI, we randomly selected fifty mature leaves from the parts of the crown used for the LAI measurements (10 leaves at each LAI measurement point). We calculated the CCI value for each leaf as the mean of three measurements of this leaf. We took all measurements in early hours so as to avoid metric fluctuations resulting from the movement of the chloroplasts (Nauš *et al*., 2010). In order to have an estimate of the mean chlorophyll content for each tree (MCL_L), we transformed CCI, which is a relative value, to chlorophyll concentration (μmol/m^2), using the universal equation described by Parry *et al*. (Parry *et al*., 2014) (μmol m^{-2} = −84.3 + 98.6 × (CCI) $^{0.505}$); we then converted this value to mg/m^2 of leaf surface by multiplying with the weighted average mass of both types of chlorophyll (0.9 mg/μmol). Finally, we estimated the total chlorophyll of each tree (TCL_T), in g, using the formula TCLT = MCLL × CA × LAImean × 10^{-3}. We used LAI_{mean} in the previous equation because when multiplied by CA, it gives the best possible estimation, in m^2, of the total foliage area of each tree. As adult olive trees have very slow growth rates (Masmoudi–Charfi and Ben Mechlia, 2007), we measured the other phenotypic traits (H, DBH, CA, SDV, LAI, CCI) only in the first year.

B2.4 Olive Leaf Spot Disease Detection

Among many different diseases affecting olive trees, one of the most widespread, both worldwide and in Lesvos, is the olive leaf spot (OLS) or Cycloconium leaf spot, a foliar disease caused by the fungus *Spilocaea oleagina* (Castagne) Hughes. The main symptoms of OLS can be detected visually and include dark green to black round spots surrounded by a yellow halo on leaves (Salman, 2017). OLS causes defoliation and progressive death of shoots and branches, leading to de–growth and productivity reduction of up to 20% (Obanor *et al*., 2008). In trees, such as those found in traditional olive groves, the lack of management practices, and competition for resources, leads to the formation of a tall and dense crown, which, in combination with the re–naturalization processes, in–creases humidity within the groves and raises the infection likelihood (Sanei and Razavi, 2011). At the same time, chemical fungicides are avoided for obvious reasons, and thus, the infection remains in the trees.

To investigate the presence of the disease, we visually examined the leaves in which we measured CCI (50 leaves per tree) at the end of November. This is within the peak growth period of the fungus, when cool, humid conditions prevail (Obanor *et al*., 2008). We evaluated OLS severity by recording the percentage of infected leaves per tree (PIL), then estimating the total infected leaf area of each tree (TIA) by multiplying PIL with CA and LAI_{mean} (TIA = PIL × CA × LAI_{mean}). We further calculated OLS to show the presence or absence of the disease for each tree.

B2.5 Collection and Processing of Olive Trees' Infrared Images

We photographed the trunks of the 80 sampled olive trees using a handheld thermal camera (Testo 875–1i, Testo SE & Co. KGaA, Lenzkirch, Germany), with a thermal resolution of < .08 °C and thermal sensitivity of <50 mK, which extracts infrared images with a spatial resolution of 160 × 120 pixels. To avoid errors resulting from (a) the effect of atmospheric composition (e.g., floating particles, soil

dust) (Minkina, W., & Dudzik, 2009) and (b) temperature inaccuracies due to the entrance of solar radiation through the tree canopy, we set the orientation of the camera for each olive tree individually to avoid patches of direct solar radiation or shading, and we carried out IRT only on rainless and windless days and in the early morning hours, at a standard distance of 5.0 m from the trunk and at a height of 1.3 m, ensuring that the entire tree trunk was captured. We kept the emissivity value at the constant level of .95 suitable for tree trunks (Briscoe *et al*., 2014), and we calibrated the collected infrared images using meteorological data: ambient temperature (T_{amb}), relative humidity (RH), and solar irradiance (SI), which we obtained, under each olive tree canopy, with a portable weather station and a solar radiation meter (Amprobe SOLAR–100).

We initially processed the collected infrared images using the TESTO IRSoft® (v. 4.3) software package and, afterward, we distinguished the areas of interest (tree trunks and lower part of main branches) from other objects in the background by using the ArcGIS Analysis toolbox (v. 10.2) (ESRI Inc., Redlands, CA, USA). Specifically, we exported the calibrated infrared images from the TESTO software, and then imported them into the ArcGIS software in a text file format (**Figure B2**). Thereafter, we converted each text file to a raster layer, and we selected the tree trunk and branches area and manually bounded them by a unique polygon in shapefile format. In this process and in order to avoid errors caused by leaf surfaces, we selected branches that had the least possible leaf cover. Finally, we extracted the temperature values within the tree trunk areas (**Figure B3a, b**) and organized them into a database for statistical analysis.

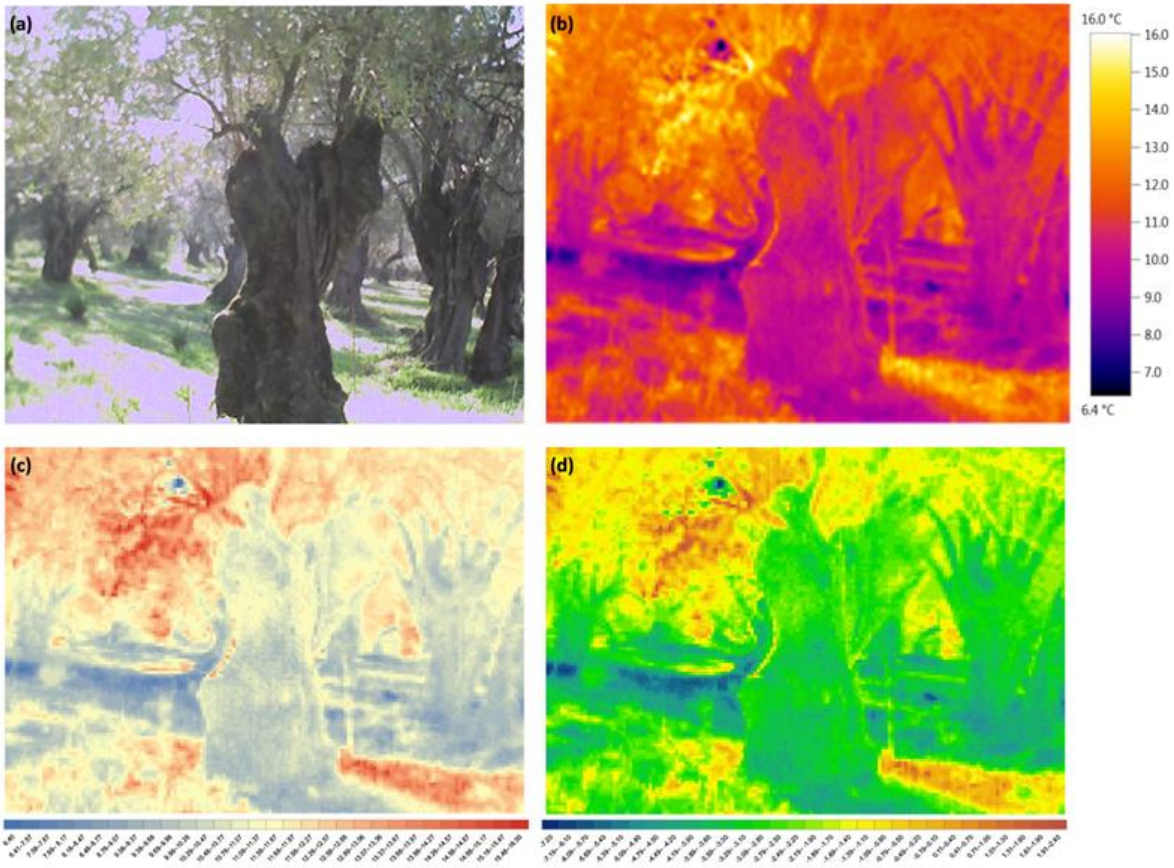

Figure B2. Main methodological procedure of an individual olive tree sample for extracting the trunk temperature data: upper left is the RGB (visible) image (a); upper right is the infrared image after calibration using the TESTO software (b); lower left is the calibrated image after imported in ArcGIS, as a raster layer (c); lower right is the final infrared image (d), as a raster layer, after converting each pixel to correspond to the temperature difference of the tree trunk from the environment (ΔT_{pixel}).

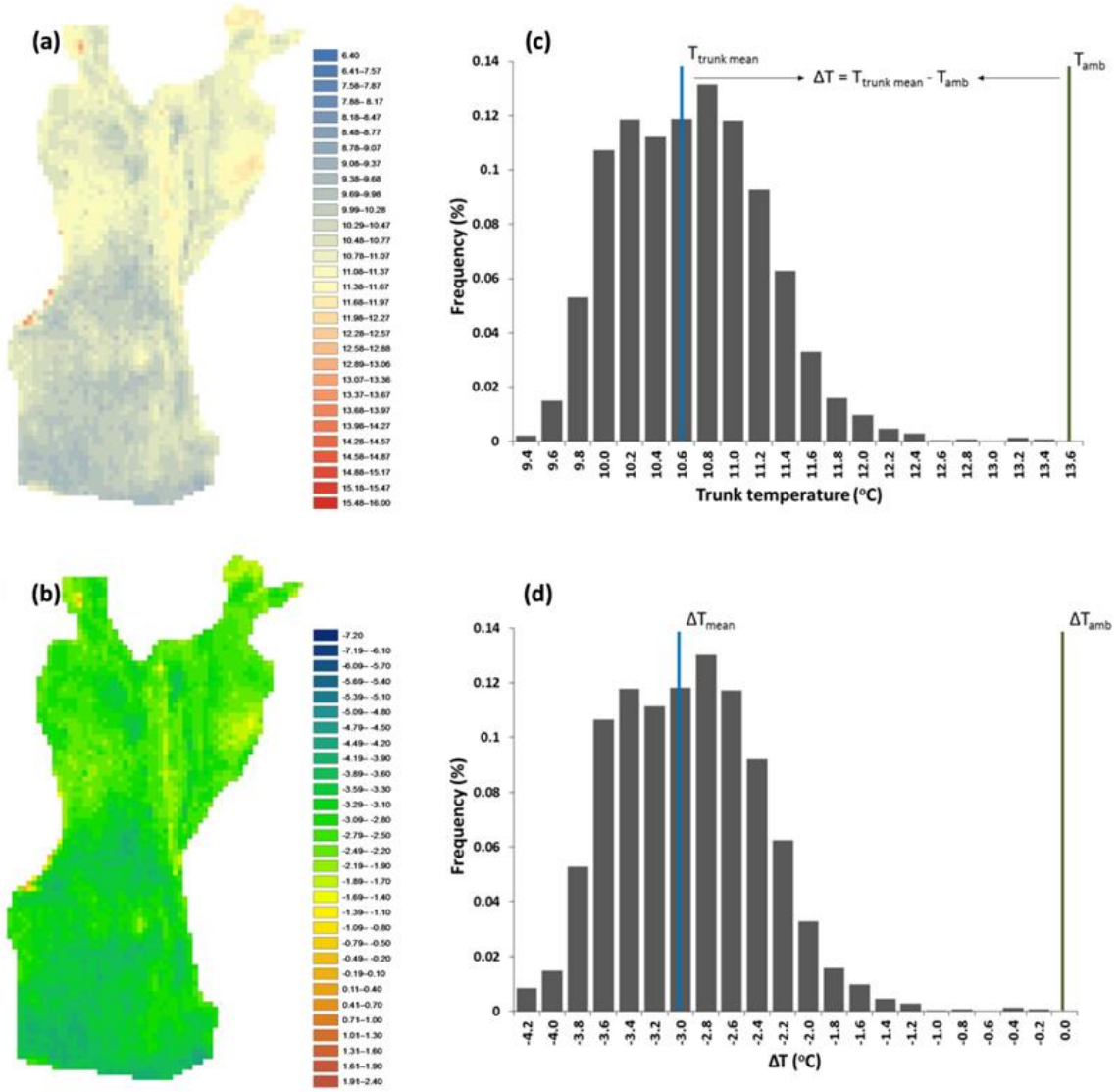

Figure B3. Trunk of an individual olive tree sample which was exported with the use of ArcGIS Analysis toolbox, as well as the histogram of its pixel values; (a, c) refers to the actual trunk temperature along with its histogram, while (b, d) refers to the trunk ΔT along with its histogram distribution. The blue line in the two histograms corresponds to the mean trunk (c) and ΔT (d) temperature values. The green line corresponds to Tamb in both histograms.

B2.6 Estimation of Olive Trees' Thermal Profile

In order to define the trees' thermal profile, we derived a set of thermal variables describing the response of the tree trunk and branches to ambient temperature by analysis of the trunk temperature histograms. In correspondence with the canopy temperature depression index (Idso *et al*., 1981), we subtracted the trunk temperature value of each pixel (T_{pixel}) from Tamb ($\Delta T_{pixel} = T_{pixel} - T_{amb}$) to obtain a unique pixel value in response to Tamb, thus creating a new histogram for each tree based on ΔT (**Figure B3**).

In order to assess the state of each olive tree as a whole, the effect of outliers and skewed data had to be avoided, hence, from each histogram, we calculated the inter–quartile range (IQR) instead of the range. However, assessing the state of individual characteristics that appear on the tree trunk and which are directly associated with the tree's health, such as wounds or other external abnormal indications, requires the study of the extreme ΔT_{pixel} values. In any case, the trunk's structural defect

patches are expected to exhibit high dissimilarity of their ΔT distribution compared to the healthy part of the trunk, and therefore we used the interpercentile ranges of each trunk histogram ($\Delta T_{05} - \Delta T_{25}$ (IPR_1) and $\Delta T_{75} - \Delta T_{95}$ (IPR_2)) separately as the most appropriate statistical metric to assess trunks' individuality. Furthermore, when these values are added together, they define the outer percentile range (OPR), which represents the required information regarding all the external or/and internal abnormalities of the trunk. Lastly, we calculated the extent of ΔT defect patches (EΔT) using the ratio of the actual number of pixels contained between the limits $\mu - 3\sigma \leq np \leq \mu - 2\sigma$ and $\mu + 2\sigma \leq np \leq \mu + 3\sigma$ to the total pixels of each tree trunk surface.

B2.7 Statistical Analysis

We used SPSS software (v. 25.0. Armonk, NY: IBM Corp.) for all statistical analyses. All the assumptions required were met and statistical significance was assumed at the 5% level. Summary statistics are expressed as means ± standard deviation (SD).

Prior to further analysis, we tested for possible differences in microclimate between the two sites due to the existing small differences in topography and altitude. Using in–dependent sample t–tests to compare microclimate variables recorded during infrared image collection, we did not find any statistically significant differences between the two sites (T_{amb} (t (40) = −.169, p = .866); SI (t (40) = .730, p = .468)), with the exception of relative humidity (RH (t (40) = 8.252, p = .001)). Therefore, we decided that treating the two sites separately was not justified and, thus, we pooled the data for the two sites.

For modeling the relationship of tree productivity with tree architectural and vitality metrics, chlorophyll concentration, and OLS infected area, as well as tree thermal variables, we visually examined their associations in scatterplots and assessed their relation–ship using Pearson's correlation coefficient (r). Next, we used multiple linear regression, with a backward elimination procedure for significant variable selection. To check for linear dependence, all independent variables were correlated to each other and we used the variance inflation factor (VIF), with a threshold value of < 3 (Zuur *et al.*, 2010) as an indicator of multicollinearity. Variables with the highest VIF were sequentially dropped from the model. We implemented this analysis both separately for each set of variables (architectural and vitality set, OLS set, thermal variables set) and by combining them all together for (a) each year's productivity and (b) for the mean productivity of all harvest years.

For examining the potential effect of OLS on tree vitality, we chose a generalized linear model. In correspondence with the previous procedure, we used architectural, vitality, and thermal metrics as predictor variables, both separately and in combination; final models were reached with backward stepwise elimination, while Nagelkerke's R^2 was used as an indication of the amount of variation explained by the model, while the overall significance of the model was tested with the Hosmer and Lemeshow goodness of fit test. To assess the discrimination ability of the model, a classification table of observed and predicted values regarding the OLS was computed and evaluated by receiver operating characteristic (ROC) curve analysis.

Finally, we used hierarchical clustering to identify any homogeneous tree groups with an analysis of variance approach to assess intercluster distances (Ward's method). To avoid problems caused by different measuring scales, we standardized the variables using Z–scores and we conducted one–way ANOVA, as well as Tukey's post hoc, tests to determine which phenotypic traits and thermal variables of olive trees are significantly differentiated between cluster groups.

B.3 Results

B3.1 Descriptive Statistics of Sample Olive Trees and Leaves

As recorded during data collection, mean T_{amb} was 13.63 ± 2.16 °C, mean RH was 67.72 ± 18.75%, and mean SI was 390.45 ± 136.77 W/m^2. The sampled olive trees had a mean height of 7.25 ± 2.74 m, mean DBH of 74.41 ± 35.45 cm, and mean CA of 51.78 ± 24.69 m^2. Descriptive statistics of olive tree architecture, vitality, and thermal profile traits are presented in **Table A1**.

Table B1. Descriptive statistics for olive tree traits (N = 80).

Variables	Mean	SD	S.E.	Min	Max	CV
			Olive Tree Architecture			
H (m)	7.25	2.74	.30	2.60	17.20	37.79
DBH (cm)	74.41	35.45	3.96	21.66	192.99	47.64
CA (m^2)	51.78	24.69	2.76	14.19	125.88	47.68
			Olive Tree Vitality			
Pr (kg) (4 years mean)	39.60	16.49	1.84	5.00	77.50	41.64
PS (4 years mean)	5.91	2.14	.24	1.00	12.00	36.20
US (4 years mean)	3.50	1.87	.20	.00	9.00	53.42
SR (4 years mean)	.60	.15	.01	.29	1.00	25.00
SDV	.014	.011	.001	.00	.07	78.57
Age	245.94	74.80	8.36	134.62	496.15	30.41
LAI_{mean}	2.11	.75	.17	.10	6.80	35.54
LAI_{range}	2.53	1.16	.13	.90	5.50	45.84
			Chlorophyll Concentration			
CCI (n = 400)	105.37	34.67	3.87	39.29	159.45	32.90
MCL_L (g/m^2)	.84	.16	.02	.49	1.07	19.04
TCL_T (g)	98.58	72.20	11.78	3.01	598.42	73.24
			OLS Parameters			
PIL	.24	.28	.03	.00	.80	116.66
TIA (m^2)	20.36	32.36	3.61	.00	190.00	158.93
			Thermal Variables			
ΔT	−1.72	1.32	.14	−4.77	1.98	−76.74
IQR	.72	.33	.03	.21	2.46	45.83
IPR_1	.51	.21	.02	.15	1.14	41.17
IPR_2	.46	.21	.02	.14	1.33	45.65
OPR	.98	.38	.04	.29	2.33	38.77
ETD	.31	.03	.004	.23	.42	9.67

In terms of the total annual productivity, the sampled olive trees produced a total of 4335 kg, 3035 kg, 3050 kg, and 2259 kg in the 2017, 2018, 2019, and 2020 harvest years. The variation of productivity for each site is presented in **Figure B4**, while a detailed description of the productivity of both sites, as well as PS, US, and SR per harvest season, is presented in **Table BS1** in the Appendix.

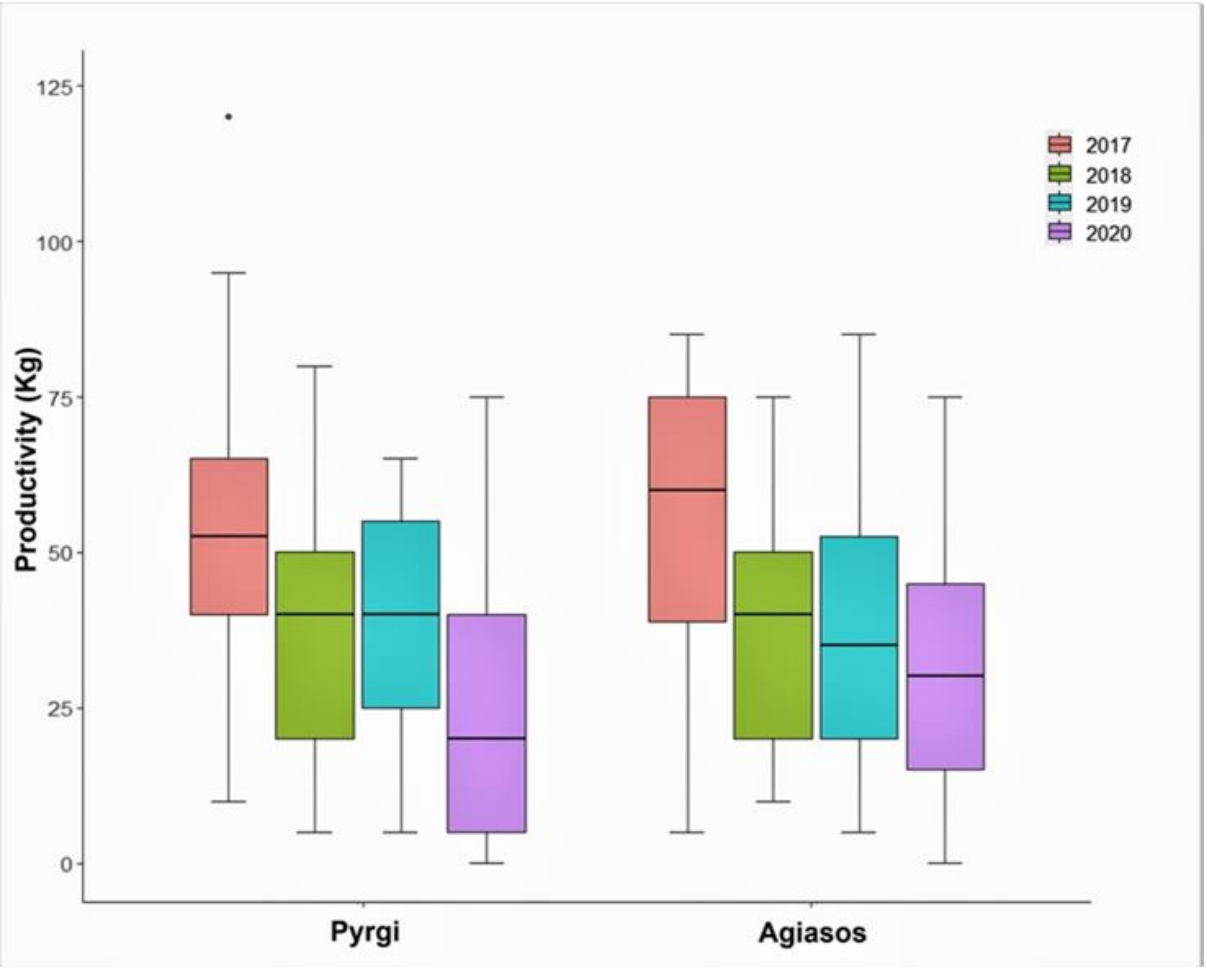

Figure B4. Box plot showing the mean annual productivity for the four harvest seasons. Horizontal lines: medians; boxes: interquartile ranges (25–75%); whiskers: data ranges.

B3.2 Relationships among the Olive Tree Traits

The analysis of tree trait variables revealed significant associations between them, both positive and negative (**Figure B5**). Productivity exhibited (a) significant positive cor–relations with SR ($r = .34$; $p = .002$), LAI_{mean} ($r = .56$; $p < .001$), MCL_L ($r = .63$; $p < .001$), and TCL_T ($r = .36$; $p < .001$), and (b) significant negative correlations with SDV ($r = -.51$; $p < .001$), LAI_{range} ($r = -.58$; $p < .001$), and PIL ($r = -.58$; $p < .001$). Concerning the relationship between productivity and tree thermal profile variables, there were significant negative correlations with almost all of the thermal variables (IQR: $r = -.69$, $p < .001$; IPR_1: $r = -.47$, $p < .001$; IPR_2: $r = -.55$, $p < .001$; OPR: $r = -.59$, $p < .001$; ETD: $r = -.35$, $p = .002$), except for ΔT.

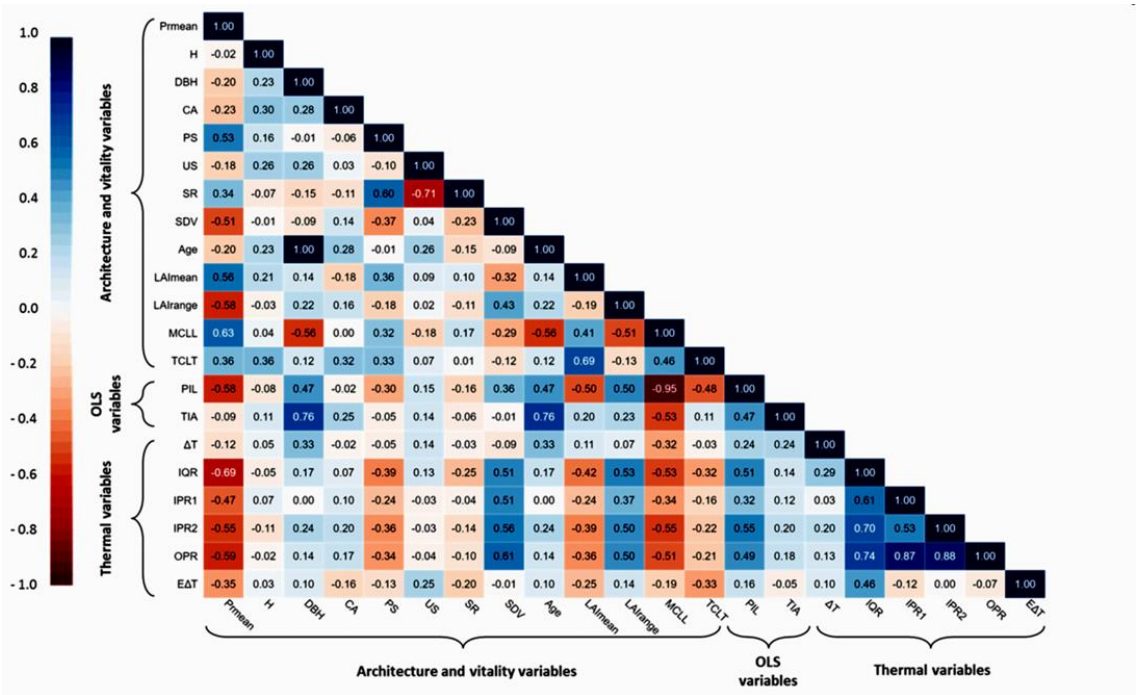

Figure B5. Pearson's r correlation matrix showing the relationships between olive tree architectural, vitality, OLS, and thermal variables. For clarity, CCI, which refers to leaves, is omitted. Red and blue colors indicate positive and negative correlations, respectively, while intensity of color indicates the strength of the relationship. All correlation coefficients above .3 or below −.3 are statistically significant ($p < .05$).

The analyzed architecture and vitality traits showed different relationships among them, which are presented in detail in **Figure B5**. Focusing on individual relationships of thermal variables with architecture and vitality traits of the olive trees, the thermal variability measures (IQR, IPR_1, IPR_2, OPR) were positively correlated with SDV, LAIrange, and PIL, and negatively correlated with LAI_{mean}, MCL_L, and TCLT (**Figure B5**). With regard to OLS variables, the percentage of infected leaves per tree (PIL) and the total infected area of each tree (TIA) followed the same pattern, showing positive correlation with DBH, age, and LAI_{range}, and negative correlations with MCLL (**Figure B5**).

B3.3 Effect of Tree Traits on Productivity

The above examination of traits is a generalized depiction of existing associations. However, to explain and predict the annual productivity of traditionally cultivated olive trees, it is necessary to form a network of variables that can provide the basis for sustainable agricultural practices, which may provide essential information on the resilience and health state of the traditional olive groves.
To obtain prediction models for productivity based on tree traits, we performed multiple linear regression analysis with backward elimination. We tested each set of variables separately, as well as all variables together. We also calculated the squared semi–partial coefficient as a measure of the proportion of total variance uniquely explained by each trait. The analyses for productivity for each harvest season resulted in a total of 20 statistically significant models; four for each season (**Tables BS2–BS5** in the Appendix), and another four concerning the average tree productivity of those harvest seasons (**Table B2**).

The results indicate that either specific traits or combinations of them, depending on each variable set, are statistically significant predictors of productivity. Specifically, for the mean annual olive tree productivity, the model for architecture and vitality traits was significant ($F(4, 75) = 31.85$, $p < .001$), with an adjusted R^2 of 61%.The final models for the OLS and thermal variables were also significant ($F(2, 77) = 23.98$, $p < .001$, $R^2 = .368$; $F(1, 78) = 69.122$, $p < .001$, $R^2 = .463$), as was the final model

with all variables (F (6, 73) = 31.98, p < .001). This last model had the greatest explanatory power (R^2 = .702) of all final models. The predictors' individual importance, evaluated by sr^2, showed that: (a) for the "architecture and vitality traits" model, LAI_{mean}—controlling for the effects of the other predictors—expressed 8.23% of the model's total variance, (b) for the "OLS" model, PIL had a unique contribution of 37.6%, (c) for the "thermal" model, IQR contributed by 46.9%, and (d) for the "combination" model, MCL_L uniquely contributed by 13.7%.

Table B2. Final models obtained from multiple linear regression analyses for estimating Prmean. All multiple regression models were statistically significant (p < .05). The slope of the predictor variable for the response variable (B), the standard error for the slope (SE B), the standardized beta (β), the t–test statistic (t), the probability value (p), the squared semi–partial coefficient (sr^2), the regression–adjusted coefficient for the multiple regression model (R^2), and the predictive capability of the models (F). The regression equations for each model are presented in *italics*.

Variables Set	Response Variable	Predictor Variables	B	SE B	β	t	*p*	sr^2	Adj. R^2	F
Architecture and Vitality Traits	Pr_{mean}	(constant)	21.50	8.84		2.43	.01		.610	31.85
		SDV	-282.49	114.39	-.20	-2.47	.01	.030		
		LAI_{mean}	3.42	.83	.32	4.08	.00	.082		
		LAI_{range}	-4.04	1.23	-.28	-3.27	.00	.053		
		MCL_L	28.36	8.72	.28	3.25	.00	.052		
Regression equation		*$Pr_{mean} = 21.50 - 282.49 \times SDV + 3.42 \times LAI_{mean} - 4.04 \times LAI_{range} + 28.36 \times MCL_L$*								
OLS	Pr_{mean}	(constant)	46.99	1.97		23.77	.00		.368	23.98
		PIL	-39.57	5.76	-.69	-6.86	.00	.376		
		TIA	.12	.05	.24	2.37	.02	.044		
Regression equation		*$Pr_{mean} = 46.99 - 39.57 \times PIL + .12 \times TIA$*								
Thermal	Pr_{mean}	(constant)	63.65	3.19		19.95	.00		.463	69.12
		IQR	-33.33	4.00	-.68	-8.31	.00	.469		
Regression equation		*$Pr_{mean} = 63.65 - 33.33 \times IQR$*								
Combination	Pr_{mean}	(constant)	5.55	10.86		.51	.61		.702	31.98
		CA	-.16	.04	-.25	-3.75	.00	.052		
		SR	16.26	6.78	.15	2.39	.02	.021		
		LAI_{range}	-2.31	1.10	-.16	-2.10	.04	.016		
		MCL_L	54.23	9.16	.55	5.91	.00	.137		
		TIA	.18	.04	.36	4.58	.00	.072		
		IQR	-14.81	3.91	.30	-3.78	.00	.054		
Regression equation		*$Pr_{mean} = 5.55 - .16 \times CA + 16.26 \times SR - 2.31 \times LAI_{range} + 54.23 \times MCL_L + .18 \times TIA - 14.81 \times IQR$*								

B3.4 Modeling the Incidence of OLS

To examine if olive tree phenotypic traits can explain the incidence of OLS disease, we used binary logistic regression models (BLR); we tested three distinct models to explain the presence of the disease, based on (a) architectural and vitality variables, (b) thermal variables, and (c) the combination of the significant traits and thermal variables, which had emerged from the first two models.

Regarding the olive tree architectural and vitality traits, a preliminary analysis suggested that the assumption of multicollinearity was met (tolerance = .741), while the inspection of standardized residuals values showed that there were no outliers. To correctly discriminate between trees with and without OLS symptoms, we selected the area under the ROC curve (AUC) as a measure of the average value of sensitivity for all possible values of specificity, with a threshold (.513) resulting from

Youden's index (Youden, 1950). The area under the ROC curve (AUC = .988; S.E. = .001; 95% CI .967–1.000; p = .0001; **Figure BS1** in the Appendix) correctly classified trees with and without symptoms in 97.5% of cases. The BLR model identified MCL_L as the one important factor which best separates trees with OLS disease symptoms from those without symptoms (χ^2 (1, N = 80) = 89.04; p < .0001; **Table B3**), with a predicted classification accuracy of 95.7% for infected and 100% for non–infected olive trees. The Nagelkerke R^2 value indicated that the model could explain 90.5% of the total variance of MCL_L, while the Hosmer–Lemeshow test gave a chi–square value of 1.926 (p > .05), meaning that the model fits the data at an acceptable level.

Focusing on detecting the occurrence of OLS symptoms using the thermal variables, the BLR model identified IQR as the most significant among the six variables entered in classifying olive trees with or without symptoms (χ^2 (1, N = 80) = 27.37; p = .0001; **Table B3**). The model's classification accuracy was 80%; 72.7% for non–infected and 85.1% for infected trees, as estimated by the area under the ROC curve (AUC = .833; S.E. = .046; 95% CI .743–.923; p = .0001; Youden's index = .506; **Figure BS1** in the Appendix). The Nagelkerke R^2 showed that IQR can explain 39% of the total variance of the data, while the Hosmer–Lemeshow test showed that the model's goodness–of–fit can be accepted (χ^2 = 16.685; p > .05).

Finally, considering the possibility of combining the variables from previous models, the BLR model identified only MCLL as the factor which best classifies infected and non–infected trees, giving the same results as the first model.

Table B3. Logistic regression models for the prediction of infected and non–infected olive trees. B = logistic coefficient; S.E. = standard error of estimate; Wald = Wald chi–square; df = degree of freedom; p–value = significance.

Architecture and Vitality Traits					
Predictor	**B**	**S.E.**	**Wald's χ^2**	**df**	***p*–Value**
MCL_L	−112.33	39.62	8.03	1	.005
Constant	105.37	37.43	7.92	1	.005
Thermal Variables					
Predictor	**B**	**S.E.**	**Wald's χ^2**	**df**	***p*–Value**
IQR	6.94	1.82	14.40	1	.0001
Constant	−4.18	1.17	12.75	1	.0001

B3.5 Cluster Analysis of Olive Trees

With the aim of identifying homogeneous tree groups with similar phenotypic traits, we carried out hierarchical classification, using Ward's hierarchical clustering method. In order to display the number of potential clusters, we initially chose variables that had the greatest impact both in estimating olive tree productivity and explaining the incidence of OLS disease. Thereafter, we separated each case (case = olive tree) into its own individual cluster (agglomerative approach), and we used a dendrogram plot based on the squared Euclidean distance for cluster visualization. The resulting dendrogram showed that the olive trees examined could be classified into three general groups with similar characteristics (Figure 6); Group 1 (G1) included 39 trees, Group 2 (G2), 21, and Group 3 (G3), 20.

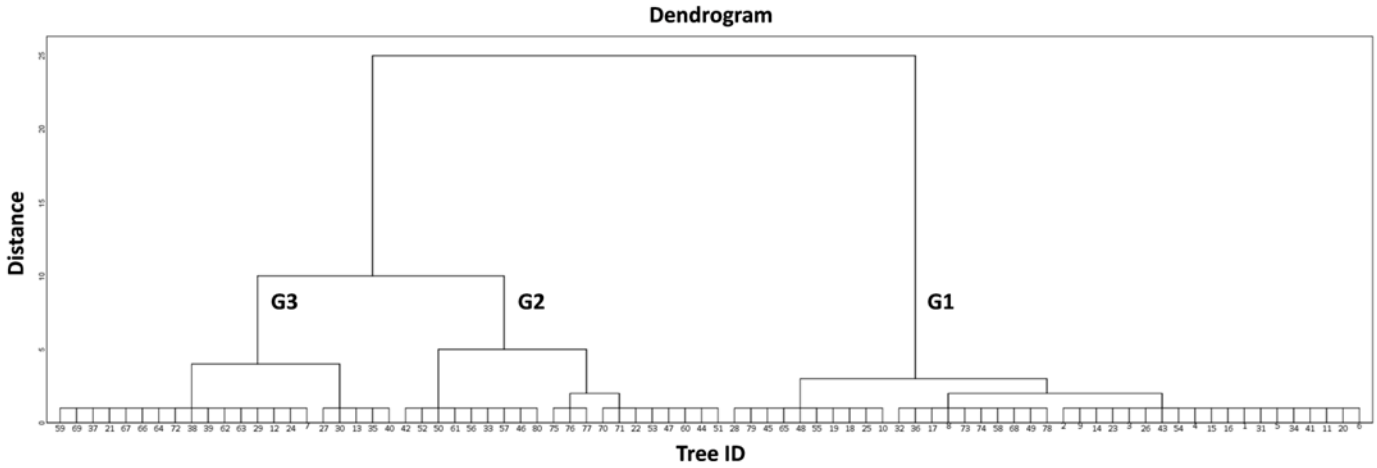

Figure B6. Dendrogram of the 80 olive trees that illustrates the dissimilarity as evaluated between Pyrgi and Agiasos sites. Numbers along branches indicated different groups.

The trees of G1 group exhibited greater height, crown area, LAImean, productivity, and chlorophyll concentration and low OLS parameters. On the contrary, trees in the G3 group displayed characteristics that describe a poor condition; high OLS parameters, greater age, and higher SDV, as well as low vitality metrics (LAI_{mean}, MCL_L, TCL_T) and lower productivity. The G2 group were intermediate between the other groups (**Table B4**). One–way ANOVA gave statistically significant differences among groups, concerning almost all the olives' phenotypic traits (DBH, Pr_{mean}, PS, US, SDV, age, LAI_{mean}, $LAIr_{ange}$, CCI, MCL_L, TCL_T, PIL, TIA) ($p < .05$).

Furthermore, examining the effect of cluster groups on thermal variables, one–way analysis of variance showed significant relationships with ΔT ($F(2, 77) = 6.18$, $p = .03$), IQR ($F(2, 77) = 13.82$, $p = .001$), IPR2 ($F(2, 77) = 16.54$, $p = .001$), and OPR ($F(2, 77) = 8.30$, $p = .001$). Tukey's HSD test for multiple comparisons found that the mean value of (a) ΔT was significantly different between G2 and G3 ($p = .002$, 95% C.I. = −2.29, −.43), (b) IQR differentiated between G1 and G3 ($p = .001$, 95% C.I. = −.60, −.22), as well as between G2 and G3 ($p = .001$, 95% C.I. = −.56, −.12), (c) IPR_2 was different among G1 and G3 ($p = .001$, 95% C.I. = −.37, −.13) and G2 and G3 ($p = .001$, 95% C.I. = −.43, −.15), and (d) OPR was also significant different between G1 and G3 ($p = .001$, 95% C.I. = −.59, −.14) and G2 and G3 ($p = .006$, 95% C.I. = −.60, −.08).

Table B4. Descriptive statistics for olive trees' traits according to the three clustering groups.

	G1 (n = 39)		G2 (n = 20)		G3 (n = 21)	
Variables	**Mean**	**SD**	**Mean**	**SD**	**Mean**	**SD**
Tree Architecture						
H (m)	8.01	3.06	6.50	2.52	6.54	1.93
DBH (cm)	72.21	30.64	51.49	18.68	100.31	40.10
CA (m^2)	54.52	24.63	48.99	30.87	49.36	17.91
Tree Vitality						
Pr (kg)	45.01	12.52	44.85	15.17	24.63	15.44
PS	6.55	2.00	5.71	2.29	4.92	1.93
US	3.79	1.80	2.50	1.00	4.04	2.29
SR	.60	.15	.65	.16	.55	.14
SDV	.012	.009	.012	.010	.019	.015
Age	241.31	64.66	197.58	39.43	300.60	84.62
LAI_{mean}	3.61	1.11	1.82	1.10	1.23	1.19
LAI_{range}	2.29	1.09	2.11	.79	3.39	1.19

Tree and Leaf Chlorophyll Concentration						
CCI (n = 400)	125.10	20.74	117.77	18.98	56.93	14.57
MCLL (g/m^2)	.93	.088	.90	.08	.60	.08
TCLT (g)	190.76	103.11	51.04	19.77	37.90	42.73
OLS Parameters						
PIL	.06	.09	.16	.16	.67	.13
TIA (m^2)	15.28	25.76	8.69	9.48	40.89	46.48
Thermal Variables						
ΔT	−1.77	1.15	−2.36	1.38	−1.00	1.28
IQR	.59	.18	.66	.20	1.00	.47
IPR_1	.47	.18	.53	.19	.58	.26
IPR_2	.40	.13	.37	.08	.66	.29
OPR	.88	.26	.90	.23	1.25	.53
ETD	.30	.03	.31	.03	.32	.05

B.4 Discussion

Our study represents the first attempt to monitor the pressures and the overall state of trees in traditional olive groves which are located on the island of Lesvos, within a part of the recognized European HNVf. For this, a crucial step was to separate the island's extensive olive groves into traditional and nontraditional. However, their identification was challenging, as their exact boundaries were not mapped, and there was no accompanying information on the individual cultivation methods used at the grove level nor any information on criteria used to define each olive grove as a traditional one. Having determined the boundaries of the traditional olive groves, our analysis focused on areas with a clear long–term absence of cultivation practices so that we have the unequivocal image of the island's traditionally grown olive tree state. After all, the agricultural land–scape of the island of Lesvos has changed since the 1990s due to land abandonment (Kizos *et al*., 2010) and, with it, cultivation practices have differentiated; nowadays, "cultivation" is often restricted to the mere harvest of olives. In some cases, pruning is also carried out, which abruptly modifies the vegetative–productive balance of the tree (pers. obs.). Therefore, an attempt was made to find traditional olive groves with clear features of cultivation practices of the past, obtaining a glimpse into the state of olive groves in the Mediterranean basin, as well as of Lesvos terraced groves, of previous decades (Lo Bianco *et al*., 2021). These practices involved forming the trees' shape to a great height and crown area, in order to overcome environmental stress and to produce larger biennial crops, by being able to accumulate water and nutrients in their large trunk and branches, and their extensive canopy and root system. Modern cultivation practices are substantially differentiated in terms of techniques (irrigation, fertilization, mechanical harvesting, pruning) (Lo Bianco *et al*., 2021) and shape of trees, aiming at low–growing irrigated trees, with a specific leaf area that produces a constant crop annually (International Olive Council., 2007).

Having identified and located traditional olive groves, we introduced a comprehensive methodological framework for traditional olive grove productivity prediction, including both easily obtainable tree trait information, which can be recorded with simple tools even with the knowledge and experience of an average olive grower, and additional information obtained with more specialized, but noninvasive, tools and techniques. Contrary to intensive agricultural systems, assessing productivity in traditional olive groves is acceptable without continual monitoring of a large set of physiological and environmental variables because immediate interventions are not possible and, occasionally, even not desirable. It should be noted that traditional olive groves tend to be less easily accessible than more intensively grown olive groves, thus, minimizing the number of necessary field visits is important. We selected techniques that can be used to collect field data in one or a few sessions, at the correct time of year, to increase the applicability of our results by both growers and cooperatives as well as by land management and nature conservation authorities.

As the main concern of all those involved in olive growing is tree productivity, we placed particular emphasis on this parameter, bearing in mind that a typical olive tree in favorable environmental conditions and with the proper management practices (regular pruning, fertilization, soil management, pest and disease control) can be productively efficient for more than 100 years (Ozturk *et al*., 2021). However, in traditional olive groves, in which the trees are much older, the absence of effective cultivation practices, in conjunction with biotic and abiotic pressures (e.g., phloem shoot–to–root flow depression due to wood decay), leads to inner crown leaf drop and retention of foliage on the outer part of the crown. Simultaneously, the inner branches start to be replaced by others on the outside and, thus, the available resources are invested in nonproductive structures (Paoletti *et al*., 2021; Fernandez–Escobar *et al*., 2013), resulting in decreased productivity as trees trade reproductive for vegetative activity (Paoletti *et al*., 2021; International Olive Council., 2007). Thus, in contrast with other studies (Stateras and Kalivas, 2020; Sola–Guirado *et al*., 2017), we took into account four consecutive years for estimating average annual productivity as well as the

average renewal of productive shoots. Theoretically, we should be able to consider only two productivity years, due to biennial fruiting, but we noticed that, in our case, the alternate bearing was not very clear (**Figure B4**), so we chose to include all four years. Moreover, the activation of metabolic pathways related to the expression of alternate bearing is affected by a wide range of climatic events which influence the vegetative and reproductive development of olives (Lavee, 2007), especially traditional ones, which we could not control.

The investigation of the relationship between productivity and the architecture and vitality traits of the olive trees revealed significant evidence in linking these traits with traditional olive grove functioning as a productive system. Of the twelve distinct traits that were either measured or calculated (e.g., MCL_L, TCL_T), five were found to be positively related (PS, SR, LAI_{mean}, MCL_L, TCL_T) and two negatively related (SDV, LAI_{range}) to productivity (**Figure B5**). Resistance mechanisms against biotic and abiotic stressors are reduced in aged olive trees (Sofo *et al*., 2008), such as ours, and physiological adaptation mechanisms (e.g., high photosynthetic rate with low stomatal conductance) are affected by reduced vegetative activity (Gargouri *et al*., 2012; Chartzoulakis *et al*., 1999); these effects are compatible with the negative productivity relationships with OLS variables.

On the one hand, the highest positive correlations which were observed between productivity and MCL_L and LAI_{mean} confirmed the already established view that these traits are considered ideal biophysical indices for the description of these relationships (Liu *et al*., 2019). Regarding MCL_L, it is well known that, despite being the essential driver of photosynthesis, and consequently olive productivity, it should be used in combination with LAI (Heege, 2013), which is an important criterion in evaluating olive trees' state, as it shows the degree to which a tree can photosynthesize. In our case, the LAImean for the 80 olive trees was particularly low (2.11 ± .75), compared with the optimal value of 6 for achieving high olive yields (International Olive Council., 2007). Apart from this, we consider that the LAI values that we found are more representative of old, rather than young, olive groves, as similar studies for measuring LAI in an old olive grove in Italy found a value of 3.5 (Čermák *et al*., 2007) and, in an intensive mature grove in Tunisia, a value of 2.8 (Aïachi *et al*., 2016).

On the other hand, the negative correlations between productivity and SDV and LAIrange, and both the relationship between them ($r = .427$; $p < .0001$) and their relationship with other significant traits (e.g., MCL_L, PIL), identify two very important parameters for estimating olive tree health. To the best of our knowledge, there is no other relevant study to use both of these traits as estimators of olive tree health. Nevertheless, we consider that it is of great importance, as LAI_{range} highlighted the deviation of olive trees from a healthy state, with extreme differences in LAI values taken into account, while SDV estimated the possible extent of the trees' phloem shoot–to–root flow depression, by quantifying its structural abnormalities. In parallel, SDV is a crucial connecting link between olive tree vitality metrics and infrared thermography; it describes trunk growth patterns, which may exhibit cracks, wounds, detached bark, and cankers, and it shows a positive correlation with almost all the thermal statistical variables which describe the thermal profile of olive trees (**Figure B5**).

These relationships result from olive tree hydraulic physiology, as olive trees have developed different strategies to sustain a balance between water supply and water loss (Johnson *et al*., 2016), by either adapting their leaf and root distribution (Van Hees, 1997) or by entire branch failure (Rood *et al*., 2000). Regarding their trunks, the alteration of their hydraulic properties due to less plasticity leads to interrupting the water supply to all trunks' neighboring segments (Domec *et al*., 2012). Thus, possible hydraulic failure in conductive tissues, related to both water supply conditions and xylem anatomical characteristics (López–Bernal *et al*., 2010), causes the surface temperature of the tree trunk to fluctuate (Burcham *et al*., 2012) and reflects tree health. IRT can detect these fluctuations, indicating potential disturbances, when temperature distribution is uneven, or a

healthy state when surface temperature is homogenous (Omran, 2017; Catena and Catena, 2008). In our case, the exported thermal variables allowed the reliable detection of SDV, while their association with other significant phenotypic traits provided critical insights into the conservation state of traditional olive groves.

Given the prominence of traditional olive groves both on the island of Lesvos and in other parts of Greece (Giourga *et al*., 2008), a detailed analysis regarding their productivity estimation based on both trees' phenotypic traits and their thermal properties is required. However, for productivity assessment, it is important to take into account the possible susceptibility of traditionally grown olive trees to disease infestations. In this context, we have created a suite of important features, derived from the linear and the logistic models, which can satisfactorily explain traditional olive grove dynamics.

The high explanatory nature of the four linear models, using different predictor groups, showed that the four–year average productivity of the traditional olive trees can be explained to a very high degree. This high explanatory power, as indicated by the coefficient of determination values, especially in the "architecture and vitality traits" model (R^2 = .610) and in the "combination" model (R^2 = .702), showed that there are specific features of olive trees that can disclose the variation levels of their productivity (**Table B2**). We consider this to be extremely important if one considers that parameters that would potentially enhance our models, such as slope and aspect at individual tree level, slope and aspect of terraced sites, soil nutrient content, and trees' competition levels, which were essential in other predictive models for olive tree productivity (Stateras and Kalivas, 2020), were not taken into account. The separate examination of each harvest season, although with a lower explanatory power in three out of four years, followed a similar pattern: the "architecture and vitality traits" and the "combination" models showed an explanatory power ranging from 41.5% to 60.2% (**Tables BS2–BS5**).

It is noteworthy that, even though the model based on thermal variables showed moderate interpretive power in estimating of Prmean (R^2 = .463) (**Table B2**), lower still for individual years (24.5–35.4%) (**Tables BS2–BS5**), infrared thermography appears to be a valuable method for obtaining precise data for productivity estimation. Among the extracted thermal variables, only IQR had an important contribution to Prmean in the "thermal" model, while in the "combination" model, IQR showed the third–largest unique contribution (5.4%) out of the six predictive factors. Additionally, the negative coefficient of IQR demonstrates an inverse relationship of IQR with productivity, supporting the view that a uniform tree trunk surface temperature distribution is associated with a healthy tree state and higher productivity.

The dependence of productivity from OLS severity metrics indicated a moderate to low inverse effect (R^2 = .368; **Table B2**), which strengthens the argument, also reported by MacDonald *et al*. (MacDonald *et al*., 2000), that this fungal disease is probably responsible for the reported low productivity of the infected olive trees. Indeed, by repeating the multiple linear regression with the poor condition group of trees (G3), the explanatory power of the model rises to 46.5% ($F(2, 19) = 18.41$, $p < .001$, R^2 = .465), having TIA as the only statistically significant explanatory variable in the final model. Following the same procedure for the G1 and G2 groups did not yield any significant results. The age of the G3 olive trees (300.60 ± 84.62 years) also played an important role; controlling for the effect of age, the correlation of Prmean with PIL had a negative nonsignificant coefficient ($r = -.44$; $p = .053$) and a positive nonsignificant coefficient with TIA ($r = .26$; $p = .254$).

Assessing the olive tree infection by OLS indicated that 58.75% of the studied trees were infected. The presence of fungal pathogens is difficult to control as their populations show spatiotemporal and genetic variability, depending, to a large extent, on humidity and ambient temperature, while

climate change increases the risk of infection in trees (Garrett *et al*., 2016). The logistic regression models had a high discriminatory performance and were quite informative regarding the predictors of both architecture and vitality traits and thermal variables groups, indicating that the probability of OLS infection could be predicted accurately by MCL_L and IQR. On the extremely high predicted classification accuracy of MCL_L (95.7%), trees with no symptoms presented a mean MCL_L of .98 ± .03 g/m^2, while those classified as infected had a much lower value of MCL_L (.73 ± .14 g/m^2). This differentiation occurs as the infected leaves undertake a gradual deterioration of their cytoplasmic contents, resulting in the degradation of chloroplasts and the progressive disappearance of chlorophyll (Lanza *et al*., 2017). From the standpoint of assessing OLS presence using thermal variables, it is understood that both the classification accuracy (80%) and the degree of explanatory power of the model (39%) are not ideal to suggest the use of IRT for detecting infection in olive trees. However, we must keep in mind that the examined thermal variables (IQR) (a) had a substantial difference between infected (.85 ± .38) and non–infected trees (.55 ± .13), and (b) were calculated from infrared images of the tree trunk and not from the leaves, which is the main organ that this disease affects. In addition, IRT has been proved to be a valuable method for identifying biotic stresses by analyzing temperature alterations in plant leaves (Ishimwe *et al*., 2014).

The classification of the 80 trees in three classes (G1, G2, G3) enabled tree health state categorization at a population level, as the group G1 includes olive trees that are in a good condition, G2 includes trees in an intermediate state, and group G3 contains trees which are in poor condition. Moreover, specific traits of the olive trees' groups can be adequately described, to some extent, by the extracted thermal variables, as shown by the initial examination of the relationships between them (**Figure B5**). In particular, it is noted that G1 and G3 display the lowest and highest values in all thermal variables, respectively, while G2 lies somewhere in between, except for ΔT (Table 4).

The high ΔT value of the G3 trees indicated their low temperature distance from Tamb; this means that the tree trunk has a faster response to ambient temperature indicative of hollows within the trunk where the air enters and heats the trunk surface faster. Paradoxically, regarding a particularly important thermal variable describing the actual extent of defect patches (EΔT), we did not find any statistically significant differences between the examined groups ($F(2, 77) = 2.97$, $p = .057$); this suggests that the area of any abnormalities is not as important, at least for traditional olive groves, as their intensity, described by the IQR for the whole tree and by the OPR for individual elements of the trunk. Hence, the three classes that describe the health state of olive trees (good, intermediate, poor) correspond to specific value ranges of these thermal variables. Poor condition corresponds to the highest values of the extracted thermal variables, while good condition corresponds to the lowest values.

Thus, combining the results of productivity assessment, infected trees' identification, and hierarchical classification, we can conclude that mainly IQR and secondarily OPR can be considered as indicators of olive trees' health state. The low value of these indices confirms the homogeneous temperature distribution on the tree trunk, as originally described by Catena and Catena (Catena and Catena, 2008), and identifies high values of vitality traits simultaneously with the absence of the OLS disease. Therefore, these indices are appropriate for measuring the thermal profile of each olive tree and for assessing its health state.

In conclusion, our results provide evidence for a combinatory methodological framework for traditional olive grove productivity prediction, taking into account typical phenotypic, spectral, and thermal tree traits. We further demonstrate that it is possible to detect the incidence of OLS in traditional olive groves and to classify olive trees into different health state categories using the same variables. Although infrared images did not provide the best prediction of tree productivity, nor the optimal classification for OLS incidence, nonetheless, they could give satisfactory

information for a rapid first assessment of the health and productivity of a traditional olive grove noninvasively. Combined with long–established methods and tools of assessing health and productivity, such as LAI and chlorophyll concentration, they can further improve the predictive power to a very high level. Overall, this study establishes a foundation for the design and application of appropriate management measures of traditional olive groves using a relatively simple and time–saving, but sufficiently accurate, methodology.

Appendix BS

Table BS1. Descriptive statistics for olive tree productivity for all the examined harvest years (N = 80).

Year	Pyrgi site				Agiasos site				Both sites			
	Pr (kg)	PS	US	SR	Pr (kg)	PS	US	SR	Pr (kg)	PS	US	SR
2017	53.50 ± 21.72	4.92 ± 2.54	3.6 ± 2.14	.56 ± .22	54.88 ± 21.59	4.87 ± 2.77	3.47 ± 1.58	.55 ± .19	54.19 ± 21.53	4.9 ± 2.64	3.53 ± 1.87	.55 ± .20
2018	37.12 ± 18.00	6.12 ± 2.72	3.6 ± 2.14	.62 ± .19	38.75 ± 18.21	4.95 ± 2.70	3.47 ± 1.58	.56 ± .18	37.93 ± 18.01	5.53 ± 2.76	3.53 ± 1.87	.59 ± .19
2019	38.87 ± 16.23	6.72 ± 3.29	3.6 ± 2.14	.64 ± .16	37.37 ± 21.72	7.62 ± 4.36	3.47 ± 1.58	.65 ± .17	38.12 ± 19.06	7.17 ± 3.87	3.53 ± 1.87	.64 ± .17
2020	25.32 ± 23.81	5.6 ± 4.51	3.6 ± 2.14	.61 ± .22	31.15 ± 21.52	6.52 ± 3.74	3.47 ± 1.58	.61 ± .17	28.23 ± 22.74	6.06 ± 4.14	3.53 ± 1.87	.61 ± .20

Table BS2. Final models obtained from multiple linear regression analyses for estimating productivity of 2017 harvest season. All multiple regression models were statistically significant ($p < .05$). The slope of the predictor variable for the response variable (B), the standard error for the slope (SE B), the standardized beta (β), the t–test statistic (t), the probability value (p), the squared semipartial coefficient (sr^2), the regression–adjusted coefficient for the multiple regression model (R^2), and the predictive capability of the models (F).

Variables set	Response Variable	Predictor Variables	B	SE B	β	t	p	sr^2	Adj. R^2	F
Architecture and Vitality Traits	Pr_{2017}	(constant)	66.19	6.03		10.97	.00		.418	19.93
		SDV	−490.30	182.26	−.26	−2.69	.00	.053		
		LAI_{mean}	4.21	1.24	.31	3.40	.00	.085		
		LAI_{range}	−6.11	1.75	−.33	−3.48	.00	.089		
OLS	Pr_{2017}	(constant)	60.56	2.81		21.50	.00		.246	13.921
		PIL	−43.15	8.21	−.58	−5.25	.00	.263		
		TIA	.21	.07	.32	2.92	.00	.081		
Thermal	Pr_{2017}	(constant)	79.87	4.73		16.88	.00		.306	35.91
		IQR	−35.63	5.94	−.56	−5.99	.00	.310		
Combination	Pr_{2017}	(constant)	89.66	5.83		15.37	.00		.447	13.76
		CA	−.18	.08	−.21	−2.39	.02	.040		
		LAI_{range}	−4.06	1.95	−.22	−2.08	.04	.030		

	PIL	−24.66	8.77	−.33	−2.81	.00	.055
	TIA	.23	.06	.35	3.52	.00	.086
	IQR	−19.58	6.73	−.31	−2.90	.00	.059

Table BS3. Final models obtained from multiple linear regression analyses for estimating productivity of 2018 harvest season. All multiple regression models were statistically significant ($p < .05$). The slope of the predictor variable for the response variable (B), the standard error for the slope (SE B), the standardized beta (β), the t–test statistic (t), the probability value (p), the squared semipartial coefficient (sr^2), the regression–adjusted coefficient for the multiple regression model (R^2), and the predictive capability of the models (F).

Variables set	Response Variable	Predictor Variables	B	SE B	β	t	p	sr^2	Adj. R^2	F
Architecture and Vitality Traits	Pr_{2018}	(constant)	42.71	5.01		8.51	.00		.425	20.46
		SDV	−393.50	151.61	−.25	−2.59	.01	.048		
		LAI_{mean}	4.48	1.03	.39	4.34	.00	.137		
		LAI_{range}	−4.07	1.46	−.26	−2.78	.00	.056		
OLS	Pr_{2018}	(constant)	43.17	2.41		17.88	.00		.209	11.42
		PIL	−33.6	7.04	−.54	−4.77	.00	.228		
		TIA	.15	.06	.28	2.45	.01	.060		
Thermal	Pr_{2018}	(constant)	60.97	3.82		15.96	.00		.354	44.31
		IQR	−31.96	4.80	−.60	−6.65	.00	.362		
Combination	Pr_{2018}	(constant)	35.18	7.27		4.83	.00		.464	23.80
		SR	17.84	7.82	.19	2.28	.02	.035		
		LAI_{mean}	3.64	1.00	.32	3.50	.00	.083		
		IQR	−23.5	4.85	−.44	−4.84	.00	.159		

Table BS4. Final models obtained from multiple linear regression analyses for estimating productivity of 2019 harvest season. All multiple regression models were statistically significant ($p < .05$). The slope of the predictor variable for the response variable (B), the standard error for the slope (SE B), the standardized beta (β), the t–test statistic (t), the probability value (p), the squared semipartial coefficient (sr^2), the regression–adjusted coefficient for the multiple regression model (R^2), and the predictive capability of the models (F).

Variables set	Response Variable	Predictor Variables	B	SE B	β	t	p	sr^2	Adj. R^2	F
Architecture and Vitality Traits	Pr_{2019}	(constant)	12.26	16.413		.74	.45		.415	15.03
		DBH	.18	.06	.34	3.07	.00	.070		
		CA	−.15	.07	−.20	−2.12	.03	.033		

		LAI_{range}	−7.03	1.68	−.43	−4.16	.00	.128		
		MCL_L	45.06	14.03	.39	3.21	.00	.076		
OLS	Pr_{2019}	(constant)	43.33	2.63		16.42	.00		.157	8.34
		PIL	−31.46	7.7	−.47	−4.08	.00	.178		
		TIA	.13	.07	.22	1.87	.06	.037		
Thermal	Pr_{2019}	(constant)	61.12	4.17		14.66	.00		.313	37.2
		IQR	−31.90	5.24	−.57	−6.09	.00	.322		
Combination	Pr_{2019}	(constant)	59.35	5.99		9.90	.00		.452	22.73
		LAI_{mean}	2.55	1.11	.21	2.29	.02	.036		
		LAI_{range}	−6.71	1.61	−.41	−4.17	.00	.120		
		IQR	−14.66	5.99	−.26	−2.44	.02	.041		

Table BS5. Final models obtained from multiple linear regression analyses for estimating productivity of 2020 harvest season. All multiple regression models were statistically significant ($p < .05$). The slope of the predictor variable for the response variable (B), the standard error for the slope (SE B), the standardized beta (β), the t–test statistic (t), the probability value (p), the squared semipartial coefficient (sr^2), the regression–adjusted coefficient for the multiple regression model (R^2), and the predictive capability of the models (F).

Variables Set	Response Variable	Predictor Variables	B	SE B	β	t	p	sr^2	Adj. R^2	F
Architecture and Vitality Traits	Pr_{2020}	(constant)	46.55	5.34		8.71	.00		.602	30.86
		DBH	−.39	.04	−.61	−8.46	.00	.361		
		SDV	−428.23	148.24	−.22	−2.89	.00	.042		
		LAI_{mean}	3.75	1.51	.26	2.49	.01	.031		
		TCL_T	.06	.02	.30	3.00	.00	.045		
OLS	Pr_{2020}	(constant)	40.84	2.59		15.77	.00		.407	55.26
		PIL	−50.56	6.80	−.64	−7.43	.00	.414		
Thermal	Pr_{2020}	(constant)	52.62	5.21		10.09	.00		.245	26.65
		IQR	−33.83	6.55	−.50	−5.16	.00	.255		
Combination	Pr_{2020}	(constant)	46.556	5.34		8.71	.00		.602	30.86
		DBH	−.39	.046	−.61	−8.46	.00	.361		
		SDV	−428.23	148.24	−.22	−2.89	.00	.042		
		LAI_{mean}	3.75	1.51	.26	2.49	.01	.031		
		TCL_T	.06	.02	.30	3.00	.00	.045		

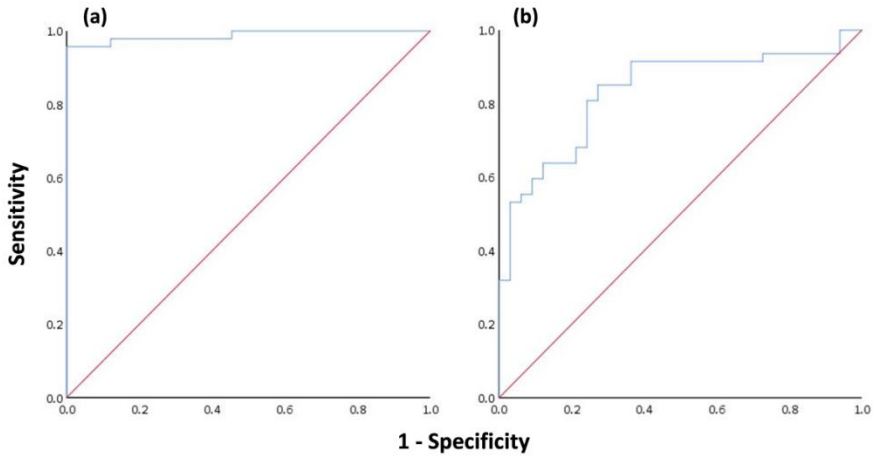

Figure BS1. The ROC curves for logistic regression models using (a) the architecture and vitality traits and (b) the thermal variables.

References

1. Altieri, M.A. Linking Ecologists and Traditional Farmers in the Search for Sustainable Agriculture. *Front. Ecol. Environ.* **2004**, *2*, 35.
2. Jarvis, D.; Brown, A.H.D.; Cuong, P.H.; Collado–Panduro, L. A global perspective of the richness and evenness. *Proc. Natl. Acad. Sci. USA* **2008**, *105*, 5326–5331.
3. Achtak, H.; Ater, M.; Oukabli, A.; Santoni, S.; Kjellberg, F.; Khadari, B. Traditional agroecosystems as conservatories and incubators of cultivated plant varietal diversity: the case of fig (*Ficus carica* L.) in Morocco. *BMC Plant Biol.* **2010**, *10*, 28–28.
4. Fischer, J.; Hartel, T.; Kuemmerle, T. Conservation policy in traditional farming landscapes. *Conserv. Lett.* **2012**, *5*, 167–175.
5. Beaufoy, G.; Jones, G. *HNV Farming in England and Wales–Findings from Three Local Projects*; EFNCP: Portree, UK, 2012; ISBN 9781902855011.
6. Plieninger, T.; Bieling, C. Resilience–Based Perspectives to Guiding High–Nature–Value Farmland through Socioeconomic Change. *Ecol. Soc.* **2013**, *18*, https://doi.org/10.5751/es–05877–180420.
7. Lomba, A.; Guerra, C.; Alonso, J.; Honrado, J.P.; Jongman, R.; McCracken, D. Mapping and monitoring High Nature Value farmlands: Challenges in European landscapes. *J. Environ. Manag.* **2014**, *143*, 140–150, https://doi.org/10.1016/j.jenvman.2014.04.029.
8. Loumou, A.; Giourga, C. Olive groves: The life and identity of the Mediterranean. *Agric. Hum. Values* **2003**, *20*, 87–95.
9. Solomou, A.; Sfougaris, A. Comparing conventional and organic olive groves in central Greece: plant and bird diversity and abundance. *Renew. Agric. Food Syst.* **2011**, *26*, 297–316.
10. Price, M. High Nature Value Farming in Europe: 35 European Countries—Experiences and Perspectives. *Mt. Res. Dev.* **2013**, *33*, 480.
11. Pointereau, P.; Paracchini, M.L.; Terres, J.–M.; Jiguet, F.; Bas, Y.; Biala, K. *Identification of High Nature Value Farmland in France through Statistical Information and Farm Practice Surveys;* Publications Office of the EU*,* Report EUR 22786 EN; 2007; ISBN 9789279064753.
12. Poláková, J.; Tucker, G.; Hart, K.; Dwyer, J.; Rayment, M. Addressing biodiversity and habitat preservation through measures applied under the Common Agricultural Policy. **2011**, Report prepared for DG Agriculture and Rural Development, Contract No. 30–CE–0388497/00–44, Institute for European Environmental Policy, London.
13. Keenleyside, C, Beaufoy, G, Tucker, G, and Jones, G. High Nature Value farming throughout EU–27 and its financial support under the CAP. 2014, Report Prepared for DG Environment, Contract No ENV B.1/ETU//0035. Institute for European Environmental Policy, London.
14. Duarte, F.; Jones, N.; Fleskens, L. Traditional olive orchards on sloping land: Sustainability or abandonment? *J. Environ. Manag.* **2008**, *89*, 86–98.
15. Henle, K.; Alard, D.; Clitherow, J.; Cobb, P.; Firbank, L.; Kull, T.; McCracken, D.; Moritz, R.F.A.; Niemelä, J.; Rebane, M.; *et al*. Identifying and managing the conflicts between agriculture and biodiversity conservation in Europe—A review. *Agric. Ecosyst. Environ.* **2008**, *124*, 60–71, doi:10.1016/j.agee.2007.09.005.
16. De Graaff, J.; Duarte, F.; Fleskens, L.; de Figueiredo, T. The future of olive groves on sloping land and ex–ante assessment of cross compliance for erosion control. *Land Use Policy* **2010**, *27*, 33–41, doi:10.1016/j.landusepol.2008.02.006.
17. De Graaff, J.; Kessler, A.; Duarte, F. Financial consequences of cross–compliance and flat–rate–per–ha subsidies: The case of olive farmers on sloping land. *Land Use Policy* **2011**, *28*, 388–394, doi:10.1016/j.landusepol.2010.08.001.
18. Lefebvre, M.; Espinosa, M.; Gomez–y–Paloma, S. *The Influence of the Common Agricultural Policy on Agricultural Landscapes*; Publications Office of the European Union: Luxembourg, 2012; doi:10.2791/94269.

19. Brandolini, P. *The Outstanding Terraced Landscape of the Terre Coastal Slopes (Eastern Liguria)*; Soldati, M.M.M.; Ed.; Springer: Cham, Switzerland, 2017; pp 235–244; ISBN 9783319261928.
20. Modica, G.; Praticò, S.; Di Fazio, S. Abandonment of traditional terraced landscape: A change detection approach (a case study in Costa Viola, Calabria, Italy). *Land Degrad. Dev.* **2017**, *28*, 2608–2622, doi:10.1002/ldr.2824.
21. Brunori, E.; Salvati, L.; Antogiovanni, A.; Biasi, R. Worrying about "vertical landscapes": Terraced olive groves and ecosystem services in marginal land in central Italy. *Sustainability* **2018**, *10*, 1164, doi:10.3390/su10041164.
22. Benton, T.G.; Vickery, J.A.; Wilson, J.D. Farmland biodiversity: Is habitat heterogeneity the key? *Trends Ecol. Evol.* **2003**, *18*, 182–188, doi:10.1016/S0169–5347(03)00011–9.
23. Hole, D.G.; Perkins, A.J.; Wilson, J.D.; Alexander, I.H.; Grice, P. V.; Evans, A.D. Does organic farming benefit biodiversity? *Biol. Conserv.* **2005**, *122*, 113–130, doi:10.1016/j.biocon.2004.07.018.
24. Fleskens, L. Conservation Scenarios for Olive Farming on Sloping Land in the Mediterranean. Doctoral Thesis. Wageningen University: Wageningen, The Netherlands, 2007; ISBN 9789085047179.
25. Caraveli, H. A comparative analysis on intensification and extensification in mediterranean agriculture: Dilemmas for LFAs policy. *J. Rural Stud.* **2000**, *16*, 231–242, doi:10.1016/S0743–0167(99)00050–9.
26. Kizos, T.; Dalaka, A.; Petanidou, T. Farmers' attitudes and landscape change: Evidence from the abandonment of terraced cultivations on Lesvos, Greece. *Agric. Human Values* **2010**, *27*, 199–212, doi:10.1007/s10460–009–9206–9.
27. Dunjó, G.; Pardini, G.; Gispert, M. Land use change effects on abandoned terraced soils in a Mediterranean catchment, NE Spain. *Catena* **2003**, *52*, 23–37, doi:10.1016/S0341–8162(02)00148–0.
28. Salvati, L.; Ferrara, C. The local–scale impact of soil salinization on the socioeconomic context: An exploratory analysis in Italy. *Catena* **2015**, *127*, 312–322, doi:10.1016/j.catena.2015.01.008.
29. Stanchi, S.; Freppaz, M.; Agnelli, A.; Reinsch, T.; Zanini, E. Properties, best management practices and conservation of terraced soils in Southern Europe (from Mediterranean areas to the Alps): A review. *Quat. Int.* **2012**, *265*, 90–100, doi:10.1016/j.quaint.2011.09.015.
30. International Olive Council. *Production Techniques in Olive Growing*; IOC: Madrid, Spain, 2007; ISBN 9788493166366.
31. Tartaglini, N.; Calabrese, G.J. Servadei, L. Ancient olive orchards as high nature value farmland; a shared vision at euro–mediterranean level. In *A Multi–Scale and Multi–Level Approach for Conservation of Ancient Olive Orchards in the Euro–Mediterranean Region*; La Posta, A., Lacirignola, C., Mimiola, G., Eds.; CIHEAM Mediterranean Agronomic Institute: Bari, Italy, 2012; pp. 27–39.
32. Beaufoy, G. *Olives Ecosystems and Biodiversity—Considerations for Action in the EU*; IOC: Madrid, Spain, 2009; p. 26.
33. Zhang, J. Multi–source remote sensing data fusion: Status and trends. *Int. J. Image Data Fusion* **2010**, *1*, 5–24, doi:10.1080/19479830903561035.
34. Hansen, M.C.; Stehman, S.V.; Potapov, P.V.; Loveland, T.R.; Townshend, J.R.G.; DeFries, R.S.; Pittman, K.W.; Arunarwati, B.; Stolle, F.; Steininger, M.K.; *et al*. Humid tropical forest clearing from 2000 to 2005 quantified by using multitemporal and multiresolution remotely sensed data. *Proc. Natl. Acad. Sci. USA* **2008**, *105*, 9439–9444.
35. Eva, H.; Carboni, S.; Achard, F.; Stach, N.; Durieux, L.; Faure, J.F.; Mollicone, D. Monitoring forest areas from continental to territorial levels using a sample of medium spatial resolution satellite imagery. *ISPRS J. Photogramm. Remote Sens.* **2010**, *65*, 191–197, doi:10.1016/j.isprsjprs.2009.10.008.
36. Huang, Y.; Ren, Z.; Li, D.; Liu, X. Phenotypic techniques and applications in fruit trees: A review. *Plant Methods* **2020**, *16*, 1–22, doi:10.1186/s13007–020–00649–7.

37. Di Nisio, A.; Adamo, F.; Acciani, G.; Attivissimo, F. Fast detection of olive trees affected by xylella fastidiosa from uavs using multispectral imaging. *Sensors* **2020**, *20*, 4915, doi:10.3390/s20174915.
38. Castrignanò, A.; Belmonte, A.; Antelmi, I.; Quarto, R.; Quarto, F.; Shaddad, S.; Sion, V.; Muolo, M.R.; Ranieri, N.A.; Gadaleta, G.; *et al*. Semi–automatic method for early detection of xylella fastidiosa in olive trees using uav multispectral imagery and geostatistical–discriminant analysis. *Remote Sens.* **2021**, *13*, 14, doi:10.3390/rs13010014.
39. Blekos, K.; Tsakas, A.; Xouris, C.; Evdokidis, I.; Alexandropoulos, D.; Alexakos, C.; Katakis, S.; Makedonas, A.; Theoharatos, C.; Lalos, A. Analysis, modeling and multi–spectral sensing for the predictive management of verticillium wilt in olive groves. *J. Sens. Actuator Netw.* **2021**, *10*, 15, doi:10.3390/jsan10010015.
40. Berry, J.K.; Delgado, J.A.; Khosla, R.; Pierce, F. Precision Conservation for Environmental Sustainability. *J. Soil Water Conserv.* **2003**, *10*, 1–26.
41. Berry, J.K.; Delgado, J.A.; Pierce, F.J.; Khosla, R. Applying spatial analysis for precision. *J. Soil Water Conserv.* **2005**, *60*, 363–370.
42. Delgado, J.A.; Berry, J.K. Advances in Precision Conservation. *Adv. Agron.* **2008**, *98*, 1–44, doi:10.1016/S0065–2113(08)00201–0.
43. Ouis, D. Non Destructive Techniques for Detecting Decay in Standing Trees. *Arboric. J.* **2003**, *27*, 159–177, doi:10.1080/03071375.2003.9747371.
44. Ishimwe, R.; Abutaleb, K.; Ahmed, F. Applications of Thermal Imaging in Agriculture—A Review. *Adv. Remote Sens.* **2014**, *3*, 128–140, doi:10.4236/ars.2014.33011.
45. Dragavtsev, V.; Nartov, V.P. Application of Thermal Imaging in Agriculture and Forestry. *Eur. Agrophys. J.* **2015**, *2*, 15, doi:10.17830/j.eaj.2015.01.015.
46. Still, C.; Powell, R.; Aubrecht, D.; Kim, Y.; Helliker, B.; Roberts, D.; Richardson, A.D.; Goulden, M. Thermal imaging in plant and ecosystem ecology: applications and challenges. *Ecosphere* **2019**, *10*, doi:10.1002/ecs2.2768.
47. Vadivambal, R.; Jayas, D.S. Applications of Thermal Imaging in Agriculture and Food Industry–A Review. *Food Bioprocess Technol.* **2011**, *4*, 186–199, doi:10.1007/s11947–010–0333–5.
48. Chaerle, L.; Van Caeneghem, W.; Messens, E.; Lambers, H.; Van Montagu, M.; Van Der Straeten, D. Presymptomatic visualization of plant–virus interactions by thermography. *Nat. Biotechnol.* **1999**, *17*, 813–816, doi:10.1038/11765.
49. Chaerle, L.; De Boever, F.; Van Montagu, M.; Van der Straeten, D. Thermographic visualization of cell death in tobacco and Arabidopsis. *Plant Cell Environ.* **2001**, *24*, 15–25, doi:10.1046/j.1365–3040.2001.00654.x.
50. Lenthe, J.H.; Oerke, E.C.; Dehne, H.W. Digital infrared thermography for monitoring canopy health of wheat. *Precis. Agric.* **2007**, *8*, 15–26, doi:10.1007/s11119–006–9025–6.
51. Agam, N.; Cohen, Y.; Berni, J.A.J.; Alchanatis, V.; Kool, D.; Dag, A.; Yermiyahu, U.; Ben–Gal, A. An insight to the performance of crop water stress index for olive trees. *Agric. Water Manag.* **2013**, *118*, 79–86, doi:10.1016/j.agwat.2012.12.004.
52. Struthers, R.; Ivanova, A.; Tits, L.; Swennen, R.; Coppin, P. Thermal infrared imaging of the temporal variability in stomatal conductance for fruit trees. *Int. J. Appl. Earth Obs. Geoinf.* **2015**, *39*, 9–17, doi:10.1016/j.jag.2015.02.006.
53. Egea, G.; Padilla–Díaz, C.M.; Martinez–Guanter, J.; Fernández, J.E.; Pérez–Ruiz, M. Assessing a crop water stress index derived from aerial thermal imaging and infrared thermometry in super–high density olive orchards. *Agric. Water Manag.* **2017**, *187*, 210–221, doi:10.1016/j.agwat.2017.03.030.
54. Oerke, E.C.; Fröhling, P.; Steiner, U. Thermographic assessment of scab disease on apple leaves. *Precis. Agric.* **2011**, *12*, 699–715, doi:10.1007/s11119–010–9212–3.
55. Ouledali, S.; Ennajeh, M.; Zrig, A.; Gianinazzi, S.; Khemira, H. Estimating the contribution of arbuscular mycorrhizal fungi to drought tolerance of potted olive trees (*Olea europaea*). *Acta Physiol. Plant.* **2018**, *40*, 1–13, doi:10.1007/s11738–018–2656–1.

56. Catena, A.; Catena, G. Overview of thermal imaging for tree assessment. *Arboric. J.* **2008**, *30*, 259–270, doi:10.1080/03071375.2008.9747505.
57. Guo, Y.Y.; Yu, H.Y.; Kong, D.S.; Yan, F.; Zhang, Y.J. Effects of drought stress on growth and chlorophyll fluorescence of Lycium ruthenicum Murr. seedlings. *Photosynthetica* **2016**, *54*, 524–531, doi:10.1007/s11099–016–0206–x.
58. Wang, J.; Wang, T.; Shi, T.; Wu, G.; Skidmore, A.K. A wavelet–based area parameter for indirectly estimating copper concentration in Carex leaves from canopy reflectance. *Remote Sens.* **2015**, *7*, 15340–15360, doi:10.3390/rs71115340.
59. Obeidat, W.; Avila, L.; Earl, H.; Lukens, L. Leaf spectral reflectance of maize seedlings and its relationship to cold tolerance. *Crop Sci.* **2018**, *58*, 2569–2580, doi:10.2135/cropsci2018.02.0115.
60. Li, W.; Sun, Z.; Lu, S.; Omasa, K. Estimation of the leaf chlorophyll content using multiangular spectral reflectance factor. *Plant. Cell Environ*. **2019**, 42, 3152–3165.
61. Ali, M.M.; Al–Ani, A.; Eamus, D.; Tan, D.K.Y. Leaf nitrogen determination using non–destructive techniques—A review. *J. Plant Nutr.* **2017**, *40*, 928–953, doi:10.1080/01904167.2016.1143954.
62. Steele, M.; Gitelson, A.A.; Rundquist, D. Nondestructive estimation of leaf chlorophyll content in grapes. *Am. J. Enol. Vitic.* **2008**, *59*, 299–305.
63. Pavlovic, D.; Nikolic, B.; Djurovic, S.; Waisi, H.; Andjelkovic, A.; Marisavljevic, D. Chlorophyll as a measure of plant health: Agroecological aspects. *Pestic. Fitomed.* **2014**, *29*, 21–34, doi:10.2298/pif1401021p.
64. Almansoori, T.; Salman, M.; Aljazeri, M. Rapid and nondestructive estimations of chlorophyll concentration in date palm (*Phoenix dactylifera* L.) leaflets using SPAD–502+ and CCM–200 portable chlorophyll meters. *Emir. J. Food Agric.* **2021**, *33*, 532–543, doi:10.9755/ejfa.2021.v33.i7.2723.
65. Richardson, A.D.; Duigan, S.P.; Berlyn, G.P. An evaluation of noninvasive methods to estimate foliar chlorophyll content. *New Phytol.* **2002**, *153*, 185–194, doi:10.1046/j.0028–646X.2001.00289.x.
66. Mishra, K.B.; Mishra, A.; Klem, K.; Govindjee Plant phenotyping: A perspective. *Indian J. Plant Physiol.* **2016**, *21*, 514–527, doi:10.1007/s40502–016–0271–y.
67. Sánchez–Reinoso, A.D.; Ligarreto–Moreno, G.A.; Restrepo–Díaz, H. Drought–tolerant common bush bean physiological parameters as indicators to identify susceptibility. *HortScience* **2019**, *54*, 2091–2098, doi:10.21273/HORTSCI14436–19.
68. Villalobos, F.J.; Testi, L.; Hidalgo, J.; Pastor, M.; Orgaz, F. Modelling potential growth and yield of olive (*Olea europaea* L.) canopies. *Eur. J. Agron.* **2006**, *24*, 296–303, doi:10.1016/j.eja.2005.10.008.
69. Pelil, P.; Biradar, P.; Bhagawathi, A.U.; Hejjigar, I.S. Area Index of horticulture crops and its importance. *Int. J. Curr. Microbiol. Appl. Sci.* **2018**, *7*, 505–513.
70. Kosmas, C.; Danalatos, N.G.; Poesen, J.; Van Wesemael, B. The effect of water vapour adsorption on soil moisture content under Mediterranean climatic conditions. *Agric. Water Manag.* **1998**, *36*, 157–168, doi:10.1016/S0378–3774(97)00050–4.
71. Marathianou, M.; Kosmas, C.; Gerontidis, S.; Detsis, V. Land–use evolution and degradation in Lesvos (Greece): A historical approach. *Land Degrad. Dev.* **2000**, *11*, 63–73, doi:10.1002/(SICI)1099–145X(200001/02)11:1<63::AID–LDR369>3.0.CO;2–8.
72. Paracchini, M.L.; Petersen, J.–E.; Hoogeveen, Y.; Bamps, C.; Burfield, I.; Van Swaay, C. *High Nature Value Farmland in Europe—An Estimate of the Distribution Patterns on the Basis of Land Cover and Biodiversity Data*; European Comission: Luxembourg, 2008; ISBN 9789279095689.
73. European Environment Agency (EEA). Corine land cover. Available online: https://land.copernicus.eu/pan–european/corine–land–cover/clc–2012 (accessed on 10/09/2017)
74. European Environment Agency (EEA) Tree cover density. Available online: https://land.copernicus.eu/pan–european/high–resolution–layers/forests/tree–cover–density (accessed on 10/09/2017)

75. European Environment Agency (EEA). Dominant leaf type. Available online: https://land.copernicus.eu/pan–european/high–resolution–layers/forests/dominant–leaf–type (accessed on 10/09/2017).
76. Pretzsch, H.; Biber, P.; Uhl, E.; Dahlhausen, J.; Rötzer, T.; Caldentey, J.; Koike, T.; van Con, T.; Chavanne, A.; Seifert, T.; *et al*. Crown size and growing space requirement of common tree species in urban centres, parks, and forests. *Urban For. Urban Green.* **2015**, *14*, 466–479, doi:10.1016/j.ufug.2015.04.006.
77. Ryan, M. G.; Binkley, D.; Fownes, J.H. Age–related decline in forest productivity: pattern and process. *Adv. Ecol. Res.* **1997**, *27*, 213–262.
78. Fabbri, A.; Bartolini, G.; Lambardi, M.; Kailis, S.G. *Olive Propagation Manual*; CSIRO Publishing: Collingwood, VA, Australia 2004; ISBN 0–643–06676–4.
79. Cherubini, P.; Gartner, B.L.; Tognetti, R.; Bräker, O.U.; Schoch, W.; Innes, J.L. Identification, measurement and interpretation of tree rings in woody species from mediterranean climates. *Biol. Rev. Camb. Philos. Soc.* **2003**, *78*, 119–148, doi:10.1017/S1464793102006000.
80. Arnan, X.; López, B.C.; Martínez–Vilalta, J.; Estorach, M.; Poyatos, R. The age of monumental olive trees (*Olea europaea*) in northeastern Spain. *Dendrochronologia* **2012**, *30*, 11–14, doi:10.1016/j.dendro.2011.02.002.
81. Parry, C.; Blonquist, J.M.; Bugbee, B. In situ measurement of leaf chlorophyll concentration: Analysis of the optical/absolute relationship. *Plant Cell Environ.* **2014**, *37*, 2508–2520, doi:10.1111/pce.12324.
82. Nauš, J.; Prokopová, J.; Řebíček, J.; Špundová, M. SPAD chlorophyll meter reading can be pronouncedly affected by chloroplast movement. *Photosynth. Res.* **2010**, *105*, 265–271, doi:10.1007/s11120–010–9587–z.
83. Masmoudi–Charfi, C.; Ben Mechlia, N. Characterization of young olive trees growth during the first six years of cultivation. *Adv. Hortic. Sci.* **2007**, *21*, 116–124, doi:10.1400/76211.
84. Salman, M. Biological control of Spilocaea oleagina, the causal agent of olive leaf spot disease, using antagonistic bacteria. *J. Plant Pathol.* **2017**, *99*, 741–744, doi:10.4454/jpp.v99i3.3958.
85. Obanor, F.O.; Jaspers, M. V.; Jones, E.E.; Walter, M. Greenhouse and field evaluation of fungicides for control of olive leaf spot in New Zealand. *Crop Prot.* **2008**, *27*, 1335–1342, doi:10.1016/j.cropro.2008.04.007.
86. Sanei, S.J.; Razavi, S.E. Survey of Spilocaea oleagina, causal agent of olive leaf spot, in North of Iran. *J. Yeast Fungal Res.* **2011**, *2*, 33–38, doi:10.5897/jyfr11.004.
87. Minkina, W.; Dudzik, S. *Infrared Thermography: Errors and Uncertainties*; John Wiley & Sons, Ltd.: Chichester, UK, 2009; ISBN 9780470747186.
88. Briscoe, N.J.; Handasyde, K.A.; Griffiths, S.R.; Porter, W.P.; Krockenberger, A.; Kearney, M.R. Tree–hugging koalas demonstrate a novel thermoregulatory mechanism for arboreal mammals. *Biol. Lett.* **2014**, *10*, doi:10.1098/rsbl.2014.0235.
89. Idso, S.B.; Reginato, R.J.; Jackson, R.D.; Pinter, P.J. Measuring yield–reducing plant water potential depressions in wheat by infrared thermometry. *Irrig. Sci.* **1981**, *2*, 205–212, doi:10.1007/BF00258374.
90. Zuur, A.F.; Ieno, E.N.; Elphick, C.S. A protocol for data exploration to avoid common statistical problems. *Methods Ecol. Evol.* **2010**, *1*, 3–14, doi:10.1111/j.2041–210x.2009.00001.x.
91. Youden, W.J. Index for rating diagnostic tests. *Cancer* **1950**, *3*, 32–35, doi:10.1002/1097–0142(1950)3:1<32::AID–CNCR2820030106>3.0.CO;2–3.
92. Lo Bianco, R.; Proietti, P.; Regni, L.; Caruso, T. Planting systems for modern olive growing: Strengths and weaknesses. *Agric.* **2021**, *11*, 494, doi:10.3390/agriculture11060494.
93. Ozturk, M.; Altay, V.; Gönenç, T.M.; Unal, B.T.; Efe, R.; Akçiçek, E.; Bukhari, A. An overview of olive cultivation in Turkey: Botanical features, eco–physiology and phytochemical aspects. *Agronomy* **2021**, *11*, 295, doi:10.3390/agronomy11020295.
94. Fernandez Escobar, R.; de la Rosa, R.; Leon, L.; Gomez, J.A.; Testi, F.; Orgaz, M.; Gil–Ribes, J.A.; Quesada–Moraga, E.; Trapero, A. Evolution and sustainability of the olive production systems.

In Present and Future of the Mediterranean Olive Sector; Arcas, N., Arroyo López, F.N., Caballero, J., D'Andria, R., Fernández, M., Fernandez, E.R., Garrido, A., López–Miranda, J., Msallem, M., Parras, M., *et al*., Eds.; CIHEAM/IOC: Zaragoza, Spain, 2013; pp. 11–42.
95. Paoletti, A.; Rosati, A.; Famiani, F. Effects of cultivar, fruit presence and tree age on whole–plant dry matter partitioning in young olive trees. *Heliyon* **2021**, *7*, e06949, doi:10.1016/j.heliyon.2021.e06949.
96. Sola–Guirado, R.R.; Castillo–Ruiz, F.J.; Jiménez–Jiménez, F.; Blanco–Roldan, G.L.; Castro–Garcia, S.; Gil–Ribes, J.A. Olive actual "on year" yield forecast tool based on the tree canopy geometry using UAS imagery. *Sensors* **2017**, *17*, 1743, doi:10.3390/s17081743.
97. Stateras, D.; Kalivas, D. Assessment of olive tree canopy characteristics and yield forecast model using high resolution uav imagery. *Agriculture* **2020**, *10*, 385, doi:10.3390/agriculture10090385.
98. Lavee, S. Biennial bearing in olive (*Olea europaea*). *Annales* **2007**, *17*, 102–112.
99. Sofo, A.; Manfreda, S.; Fiorentino, M.; Dichio, B.; Xiloyannis, C. The olive tree: A paradigm for drought tolerance in Mediterranean climates. *Hydrol. Earth Syst. Sci.* **2008**, *12*, 293–301, doi:10.5194/hess–12–293–2008.
100. Chartzoulakis, K.; Patakas, A.; Bosabalidis, A.M. Changes in water relations, photosynthesis and leaf anatomy induced by intermittent drought in two olive cultivars. *Environ. Exp. Bot.* **1999**, *42*, 113–120, doi:10.1016/S0098–8472(99)00024–6.
101. Gargouri, K.; Bentaher, H.; Rhouma, A. A novel method to assess drought stress of olive tree. *Agron. Sustain. Dev.* **2012**, *32*, 735–745, doi:10.1007/s13593–011–0078–1.
102. Liu, Y.; Gong, W.; Xing, Y.; Hu, X.; Gong, J. Estimation of the forest stand mean height and aboveground biomass in Northeast China using SAR Sentinel–1B, multispectral Sentinel–2A, and DEM imagery. ISPRS *J. Photogramm. Remote Sens*. **2019**, 151, 277–289, doi:10.1016/j.isprsjprs.2019.03.016.
103. Heege, H.J. (Ed.) *Precision in Crop Farming*; Springer: Dordrecht, The Netherlands, 2013; ISBN 978–94–007–6759–1.
104. Čermák, J.; Gašpárek, J.; De Lorenzi, F.; Jones, H.G. Stand biometry and leaf area distribution in an old olive grove at Andria, southern Italy. *Ann. For. Sci.* **2007**, *64*, 491–501, doi:10.1051/forest:2007026.
105. Mezghani, M.A.; Hassouna, G.; Ibtissem, L.; Labidi, F. Leaf area index and light distribution in olive tree canopies (*Olea europaea* L.). *Int. J. Agron. Agric. Res.* **2016**, *8*, 60–65, doi:10.13140/RG.2.1.3193.5600.
106. Johnson, D.M.; Wortemann, R.; McCulloh, K.A.; Jordan–Meille, L.; Ward, E.; Warren, J.M.; Palmroth, S.; Domec, J.C. A test of the hydraulic vulnerability segmentation hypothesis in angiosperm and conifer tree species. *Tree Physiol.* **2016**, *36*, 983–993, doi:10.1093/treephys/tpw031.
107. Van Hees, A.F.M. Growth and morphology of pedunculate oak (*Quercus robur* L) and beech (*Fagus sylvatica* L) seedlings in relation to shading and drought. *Ann. Sci. For.* **1997**, *54*, 9–18, doi:10.1051/forest:19970102.
108. Rood, S.B.; Patiño, S.; Coombs, K.; Tyree, M.T. Branch sacrifice: Cavitation–associated drought adaptation of riparian cottonwoods. *Trees Struct. Funct.* **2000**, *14*, 248–257, doi:10.1007/s004680050010.
109. Domec, J.C.; Lachenbruch, B.; Pruyn, M.L.; Spicer, R. Effects of age–related increases in sapwood area, leaf area, and xylem conductivity on height–related hydraulic costs in two contrasting coniferous species. *Ann. For. Sci.* **2012**, *69*, 17–27, doi:10.1007/s13595–011–0154–3.
110. López–Bernal, Á.; Alcántara, E.; Testi, L.; Villalobos, F.J. Spatial sap flow and xylem anatomical characteristics in olive trees under different irrigation regimes. *Tree Physiol.* **2010**, *30*, 1536–1544, doi:10.1093/treephys/tpq095.
111. Burcham, D.C.; Leong, E.C.; Fong, Y.K.; Tan, P.Y. An evaluation of internal defects and their effect on trunk surface temperature in *Casuarina equisetifolia* L. (Casuarinaceae). *Arboric. Urban For.* **2012**, *38*, 277–286, doi:10.48044/jauf.2012.037.

112. Omran, E.S.E. Early sensing of peanut leaf spot using spectroscopy and thermal imaging. *Arch. Agron. Soil Sci.* **2017**, *63*, 883–896, doi:10.1080/03650340.2016.1247952.
113. Giourga, C.; Loumou, A.; Tsevreni, I.; Vergou, A. Assessing the sustainability factors of traditional olive groves on Lesvos Island, Greece (Sustainability and traditional cultivation). *GeoJournal* **2008**, *73*, 149–159, doi:10.1007/s10708–008–9195–z.
114. MacDonald, A.J.; Walter, M.; Trought, M.C.; Frampton, C.M.; Burnip, G. Survey of olive leaf spot in New Zealand. *N. Z. Plant Prot.* **2000**, *53*, 126–132, doi:10.30843/nzpp.2000.53.3664.
115. Garrett, K.A.; Nita, M.; Wolf, E.D.D.; Gomez, L.; Sparks, A.H. *Plant Pathogens as Indicators of Climate Change*, 1st ed.; Elsevier: Amsterdam, The Netherlands, 2016; ISBN 9780444533012.
116. Lanza, B.; Ragnelli, A.M.; Priore, M.; Aimola, P. Morphological and histochemical investigation of the response of *Olea europaea* leaves to fungal attack by Spilocaea oleagina. *Plant Pathol.* **2017**, *66*, 1239–1247, doi:10.1111/ppa.12671.

C. Investigating the effect of resin collection and detecting fungal infection in resin-tapped and non-tapped pine trees, using minimally invasive and non-invasive diagnostics

Abstract

In pine stands systematic harvesting of forest products, such as resin extraction, are known to affect trees' vitality and consequently their response to fungal diseases. The latter constitutes a serious threat for standing vigorous trees, thus early warning signals and short diagnosis time of fungal pathogens, are crucial for designing effective forest management practices. In this study, we explored the effects of the resin extraction process, which was one of the most prominent economic traditional activities throughout the Mediterranean region, on the pines' growth, and detected fungal presence in resin-tapped and non-tapped pine trees. For this, we obtained phenotypic information from 333 resin-tapped and 163 non-tapped Pinus brutia trees, in 20 forest stands, on the island of Lesvos, Greece, by combining in-situ minimally invasive (tree coring) and non-invasive diagnostics (infrared thermography), with the trees' phenotypic traits and indices. In each stand, tree cores were extracted from 34% of the total trees, while the fungal presence was confirmed (a) by the discoloration and decay patterns in the tree cores, (b) by external indicators of decay, such as fruiting bodies, and (c) by the sudden change in boring resistance during the tree cores' extraction. To evaluate the effect of resin tapping on pines' growth, we developed hierarchical multiple linear regression models controlling parameters related to pines' phenotypic traits, while for estimating the fungal presence, we used a set of logistic regression models. The results indicated that the number of tapping scars on the pines' trunk surface, resulting from the resin extraction process, explained the decrease of (a) the average annual growth of the pines by 9.2%, (b) the annual growth after the resin extraction process by 11.7%, while the explanatory power increased to 19% in the trees with a low ratio of their resin extraction age to their total age. The fungal presence was successfully classified (a) in 91.5% of the resin-tapped cases we examined, and (b) in 94.9% of the resin-tapped and non-tapped trees when combining the trees' phenotypic traits and indices with non-invasive diagnostics. These findings may contribute in monitoring forest stand dynamics in order to prevent or mitigate their degradation, and also towards effective management plans concerning the resin extraction in Greece.

Keywords

Pinus brutia, infrared thermography, hemispherical imaging, tree coring, fungal detection

C. List of Tables

C. List of Figures

C.1 Introduction

Forest ecosystems are of major importance for humankind, due to the fact that they provide a variety of ecosystem functions and services (Gamfeldt *et al.*, 2013; Brockerhoff *et al.*, 2017; Mori *et al.*, 2017) and also because of their regulating and supporting role towards biodiversity conservation in general (Watson *et al.*, 2018). However, as in any other ecosystem, they are already experiencing the effects of several major perturbations resulting from climatic alterations (Ameztegui *et al.*, 2018; Li *et al.*, 2018; Jandl *et al.*, 2019; Morecroft *et al.*, 2019), as their life expectancy does not allow them to adapt quickly to changes in environmental conditions (Ogawa-Onishi *et al.*, 2010; Gilliam, 2016; Bisbing *et al.*, 2021), with better-documented those in species phenology (Xie *et al.*, 2018; Chen *et al.*, 2019; Piao *et al.*, 2019), distribution (Dyderski *et al.*, 2018; Peterson *et al.*, 2019), and physiology (Holopainen *et al.*, 2018; Morin *et al.*, 2018; Lahive *et al.*, 2019). At the same time, forests are particularly vulnerable to several biotic (e.g. fungi, bacteria, insects, parasitic plants) and abiotic (e.g. pesticides/herbicides, soil conditions, water availability) stresses recurring throughout their life (Boa, 2003; Teshome *et al.*, 2020); their interaction (Anderegg *et al.*, 2015) along with the increasing frequency and severity of extreme weather events (IPCC, 2018), can potentially lead to changes in the availability of natural resources (Brown *et al.*, 2011; Siry *et al.*, 2018), diversification of forest areas (Nerfa *et al.*, 2020), and reduction of their productivity and their regeneration (Walmsley *et al.*, 2009; Pretzsch, Biber, Uhl, and Dauber, 2015; Gardner *et al.*, 2019).

The combination of these disruptions can be amplified by the already existing and well-known anthropogenic pressures, such as overgrazing (Hao *et al.*, 2018), increasing demand for timber (Piponiot *et al.*, 2019; Zhang *et al.*, 2020), and chronic harvesting of non-timber forest products (Lopez-Toledo *et al.*, 2018; Tieminie *et al.*, 2021). In particular, harvesting of non-timber forest products (e.g. bark, fruit, leaves, latex, resin) is generally considered less harmful with little or no ecological impact to forest ecosystems, since it does not drive to instant tree mortality (Ticktin, 2004). However, excessive exploitation of these detachable products, may change the forests' biological processes (Gaoue and Ticktin, 2008; Gaoue *et al.*, 2013), directly affecting tree physiology and forest structure, by mainly altering the trees' survival, reproduction, and growth rates (Ticktin, 2004; Endress *et al.*, 2006). In parallel, there are indirect effects with most important, the susceptibility of trees to pathogens and pests spread (Matsuhashi *et al.*, 2020). In any case, the number of invasive fungal pathogens in Europe has increased exponentially (Santini and Battisti, 2019; Prospero *et al.*, 2021), over the last four decades, with fungal infections being considered as the leading causes of infectious diseases in forest trees. Controlling fungal pathogens is difficult due to spatiotemporal and genetic variability of their populations, while climate change increases the risk of infection in forest trees (Garrett *et al.*, 2016). Altogether, these factors affect the trees by reducing their growth (Papadopoulos, 2013) and leading to an increase in their mortality (Camarero *et al.*, 2018).

One of the most important, but at the same time, less studied non-timber forest products, in terms of the impact that its harvest has on both the growth of trees and the possibility of pathogens and pests infestation, is oleoresin. Oleoresin, or simply called resin, a complex mixture of terpenoids, constitutes the most important and complex ecological, chemical, and physical defense mechanism of conifers (Trapp and Croteau, 2001; Piponiot *et al.*, 2019; Garcia-Forner *et al.*, 2021) (Trapp and Croteau, 2001; Rodrigues-Corrêa *et al.*, 2012; Garcia-Forner *et al.*, 2021); its extraction was considered a traditional forest activity with a major economic role (Palma *et al.*, 2016) especially for Mediterranean countries (Calama Sainz *et al.*, 2011; Papadopoulos, 2013). As with any other defensive trait, resin synthesis, production, transport, and maintenance has a particular metabolic cost and probably an allocation cost for the pines; terpenoids compounds are the most energetically expensive defensive metabolites (Gershenzon, 1994) competing especially with pines' growth and secondary metabolism (Züst and Agrawal, 2017). This cost has been studied in a variety of different

conifer species by investigating resin extraction's effect on trees' growth rate, with somewhat contradictory results either positive (Magnuszewski and Tomusiak, 2013; van der Maaten *et al.*, 2017) or negative (Papadopoulos, 2013; Génova *et al.*, 2014; Chen *et al.*, 2015; Rodríguez-García *et al.*, 2016; Zeng *et al.*, 2021), while others report that there is no significant effect either on the trees' growth or on their ability to respond to possible environmental changes (Williams, 2017; Du *et al.*, 2021). These contradictory and ambiguous results may be due to the different number of the extracted cores or cross-sections (disks) analyzed per tree, the tapping methods used from the resin collectors, the ratio of the resin-tapped to non-tapped trees, and the different pine species which were studied (*P. pinaster, P. halepensis, P. tabuliformis, P. massoniana, P. sylvestris, P. elliottii*). This, combined with the conifers' resin canals phenotypic and intraspecific genetic variation (Moreira *et al.*, 2015; Vázquez-González *et al.*, 2019) as well as the small number of studies available so far, does not allow a safe conclusion to be drawn on the question of whether and how exactly resin affects tree growth.

At the same time, this ecological defense trait against herbivores and pathogens predation (Phillips and Croteau, 1999; Cheng *et al.*, 2007) sterilizes and insulates damaged tissues ((Celedon and Bohlmann, 2019), by spreading out the oleoresin to the tree trunk, where their resin acids form a physical barrier sealing the wound and entrapping the pests (Wallin *et al.*, 2003) and their associated pathogenic fungi (Trapp and Croteau, 2001). However, when the resin extraction process is chronic or takes place on many distinct fronts of the pines' trunk, constant resin collection leaves the wound(s) exposed, resulting in creating optimal conditions that lead to the colonization of the trees' internal functional areas or non-functional tissues by fungal communities. The speed of wound occlusion (new tissue which has been generated in the outer wound area) (Shigo and Marx, 1977) depends on the size of the wound and the vitality of the particular tree. However, behind the occluded tissues, the internal area within the wound may be decayed over time, due to well-adapted fungal species to these conditions (Fay and de Berker, 2018). If the occlusion occurs quickly, then it is possible to cause only a simple discoloration on the wood. However, if the wound remains open for a longer period of time (e.g. to collect the resin) and the environmental conditions are favorable, then the exposed wood is going to be colonized by bacteria as well as fungal pathogens. The latter constitutes a serious threat regarding standing vigorous trees; it is among the leading causes of their mortality and contributes greatly to forest stands degradation.

For these reasons, effective monitoring through early warning signals and short diagnosis time of fungal pathogen presence, in resin-tapped and non-tapped trees, along with the study of the effect of resin extraction process on their growth, are crucial elements in preventing or mitigating the effects of the resin extraction process in coniferous forest stands.

In recent years, in order to obtain information on tree responses to past environmental stresses (Pedersen, 1998) and biotic and/or abiotic disturbances (Cherubini *et al.*, 2003), a variety of different plant phenotypic methodologies (Huang *et al.*, 2020) resulting from screening, evaluation, and diagnostic tools (Burcham *et al.*, 2012; Leong *et al.*, 2012; Goh *et al.*, 2018), invasive and non-invasive, along with conventional and well-established forestry techniques, have been developed. The combination of these phenotypic methods and tools, which are mainly used towards tree health estimation, can provide precise information regarding the scale and the extent of disturbances (Hartmann *et al.*, 2018), caused to tree tissues from wood decomposition (Johnstone *et al.*, 2010), and at the same time they can be used for investigating the effects of these disturbances to tree growth.

Minimally invasive methods such as dendrochronology (Tsen *et al.*, 2016) have been used extensively in tree-ring research for determining tree growth rate, age, and soundness for indirectly quantification of tree productivity and health (Kozlowski *et al.*, 2012), with the parallel detection of

wood decay at the drilling point (Goh *et al.*, 2018). In contrast, there are non-invasive phenotypic approaches and tools for monitoring the physiological, growth, development, stress, and other phenotypic traits of trees (e.g. leaf area, aboveground carbon/biomass, canopy structure) (Fahlgren *et al.*, 2015), which belong to the wider field of remote sensing (Torresan *et al.*, 2017), such as satellite datasets (Safari *et al.*, 2017; Pádua *et al.*, 2018), visible, fluorescence, hyperspectral, and infrared imaging (Humplík *et al.*, 2015). Among these modalities, infrared thermography (IRT) has the ability to accurately (a) estimate tree health state (Catena and Catena, 2008; Bellett-Travers and Morris, 2010; Vidal and Pitarma, 2019), (b) detect pests and fungal infestation in forest areas (Al-doski *et al.*, 2016; Asner *et al.*, 2018), and (c) estimate trees' structural abnormalities (Zevgolis, 2022b), while it is considered one of the most promising non-invasive techniques for stress-related responses of trees (Zevgolis *et al.*, 2022).

A synthesis of these methods can produce a comprehensive methodological framework and provide the necessary information for describing the effect of resin extraction on pines' growth as well as assessing the likelihood of fungal infestation in their trunks. In this light, the main aim of our research was to explore the effects of the resin extraction process, which was one of the most prominent economic traditional activities throughout the Mediterranean region, on pines' growth, and to detect fungal presence in resin-tapped and non-tapped pine trees. For this, we obtained phenotypic information from *Pinus brutia* trees on the island of Lesvos, Greece, combining in-situ minimal invasive (tree coring) and non-invasive (IRT) diagnostics, with the trees' phenotypic traits and indices derived from commonly used forestry techniques, in order to investigate the following objectives: (a) to examine the relations between pines' phenotypic traits with their thermal and humidity indices, (b) to quantify the effect of the wounds, resulting from the resin-extraction process, to the pines' mean annual growth, (c) to estimate the effect of all traits and indices on pines' growth, and (d) to examine if the pines' phenotypic parameters as well as their growth rate, can explain the presence of fungal pathogens.

C.2 Materials and methods

C2.1 Study area

Lesvos, the third-largest island of Greece in the north-eastern Aegean Sea, with an area of 1632.8 km², encompasses the largest Coniferous forests (*Pinus brutia* and *Pinus nigra*), among the islands of the Aegean sea (342.9 km^2), which are an ecologically important constituent of the Mediterranean flora, promoting the existence of the resin tapping activity since the beginning of the previous century (**Figure C1**). Located at the central part of the island is the densest and continuous, in terms of forest structure, *P. brutia* forest (220 km^2) (Palaiologou *et al.*, 2020) with its largest part belonging to the Natura 2000 Network. The island's climate is typical Mediterranean, characterized by cool-moist winters with a mean temperature of 9.6 °C in January, and warm-dry summers with a mean temperature of 27.0 °C in July (HNMS, 2021).

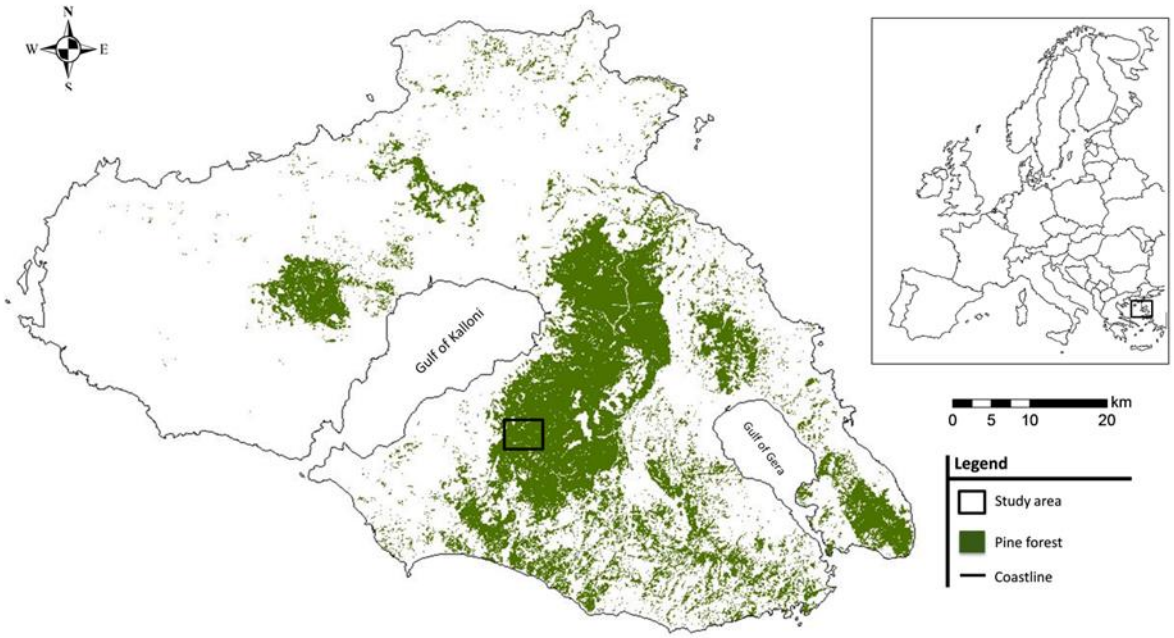

Figure C1: Map of the study area on the island of Lesvos showing the distribution of pine forests.

We randomly selected and established a total of twenty (20) forest plots of 900m^2 each (30 m x 30 m) from April to May in 2018, in a continuous and homogeneous part of the *P. brutia* forest, which was not subjected to systematic management, attempting to avoid the edge effect, grazing patches, and areas that had been logged or thinned in the previous years. All plots had a mean slope of approximately 15%, while the understory, in all plots, consisted of 45 plant species from 17 families with the predominant belonging to the families *Cistaceae*, *Fabaceae*, and *Poaceae* (pers. obs.).

C2.2 Metrics of P. brutia phenotypic traits and indices

In each stand, during the end of autumn of 2018, we documented all the *P. brutia* individuals and their phenotypic traits directly related to their architecture and vitality. All data were recorded on an inventory form, while each tree, within the 20 plots, received a unique code label for future monitoring. We recorded the typical phenotypic traits describing each tree's architectural structure and shape: (a) height (H—m), (b) diameter at breast height (DBH—cm), (c) the height at the crown base, and (d) the major and minor axes of the crown, using common forestry tools and methods (clinometer, measuring tapes, vertical sighting method) (Pretzsch, Biber, Uhl, Dahlhausen, *et al.*, 2015). Based on these traits we calculated each tree's crown area (CA—m^2) and its crown length, by

subtracting the height at the crown base from the total tree's height, in order to have an accurate estimation of each tree's crown ratio (CR). This index, resulting from the ratio of the crown length to the tree height, in addition to providing an indication of tree stability and vitality (Kontogianni *et al.*, 2011) also expresses the past cumulated competition conditions in which each individual tree grew (Soares and Tomé, 2003).

In addition, keeping in mind that trees growth is influenced by their competition with neighbouring trees during their life (Radtke *et al.*, 2003; Searle and Chen, 2020), we also calculated Hegyi's competition index (HCI) (Hegyi, 1974), one of the most popular and frequently used competing indices, which is based on the focal tree size, the tree sizes, and the distance between trees in a given stand. High values of this index equates with a high level of neighbourhood competition for the focal tree, assuming that the competition effect among the trees had not changed during the sampling period (**Figure C2**).

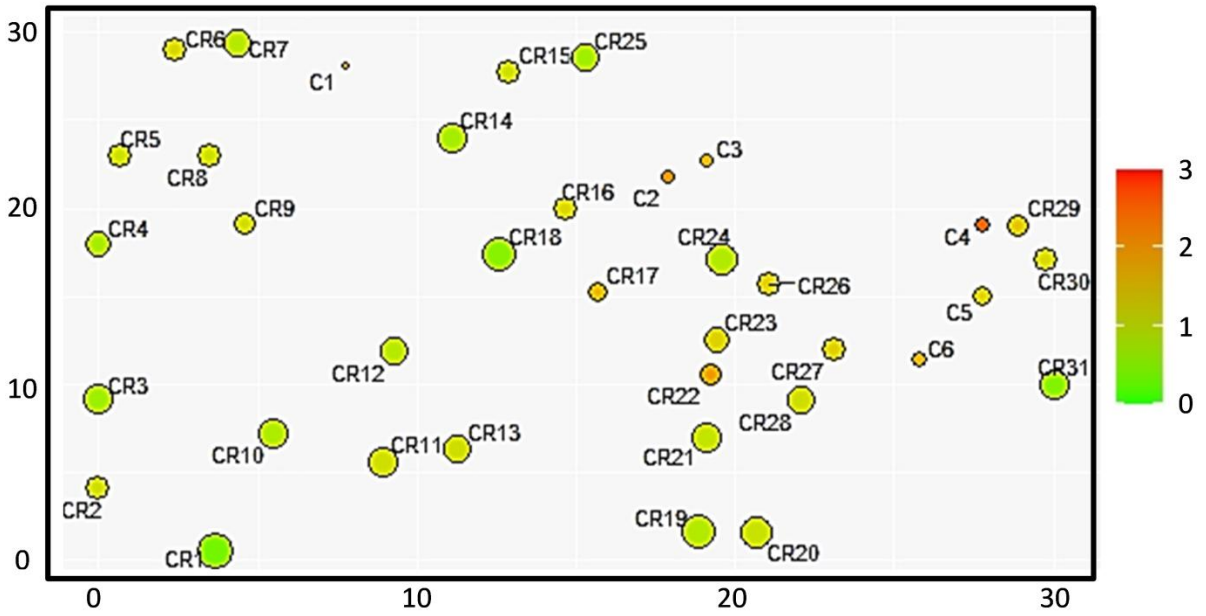

Figure C2: Sample of the spatial distribution of the *P. brutia* trees in the third plot. The trees' size is presented by the size of the circle. Larger size indicates a larger diameter. The code labels are referred to resin-tapped (with the R) and non-tapped pine trees. High values of Hegyi's index are illustrated by the red color, indicating the competition which is exerted on the specific trees.

Regarding *P. brutia* vitality, we estimated the leaf area index (LAI); LAI is an important biophysical attribute related to a variety of different ecological processes such as photosynthesis, evapotranspiration, and net primary productivity (Coops and Waring, 2001; Nakamura *et al.*, 2017). For estimating LAI, we used the hemispherical imaging method: A Canon EOS 60D camera with a wide-angle lens (hemispherical lens) was placed vertically on the trunk of each pine tree, at a height of 1.3 m from the ground, to photograph the crown area which was located both above the resin scar and the non-resinous side of the trunk (**Figure C3**). We initially processed the collected hemispherical images using the HemiView canopy image analysis software (Delta-T Devices, Cambridge, UK) in order to estimate the mean value of the leaf area index (LAI_{mean}) for the total crown of each pine. We further proceed with calculating the leaf area index for (a) the crown above the resin scar (LAI_{resin}) and above (b) the non-resin ($LAI_{non\text{-}resin}$) surface of the trunk, as well as (c) the range of LAI values for each tree (LAI_{range}). For the non-tapped pine trees we took the hemispherical images from the opposite sides of the trunk.

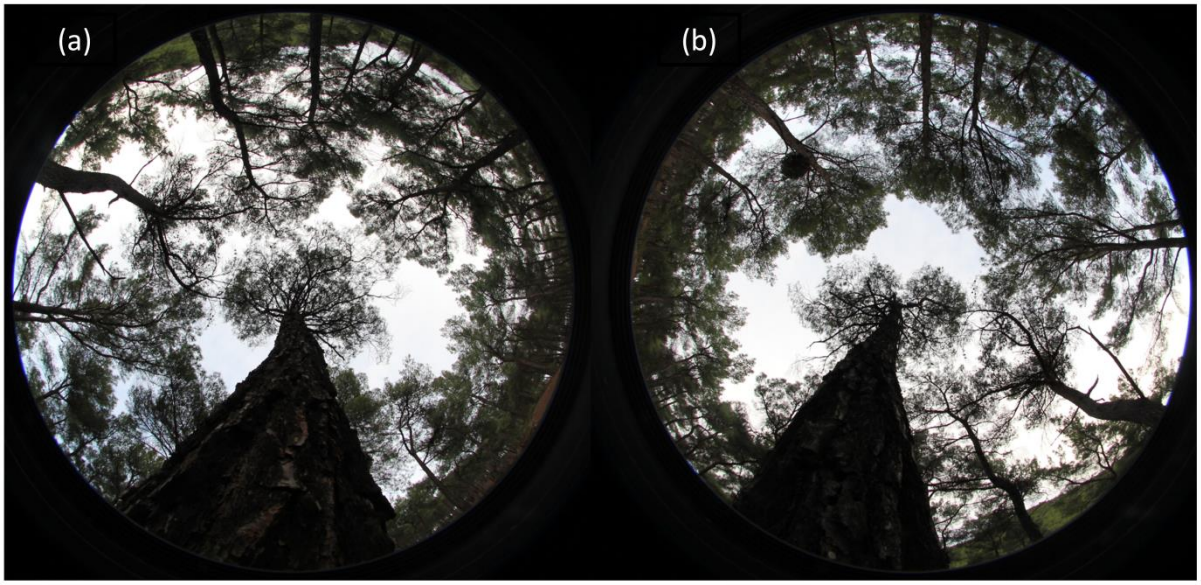

Figure C3: Sample of two hemispherical images of a *P. brutia* tree: (a) the hemispherical image from the opposite side of the scar and (b) the hemispherical image over the resin extraction area of the trunk.

Another factor of great significance, directly related to tree vitality, is the extent of the xylem and phloem tissue wounding. The effect of the "chipping method" in which the wound was created by an ax (Papadopoulos, 2013), commonly used in the island of Lesvos from the resin collectors, varied among them (Fr. E. Kakambouras, personal communication, April 12, 2018), and thus, as in any other scar (e.g. fire) it differentiated the influence of wounds on the pines' xylem tissue, based on their depth and size (Arbellay *et al.*, 2014; Rodríguez-García *et al.*, 2016). Therefore, in each tree, we measured the number of tapping scars (TS) while at the same time we recorded their dimensions: the vertical diameter (VD—cm), the horizontal diameter (HD—cm), and the internal diameter (ID—cm). From these scar traits we estimated each tree's functional perimeter (FP), as a proxy of the scar effect on the pines phloem and xylem tissue, using the formula $FP = (((\pi \times DBH) - VD) - (\pi \times DBH)) \times (\pi \times DBH)^{-1} \times 100$. Moreover, for the evaluation of the pines' mechanical integrity, we applied a strength loss equation (SL) (Smiley and Fraedrich, 1992) by taking into account the dimensions of the trees' tapping scars, and the ratio of HD to tree perimeter ($SL = HD^3 + (HD \times (\pi \times DBH)^{-1} \times (DBH^3 - HD^3) \times (100 \times ((DBH^3)^{-1}))$.

C2.3 Collection, pre-processing, and creation of thermal and humidity indices for pine trees

We performed IRT imaging on the pines' trunks using a handheld thermal camera (Testo 875-1i, Testo SE & Co. KGaA, Lenzkirch, Germany), which was calibrated, at the exact shooting moment, in the field, using ambient temperature, relative humidity, and emissivity values (e = .95) (Briscoe *et al.*, 2014), which we obtained individually for each tree under its crown, using a portable weather station and a solar radiation meter (Amprobe SOLAR-100). We took the infrared images at the part of the trunk where the oldest resin scar was located, in the early morning hours, at a standard distance of 3.0 m, in order to avoid atmospheric composition errors (Minkina and Dudzik, 2009) and temperature inaccuracies in the tree trunk, due to the entrance of solar radiation through the tree canopy. In cases where there was more than one scar, we chose to photograph the one with the largest dimensions, which was, according to resin collectors, the oldest one.

The processing of the infrared images was carried out in two stages; the first one involved an initial analysis using the TESTO IRSoft® (v. 4.3) software package, while the second one by using the ArcGIS Analysis toolbox (v. 10.2) (ESRI Inc., Redlands, CA, USA). Specifically, using the TESTO software, we initially calibrated the infrared images by inserting the meteorological data obtained in the field and

then we exported the infrared images in a text file format using two different colour palettes; the temperature image pallete and the humidity image pallete. The temperature pallete produces a dataset of temperature values for the whole image (160 x 120 pixels), in which each pixel has a particular temperature value that represents the tree trunks' adaptation to environmental conditions. Accordingly, the humidity pallete is calculated, for each pixel, taking into account the relative surface moisture of the trunk. In the second stage, we inserted the text file in the ArcGIS toolbox, we converted the text file to a raster dataset and point features (each point had a particular temperature or humidity value), and then we selected manually the pines' trunks by creating a unique polygon for each tree, in a shapefile format. In this way, we isolated the trunk of each examined pine from the other trees in the background, and thereafter we extracted the temperature and humidity values within each tree trunk's area (**Figure C4**).

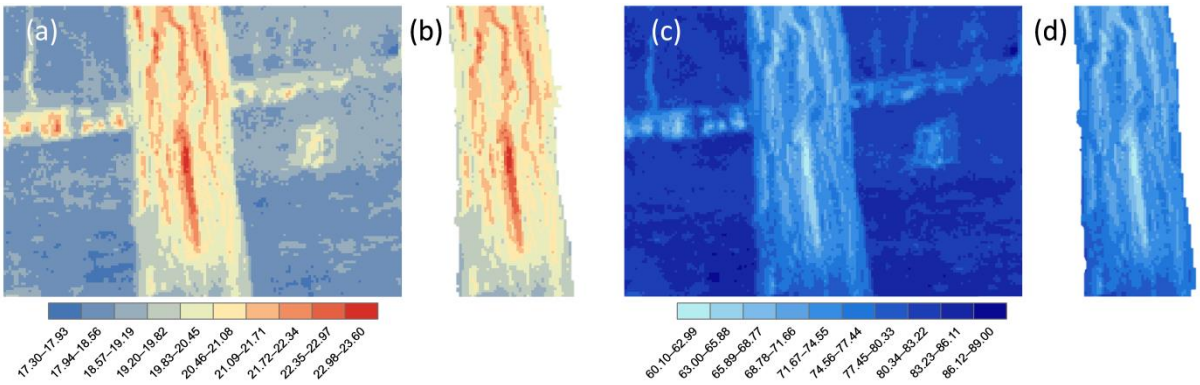

Figure C4: Main methodological procedure of extracting the tree trunks' temperature and humidity values with the use of ArcGIS Analysis toolbox: (a) refer to the calibrated image after being imported in ArcGIS, as a raster layer, using the temperature pallete; (c) refer to the calibrated image using the humidity pallete; (b) and (d) refer to the pines' trunk after the polygon creation using a shapefile format.

In order to create thermal and humidity indices for the pine trees, we extracted the trunk temperature and humidity values, based on the tree trunk histogram, and we initially calculated the typical central tendency and variability measures. Due to the fact that assessing the scars as individual traits, appearing on the pines' trunks, directly related to the pines' health state requires the study of extreme temperature and humidity values, we chose to use the interquartile trunk temperature (T_{IQR}) and humidity (H_{IQR}) range, in order to assess the state of each pine tree holistically. We avoided the use of range metrics, as the effect of outliers would significantly affect our analysis.

C2.4 Assessment of pines' growth and wood decay fungi presence

In each stand, during the autumn of 2019, we obtained tree cores from the 34% of the total standing trees, by random sampling, in order to diminish the possible impact of this technique on the tree population. Following the best-practice guidelines presented by Tsen *et al*. (2016), we chose to extract tree cores, with the use of a 5 mm increment borer, from both resin-tapped and non-tapped pine trees. In particular, we extracted two cores from each resin-tapped tree, one from the tapping face where the oldest resin scar was located, and the other from the living part of the stem, above the tapping face, at approximately 1.3 m above the ground. In addition, we extracted one increment core from each non-tapped tree, at breast height. We did not obtain two cores from the non-tapped trees, as it has been shown that decreasing the sampling effort per tree reduces the possibility of pathogenic inoculation (Tsen *et al.*, 2016). Thereafter, the core samples were brought back to the Biodiversity Conservation Laboratory at the University of the Aegean, and we mounted them on wooden holders in order to air-dry. We highlighted their annual rings, by using an electric planar and a few finer grit sandpapers, progressively, up to 1200 grit, and we scanned each core with a

CanoScan LiDE 400 (Canon Inc., Tokyo, Japan) at a resolution of 600 dpi. We used the software program CooRecorder (version 9.3.1., Cybis Elektronik and Data AB, Sweden) to mark and measure annual growth rings, while we estimated a variety of different variables related to the pines' tree-ring information: (a) total age, (b) age in which they were resin-tapped, (c) mean annual growth (AG_m), (d) mean annual growth before resin-tapped (AG_{br}), and (e) mean annual growth after the resin tapping (AG_{ar}). Based on these metrics, we calculated the ratio of the pines' resin-tapped age to their total age (RT), as we considered this an essential parameter that influences pines' growth.

Finally, we examined the obtained cores for fungal colonization, based on descriptions of discoloration and decay patterns (Shigo and Marx, 1977), by visual and stereoscopic observations. At the same time, we had also inspected each tree, during the establishment of the plots, for the occurrence of external indicators of decay, including fruiting bodies presence (Nicolotti *et al.*, 2010). However, due to the fact that the presence and distribution of fruiting bodies on a tree can give misleading information (Luana *et al.*, 2015), we also paid attention to the sudden change in boring resistance during the tree cores' extraction. We categorized this into normal and abnormal (the drill entered into the pine trunk very easily), and we combined these parameters into one binary variable (fungal presence = 1, fungal absence = 0), by combining information from cores' discoloration, fruiting bodies' presence, and drilling resistance.

C2.5 Data analysis

All the statistical analyses were carried out using SPSS software (v. 25.0. Armonk, NY: IBM Corp.). The assumptions required were all met and statistical significance was assumed at the 5% level. Summary statistics are expressed as means ± standard deviation (SD).

For examining the relationships between the pines' phenotypic traits and the thermal and humidity indices, we visually examined their associations in scatterplots and assessed their relationship using Pearson's correlation coefficient (r).

For evaluating the effect of the resin extraction process on pines' growth, we developed hierarchical multiple regression models, controlling parameters related to both their phenotypic traits and indices. Thereafter, we modelled the effect of all the measured traits and indices on pines' growth, by performing multiple linear regression analysis with a backward elimination procedure.

We also developed binary logistic regression (BLR) models to estimate the presence of the fungal pathogens explained by phenotypic traits, thermal and humidity indices, and growth rate, both in resin-tapped and non-tapped pine trees. We evaluated the predictor variables through a backward stepwise procedure, in order to maintain the optimal models, while we used Nagelkerke's R^2 as an indication of the amount of variation explained by the model, and we tested the overall significance of the model using the Hosmer–Lemeshow goodness of fit test. Finally, we assessed the discrimination ability of the model by creating a classification table of observed and predicted values of fungal presence, which we evaluated by receiver operating characteristic (ROC) curve analysis.

C.3 Results

C3.1 *P. brutia* phenotypic traits and indices

In our twenty study plots, we recorded a total of 496 pine trees of which 333 were resin-tapped and 163 were non-tapped. The sampled pine trees had a mean H of 14.01 ± 4.07 m, mean DBH of 38.26 ± 11.48 cm, and mean CA of 53.95 ± 38.32 m^2. During the data collection, the meteorological conditions, measured under the crown of each examined pine tree, displayed a mean temperature of 16.01 ± 4.26 °C, relative humidity 62.86 ± 10.57 %, and solar intensity of 5.03 ± 4.84 W/m^2. These data were taken in order to calibrate correctly the infrared images. The trees presented a mean trunk temperature of 15.92 ± 4.70 °C, a minimum temperature of 15.19 ± 4.61 °C, and a maximum temperature of 17.19 ± 4.91 °C. Corresponding to the above, the pines' mean surface humidity was 62.52 ± 10.52 %, with a minimum of 58.34 ± 11.21 %, and a maximum of 65.75 ± 10.58 %. Analytical descriptive statistics regarding the pine trees' architecture, vitality, and thermal and humidity indices are presented in **Table C1**.

Table C1. Descriptive statistics for pine traits (N = 496).

Phenotypic traits	**Resin-tapped** (N = 333)		**Non-tapped** (N = 163)		**Total** (N = 496)	
	Mean	**SD**	**Mean**	**SD**	**Mean**	**SD**
***P. Brutia* architectural traits**						
H (m)	14.77	3.98	12.45	3.79	14.01	4.06
DBH (cm)	43.69	9.47	27.17	5.84	38.26	11.48
CA (m)	69.82	36.52	21.53	13.42	53.95	38.32
CR	.39	.11	.32	.11	.37	.11
HCI	1.01	.91	2.15	2.21	1.39	1.57
***P. Brutia* vitality traits**						
LAI_{mean}	1.07	.44	1.26	.46	1.13	.45
LAI_{resin}	.87	.57	1.34	.54	1.03	.60
$LAI_{non\text{-}resin}$	1.27	.51	1.18	.50	1.24	.51
LAI_{range}	.58	.45	.32	.39	.50	.45
TS (n)	2.62	2.11	.00	.00	1.76	2.12
VD (cm)	57.60	33.80	.00	.00	38.67	38.73
HD (cm)	14.30	5.32	.00	.00	9.60	8.01
ID (cm)	7.23	3.34	.00	.00	4.85	4.36
FP (%)	−10.67	3.67	.00	.00	−7.16	5.85
SL (%)	9.96	2.76	.00	.00	6.69	5.20
***P. Brutia* thermal and humidity indices**						
T_{IQR}	1.02	.44	.33	.19	.80	.50
H_{IQR}	3.69	1.57	1.47	.97	2.96	1.75

C3.2 Relationships between pines' phenotypic traits and thermal and humidity indices

The correlation matrix revealed that statistically significant associations existed between the pines' phenotypic traits, and the thermal and humidity indices, both direct and inverse (**Figure C5**). In almost all cases, the architectural traits exhibited positive relations among them, with the exception of HCI. The examination of the relationships between the architectural traits and the leaf area indices (LAI_{mean}, LAI_{resin}, $LAI_{non\text{-}resin}$, LAI_{range}) did not show any significant correlations, with the exception of the positive correlation, which was observed between DBH and LAI_{range} ($r = .22$; $p = .001$), and the negative correlation between CA and LAI_{resin} ($r = -.21$; $p = .001$). Contrastingly, DBH had significant moderate to high positive correlations with all the variables related to tapping scars

and their dimensions, ranged between .50 to .67 (p = .001), and a significant negative correlation with FP (r = −.47; p = .001). The CA and CR traits followed the same pattern with the coefficient values ranging between .44 to .54 (p =.001) for CA, and between .11 (p = .18) to . 29 (p = .001) for CR, while a negative correlation was observed with FP for both traits (CA: r = −.41, p = .001; CR: r = −.23, p = .001). The HCI presented significant negative relationships with almost all the examined trees' phenotypic traits. Focusing on the leaf area indices, the investigation of their relationship with the tapping scars' variables (TS, VD, HD, ID, FP, SL) yielded moderate positive and negative statistically significant relationships; the higher were observed between LAI_{resin} with all of the them (TS: r = −.30, p = .001; VD: r = −.37, p = .001; HD: r = −.41, p = .001; ID: r = −.41, p = .001; FP: r = .43, p = .001; SL: r = −.42, p = .001), while $LAI_{non\text{-}resin}$ did not show any correlations with these variables.

Regarding the relationships of the non-invasive indices with the phenotypic traits of the pine trees, the thermal and humidity indices followed the same pattern with the thermal index showing slightly higher correlations from the humidity index. In particular, the T_{IQR} and the H_{IQR} were positively correlated (a) with the architectural traits (coefficient ranged from .21 to .56; p = .001), (b) with almost all the vitality traits (LAI_{range}, TS, VD, HD, ID, SL; coefficient ranged from .21 to .567; p = .001), and negatively correlated with LAI_{mean} (T_{IQR}: r = −.39, p = .001; H_{IQR}: r = −.34, p = .001), LAI_{resin} (T_{IQR}: r = −.55, p = .001; H_{IQR}: r = −.50, p = .001), and FP (T_{IQR}: r = −.60, p = .001; H_{IQR}: r = −.55, p = .001) (**Figure C5).**

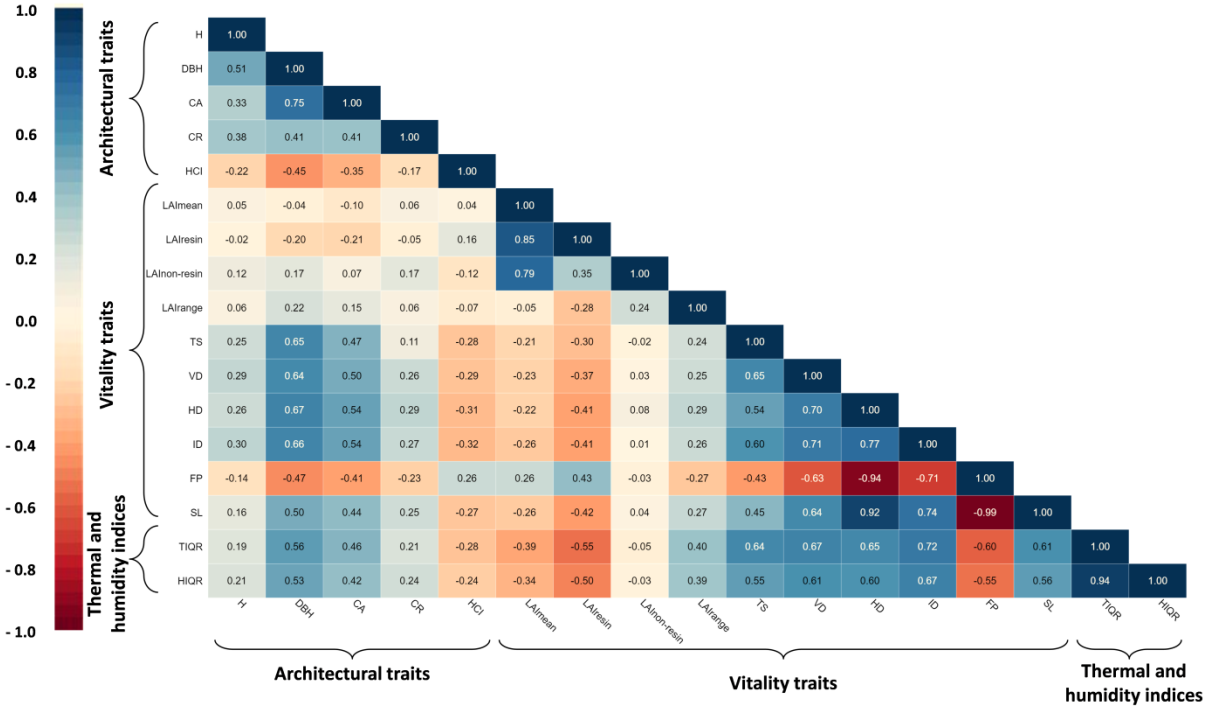

Figure C5: Correlation matrix showing the relationships between the pine trees' phenotypic traits, and the thermal and humidity indices. Red and blue colours indicate positive and negative correlations respectively, while the intensity of colour indicates the strength of the relationship. All correlation coefficients above .20 or below −.20 are statistically significant (p < .05).

C3.3 Effect of the resin extraction process on pines' growth

From the total of the 496 *P. brutia* trees, we collected cores from 175 trees, 69 were extracted from non-tapped pines, while 212 cores were from 106 resin-tapped pines. The mean age of the resin-tapped pines was 82.65 ± 19.71 years, while they were resin-tapped at the age of 33.92 ± 18.07. The resin-tapped trees had a mean AG_m of 1.94 ± .83 mm, a mean AG_{br} of 3.61 ± 2.05 mm, and a mean AG_{ar} of 1.15 ± .61 mm. The mean age of the non-tapped pines was 68.67 ± 18.33 and their AG_m was

1.77 ± .60 mm. Detailed information about the resin-tapped pines from which we collected sampling material is presented in **Table C2**.

Table C2. Descriptive statistics for resin-tapped pine trees (N = 106).

Plot	Resin-tapped	TA	RA	AG_m (mm)	AG_{br} (mm)	AG_{ar} (mm)
1	6	74.16 ± 4.30	26.00 ± 8.14	2.11 ± .65	3.99 ± 1.28	1.16 ± .31
2	6	76.33 ± 3.98	32.16 ± 20.66	1.56 ± .17	3.31 ± 1.75	.83 ± .22
3	9	76.44 ± 3.57	42.00 ± 20.54	1.52 ± .44	2.62 ± 1.28	.74 ± .56
4	2	70.50 ± 4.94	23.00 ± 2.82	3.03 ± .05	6.87 ± 1.03	1.16 ± .72
5	3	84.66 ± 6.43	41.33 ± 14.18	1.92 ± .23	2.76 ± .90	1.29 ± .18
6	5	68.60 ± 4.10	22.20 ± 1.92	2.31 ± .82	4.99 ± 1.59	1.03 ± .51
7	4	101.00 ± 6.05	45.00 ± 16.02	2.03 ± .67	3.16 ± .93	.99 ± .12
8	4	64.50 ± 16.66	30.50 ± 11.12	2.76 ± 1.29	3.61 ± 1.92	2.09 ± .79
9	5	94.60 ± 20.63	31.00 ± 21.67	1.70 ± .54	3.37 ± .72	.90 ± .26
10	5	92.60 ± 7.89	39.40 ± 30.25	1.68 ± .56	3.20 ± 1.80	1.14 ± .60
11	6	103.50 ± 10.61	47.00 ± 20.36	1.39 ± .44	2.36 ± 1.18	.91 ± .21
12	6	51.16 ± 5.49	22.00 ± 5.06	3.08 ± .72	5.08 ± 2.11	1.71 ± .40
13	5	58.20 ± 15.27	29.60 ± 17.72	3.21 ± 1.18	5.23 ± 2.00	1.83 ± 1.42
14	4	66.00 ± 3.74	41.00 ± 12.57	1.83 ± .12	2.40 ± .62	1.24 ± .23
15	7	99.42 ± 12.27	26.57 ± 17.31	1.36 ± .24	3.43 ± 1.09	.82 ± .22
16	6	104.66 ± 5.78	38.00 ± 15.25	1.25 ± .16	2.13 ± 1.19	1.01 ± .33
17	7	102.71 ± 5.22	50.00 ± 11.04	1.45 ± .22	2.15 ± .55	.89 ± .30
18	6	107.00 ± 5.54	40.66 ± 20.14	1.67 ± .35	3.19 ± 1.36	.97 ± .23
19	5	64.40 ± 5.85	24.60 ± 20.75	1.64 ± .28	3.92 ± 2.20	1.17 ± .53
20	5	68.80 ± 19.60	15.40 ± 8.44	3.01 ± 1.28	7.60 ± 4.33	1.94 ± .93

To explore the unique contribution of the effect of the wounds, resulting from the resin-extraction process, to the $AG_{m,}$ $AG_{ar,}$ and GC, we conducted a set of two hierarchical multiple regression analyses. In every model, we controlled the effects of the architectural traits and leaf area indices, while we excluded from the analysis the tapping scars' dimensions, the SL, and the thermal and humidity indices. We excluded these variables, as they are either directly related to each other or, in the case of the thermal and humidity indices, they do not provide any theoretical and/or physiological justification for explaining this effect. Variables that explain variance in AG_m and AG_{ar}, were entered in two steps. In the first step, we set as dependent variables the AG_m and AG_{ar}, individually, for the two distinct models, while the remaining phenotypic traits were the independent variables. These variables had a variance inflation factor of less than 3 and collinearity tolerance greater than 0.7, suggesting that the estimated βs are well supported. In the second step, we added the number of tapping scars (TS) as the predictor variable.

Regarding the effects of the resin extraction process on AG_m, the results of the first step indicated a significant model [$F(2, 103) = 19.509$, $p < .001$, $R^2_{adj} = .261$] with significant predictors to be DBH ($\beta = .008$, $p < .001$) and LAI_{mean} ($\beta = .075$, $p = .007$). In step two, the inclusion of TS changed the proportion of variance explained by the model, which was also significant [$F(3, 102) = 19.729$, $p < .001$, $R^2_{adj} = .349$], by an additional 9.2 % (**Table C3a**). In correspondence with the first analysis, the one that estimated the effects of the resin extraction process on AG_{ar} revealed also a significant model [$F(1, 104) = 19.523$, $p < .001$, $R^2_{adj} = .150$], with DBH as a significant predictor in step one, and a significant model [$F(2, 103) = 19.544$, $p < .001$, $R^2_{adj} = .261$], with two significant predictors (DBH, TS) in step two. The change in variance, accounted by the entrance of TS, explained an additional 11.7 % of the variance in AG_{ar} (**Table C3b**). The additional introduction of individual prognostic parameters, such as FP, did not differentiate significantly the model nor did it provide additional

explanatory power. However, the explanatory power of the model increased to a ΔR^2 of 19 %, when we chose trees with a low ratio of rein-tapped age to total age (N = 38; RT < .3).

Table C3. Hierarchical linear regression for AG_m, and AG_{ar}. The unstandardized regression coefficients (B), the standard errors (S.E.), the standardized regression coefficients (β), the t-test statistic (t), the probability value (p), the correlation coefficient (R), the adjusted R-square (R^2_{adj}), and the additional variance explained (ΔR^2).

Predictor	B	S.E.	β	t	p-value	R	$R^2_{adj.}$	ΔR^2
a. AG_m								
Step 1								
Constant	-.12	.07		-1.85	.07	.524	.261	.275
DBH	.01	.00	.43	5.06	.00			
LAI_{mean}	.08	.03	.24	2.76	.01			
Step 2								
Constant	-.15	.06		-2.38	.02			
DBH	.01	.00	.56	6.45	.00	.606	.349	.092
LAI_{mean}	.08	.03	.24	2.98	.00			
TS	-.03	.01	-.33	-3.86	.00			
b. AG_{ar}								
Step 1								
Constant	.02	.26		.09	.93	.398	.150	.158
DBH	.03	.01	.40	4.42	.00			
Step 2								
Constant	-.09	.25		-.35	.73			
DBH	.04	.01	.54	5.94	.00	.525	.261	.117
TS	-.11	.03	-.37	-4.08	.00			

In an attempt to test whether it is feasible to predict AG_m, and AG_{ar} from all the measured traits and indices, we performed multiple linear regression analysis with backward elimination. Due to the fact that the humidity index showed slightly lower correlations with the pines' phenotypic traits, we excluded it from the analysis. Results indicated that the model for predicting the AG_m was significant [F (6, 99) = 11.734, p < .001], with an adjusted R^2 of 38 %, while the model for predicting the AG_{ar} was also significant [F (4, 101) = 13.050, p < .001, $R^2_{adj.}$ = .315] (**Table C4**).

Table C4. Final models obtained from multiple linear regression analyses for estimating AG_m and AG_{ar}. All multiple regression models were statistically significant (p < .05).

Response variable	Predictor variables	B	SE B	β	t	p-value	$R^2_{adj.}$	F
AG_m	(constant)	.40	.38		1.07	.29	.380	11.734
	DBH	.04	.01	.39	3.27	.00		
	CA	.01	.00	.20	1.79	.05		
	LAI_{resin}	.34	.15	.21	2.25	.03		
	LAI_{range}	.27	.14	.15	1.87	.05		
	TS	-.08	.04	-.22	-2.37	.02		
	T_{IQR}	-.16	.07	-.21	-2.15	.03		
AG_{ar}	(constant)	-.28	.25		-1.12	.27	.315	13.050
	DBH	.03	.01	.48	5.39	.00		
	LAI_{resin}	.30	.10	.25	2.96	.00		
	LAI_{range}	.18	.11	.14	1.70	.05		
	TS	-.10	.03	-.35	-3.96	.00		

C3.4 Modelling the presence of fungal pathogens

The fungal infestation was identified in 52.5% of the examined trees (N = 92), while 46.2% (N = 81) did not present any fungal signs. Due to the fact that in two trees the identification of the presence or absence of fungi was not possible, we, therefore, removed them from the analysis. In order to examine whether non-invasive diagnostics, along with the trees' phenotypic traits, can explain the probability of the presence or the absence of fungal infestation, we used four (4) BLR models. For this purpose, we separated our dataset into two groups: the first one contained the 106 resin-tapped pines, while the second one, all the trees from which we collected the sampling material (N = 175). For the first group of trees, we ran a BLR model by using variables related to their growth rate (AG_m, AG_{ar}), their architecture and vitality traits, as well as their thermal and humidity indices. For the second group, we tested three distinct models to explain the presence of the fungal pathogens, based on (a) their architectural and vitality traits, (b) their thermal and humidity indices, and (c) a combination of all the tree traits and indices.

Regarding the resin-tapped trees, the BLR model identified five significant variables that contributed the most in predicting fungal infestation (**Table C5**). The Nagelkerke R^2 showed that these variables explained 81 % of the total variance of the data. In addition, the Hosmer–Lemeshow test showed that the model's goodness of fit can be accepted, due to the absence of chi-square significance (Hosmer–Lemeshow = 2.142; p > .05). The area under the ROC curve (AUC = .976; S.E. = .001; 95% CI .953–.998; p = 0.0001; **Figure C6**a), as a metric of the sensitivity values for all possible values of specificity, with a threshold (.676) resulting from Youden's index (Youden, 1950), classified correctly the pine trees with and without fungal presence in 91.5 % of all cases, with a predicted classification accuracy of 89.3 % for those without pathogens and 92.3 % for the infected pine trees [χ^2 (5, N = 106) = 85.83; p < .0001; **Table C5**)].

Table C5. Logistic regression models for the presence probability of fungal communities for the resin-tapped pine trees (N = 106). B = logistic coefficient; S.E. = standard error of estimate; Wald = Wald chi-square; df = degree of freedom; p - value = significance.

Predictor	B	S.E.	Wald's χ^2	df	p-value
AG_{ar}	2.50	1.02	6.01	1	.01
CR	-14.48	6.06	5.71	1	.02
FP	.23	.11	4.82	1	.03
LAI_{resin}	-4.32	1.43	9.12	1	.00
H_{IQR}	2.89	.73	15.80	1	.00
Constant	.15	2.26	.01	1	.95

Focusing on detecting the occurrence of fungal signs, using the architectural and vitality traits, in both resin-tapped and non-tapped pines, the BLR model showed an overall classification accuracy of 91.5 % (Nagelkerke R^2 = .842, Hosmer–Lemeshow = 2.630; p > .05;), 91.4 % for trees with fungal presence and 91.6% for those without [χ^2 (4, N = 173) = 175.42; p < .0001; **Table C6**a)], as estimated by the area under the ROC curve (AUC = .978; S.E. =.008; 95% CI .962 - .994; p = .0001; Youden = .594; **Figure C6**b). The model obtained using the T_{IQR} and the H_{IQR}, also had quite high classification accuracy (90.3 % for presence, 90.4 % for absence, 90.3 % in total). In this model, the H_{IQR} was the most significant factor [χ^2 (1, N = 173) = 150.11; p < .0001; **Table C6**b)], the AUC was .954 (S.E. =.016, 95% CI .923 - .985; p < .0001; Youden = .541; **Figure C6**c), the Nagelkerke R^2 was .766, and the Hosmer–Lemeshow test was 12.553 (p > .05). Lastly, the model in which we combined all the tree traits and indices, presented the higher discrimination from all the examined models; 93.5 % for fungal presence, 96.4 % for absence, and 94.9 % in total [χ^2 (5, N = 173) = 195.82; p < .0001; **Table C6**c)], as indicated by the AUC (AUC = .990; S.E. = .005; 95% CI.980–.999; p = .0001; Youden = .621; **Figure C6**d). The Nagelkerke R^2 showed that the combination of the examined variables can explain

89.6 % of the total variance of the data, while the Hosmer–Lemeshow test showed that the model's goodness-of-fit can be accepted (χ^2 = 1.899; p > .05).

Table C6. Logistic regression models for the presence probability of fungal communities for the resin-tapped and non-tapped pine trees (N = 173). B = logistic coefficient; S.E. = standard error of estimate; Wald = Wald chi-square; df = degree of freedom; p - value = significance.

a. Architectural and vitality traits					
Predictor	**B**	**S.E.**	**Wald's χ^2**	**df**	**p-value**
DBH	.24	.05	19.03	1	.00
CR	-9.68	3.49	7.70	1	.01
LAI_{resin}	-5.20	.96	29.21	1	.00
LAI_{range}	5.16	1.19	18.83	1	.00
Constant	-2.88	1.57	3.35	1	.05
b. Thermal and humidity indices					
H_{IQR}	.81	.12	47.60	1	.00
Constant	-5.83	.88	43.66	1	.00
c. Combination of tree traits and indices					
DBH	.16	.07	5.73	1	.02
CR	-10.17	4.23	5.77	1	.02
LAI_{resin}	-4.09	1.19	11.80	1	.00
LAI_{range}	3.77	1.38	7.40	1	.01
H_{IQR}	1.32	.36	13.25	1	.00
Constant	-4.44	2.07	4.60	1	.03

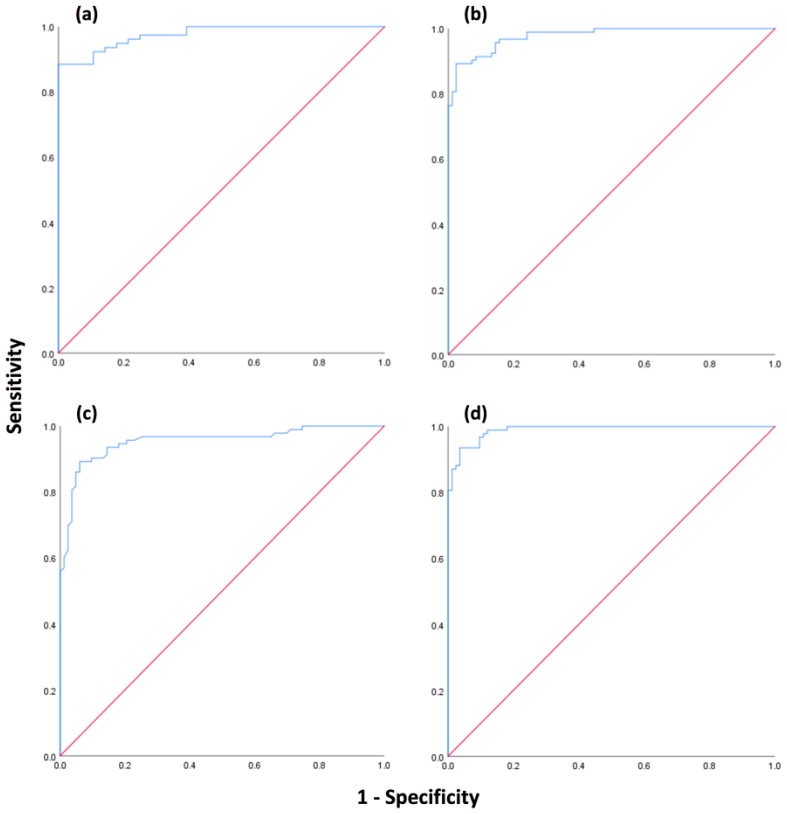

Figure C6: The ROC curves for logistic regression models using the resin-tapped trees dataset (a) and the dataset from all the sampling trees (b, c, d). ROC curve (b) refers to the Architectural and vitality variables, (c) refers to the thermal and humidity indices, and (d) refers to the combination of all the phenotypic traits and indices.

C.4 Discussion

In this study, we investigated the effect of the tapping scars, resulting from the resin extraction process, along with the presence of fungal pathogens, on pines' growth in twenty *P. brutia* forest stands. We provided a comprehensive methodological framework, which we tested in field conditions, by combining different invasive and non-invasive approaches with the trees' phenotypic traits and indices. A first reading of the proximity of the variables, constituting this methodological framework, is finding individual relations between them. Thus, by examining the correlations between the pines' phenotypic traits with their thermal and humidity indices, significant findings were illustrated, which can satisfactorily explain the dynamics of these systems by linking those traits with the trees' growth and their health estimation.

In particular, we especially gave our attention to the relationships between leaf area indices with the tapping scars' variables as, LAI is one of the most important biophysical indexes for (a) describing ecosystem structure (Zarate-valdez *et al.*, 2012) and (b) understanding vegetation growth (Musau *et al.*, 2016), by controlling within- and below- canopy microclimate, water and carbon exchange, and canopy water interception (Bréda, 2003). Furthermore, the wounded xylem and phloem tissues, from the resin extraction process would affect the shape and structure of the crown, and consequently the LAI, by interrupting or decreasing the water flow and nutrient transport, resulting in the modulation of the tree crowns' evaporation and transpiration (Liu *et al.*, 2019). After all, the trees' possible hydraulic failure in conductive tissues related to both water supply conditions and xylem anatomical characteristics, has led them in adapting their leaf distribution, in order to sustain a balance between water supply and water loss (Van Hees, 1997; López-Bernal *et al.*, 2010; Johnson *et al.*, 2016). That was the rationale behind obtaining two different LAI metrics (LAI_{resin}, $LAI_{non\text{-}resin}$) under the crown of each resin-tapped pine tree. At the same time, having in mind that the trees' competition for resources leads them to differentiate their crown structure, in terms of symmetry, we also chose to take two LAI metrics from the non-tapped pine trees. Averaging those metrics, gave us the ability to have a complete image of this indicator for each tree (LAI_{mean}), while by subtracting them we were able to obtain the range of LAI values for each tree. The LAI_{range}, a representative statistical metric describing tree vitality (Zevgolis *et al.*, 2022), highlighted the pine trees' fluctuation from a healthy condition; its greater homogeneity is directly correlated with high productivity (Leverenz and Hinckley, 1990). The positive or negative, depending on each case, statistically significant relationships which we observed between LAI metrics (LAI_{mean}, LAI_{resin}, LAI_{range}) with the tapping scars' variables, especially their relationship with the LAI_{resin}, confirms the rationale of our experimental design, to a large extent. This is further reinforced by the observed absence of any relationship between $LAI_{non\text{-}resin}$ with the tapping scars' variables.

Regarding the relationships between HCI and CR with the tapping scars' variables, both positive and negative, suggests something already known from the narratives of the resin collectors, that is, they chose to collect resin from the most vigorous trees that would give them a greater amount of resin (Fr. E. Kakambouras, personal communication, April 12, 2018). Thus, the less competition a tree has at a young age, the greater the chance of being a candidate tree for resin extraction when it reaches the desired size; this is clearly expressed by the crown ratio. In supporting this finding, the relationship of HCI with the tapping scars' variables suggests the same thing; the more competition a tree receives in the stand by its neighbouring trees, the lower the pressure is exerted from the resin collectors.

The high positive correlations between the T_{IQR} and the H_{IQR} with the tapping scars' variables, showed that these non-invasive indices can be used as a proxy when examining trees' structural defects, as it has already been discussed in various studies concerning common vegetation species of the urban environment and agricultural vegetation species (*Olea europaea*) (Zevgolis *et al.*, 2022),

including the pine trees' wounds from the resin extraction process. Moreover, their positive correlations with LAI_{range} and their negative correlations with LAI_{mean} and LAI_{resin}, can integrate those indices into a framework of commonly used indicators for assessing the forest systems' health. Nonetheless, T_{IQR} has already been considered an important and easily extracted index for estimating trees' structural abnormalities and tree health as a whole (Zevgolis, 2022) while the high positive correlation between T_{IQR} and H_{IQR}, indicates that the humidity indicator can also be used for estimating pine trees' health state. However, to be perfectly precise, when discussing the health state of the resin-tapped pine trees, as described by the LAI metrics and accordingly by their thermal and humidity indices, we should take into account the possible differences between the resin-tapped and the non-tapped trees. Thus, we used independent samples t-test to determine whether the means of those variables were significantly differentiated. We found statistically significant differences between the resin-tapped (N = 333) and the non-tapped trees (N = 163) for all the examined variables (**Figure C7**) with the exception of $LAI_{non\text{-}resin}$. In particular, there were statistically significant differences in (a) LAI_{mean} [t (494) = 4.51; p = .0001] between the resin-tapped (1.07 ± .44) and the non-tapped trees (1.26 ± .46), (b) LAI_{resin} [t (494) = 8.76; p = .0001; resin-tapped trees (.87 ± .57); non-tapped trees (1.34 ± .54)], (c) LAI_{range} [t (494) = 6.17; p = .0001; resin-tapped trees (.58 ± .45); non-tapped trees (.32 ± .39)], (d) T_{IQR} [t (494) = 18.81; p = .0001; resin-tapped trees (1.02 ± .44); non-tapped trees (.33 ± .19)], and (e) H_{IQR} [t (494) = 16.42; p = .0001; resin-tapped trees (3.69 ± 1.57); non-tapped trees (1.47 ± .97)].

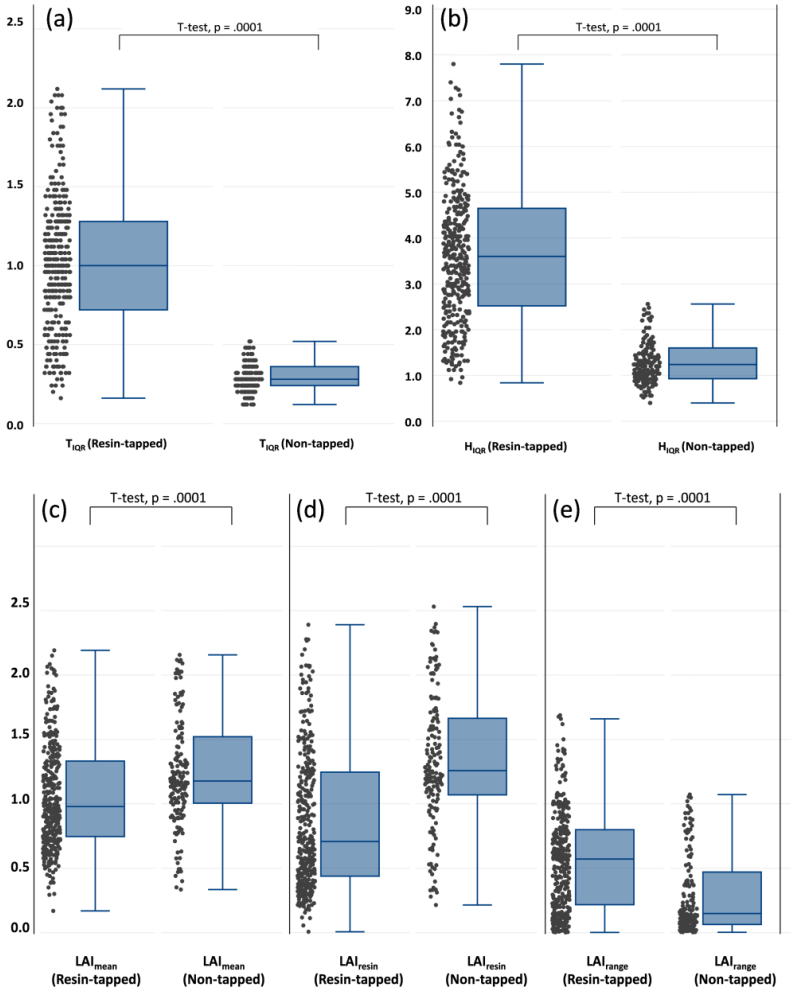

Figure C7: Box-plots showing the statistically significant differences between the resin-tapped and non-tapped pine trees: (a) the thermal index, (b) the humidity index, (c) the LAI_{mean}, (d) the LAI_{resin}, and (e) the LAI_{range}. Horizontal lines: medians; boxes: interquartile ranges (25–75%); whiskers: data ranges.

In addition to the significant differences found between resin-tapped and non-tapped pine trees, the mean values of the examined indices also constitute an important finding. In the case of the thermal index, our results confirm the definition of a healthy tree; a tree is considered healthy when its temperature is evenly distributed in the trunk (Catena and Catena, 2008). Keeping in mind the existing relationships of the examined indices, as well as the observed differences between the pines, we can conclude that along with the thermal index and the LAI, the humidity index, and the LAI_{range} can also be considered as indicators whose low values can describe a healthy pine tree.

The growth decline of the *P. brutia* trees (**Table C2**), which was illustrated by calculating the percentage change of the mean tree ring width, after the year they were wounded, was 62.95 ± 20.47 %. Trees with a low RT, exhibited a higher reduction in their growth (**Figure C8**); controlling the effect of all the architectural and vitality traits, the correlation of RT with the absolute growth change (%) before and after the wounding, had a negative significant coefficient (r = −.542; p = .0001).

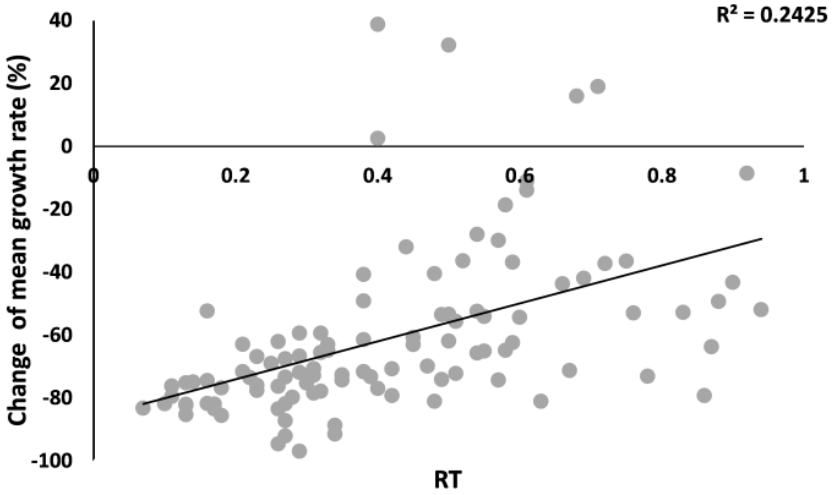

Figure C8: Scatterplot with regression line showing the relationship between the ratio of the pines' resin-tapped age to total age (RT) with the change of their mean growth rate.

When examining the effects of the tapping scars on AG_m and on AG_{ar}, the explanatory power of the hierarchical regression models increased significantly (AG_m: R^2 = .092, p = .0001; AG_{ar}: R^2 = .117, p = .0001) (**Table C3**); these findings are consistent with similar studies which were carried out on different coniferous species, showing a mean growth rate decrease of 14.1 % in *P. halepensis* (Papadopoulos, 2013) and 21.7 % in *P. massoniana* (Chen *et al.*, 2015). The extremely large growth decline in Pinus species is obviously not only due to the effect of the resin extraction process. In the island of Lesvos, as well as in other islands of the Aegean sea, growth reductions have been observed, in Pinus species, after the 1970s (Sarris *et al.*, 2007, 2011) due to the persisting drought conditions (Quintana-Seguí *et al.*, 2016), resulting in the decrease of water availability (Christopoulou *et al.*, 2021), which is directly affecting forest stands' productivity as well as their carbon sequestration (Xu *et al.*, 2017). In our case, this growth decline period is compatible with the average value of the year in which the trees were resin-tapped (1970.27 ± 22.58). Therefore, the combination of such drought-limited conditions along with the resin extraction process, as well as the possible colonization of the tapping scars by fungal species, burden the pines to a great extent and possibly leads them to high mortality (Crouchet *et al.*, 2019).

It is noteworthy that, even though the tapping scars showed low interpretive power in estimating the resin-tapped trees' mean annual growth and their mean annual growth after the resin tapping, the additional input of the trees' architectural traits (DBH, CA), vitality traits (LAI_{resin}, LAI_{range}), and the T_{IQR}, enhanced our models by increasing their explanatory power up to 38 % for AG_m and 31.5 % for

AG_{ar} (**Table C4**), confirming the aforementioned regarding the importance of such traits in describing forest dynamics. The explanatory power of the linear models, theoretically, may not be satisfactory, however, we must keep in mind that we did not use a set of parameters that would potentially enhance our models, such as climatic conditions, water availability, soil nutrient content, and slope and aspect at a stand level, which are essential in estimating the trees' growth pattern (Cherubini *et al.*, 2003; Belokopytova *et al.*, 2021), as we considered that the connection between our metrics, which is not established elsewhere, would be sufficient enough for the effective monitoring and restoring of critical forest ecosystem functions and services (Grulke *et al.*, 2020).

In this context, the short diagnosis time of fungal pathogen presence is essential for forest management. These fungal pathogens are recognized as the main current and future threat to forest ecosystems (Santini and Battisti, 2019), because of their aggressiveness and their ability to colonize xylem tissues which persists for many years (Prospero *et al.*, 2021), while, at the same time, climate change can facilitate their expansion (Garrett *et al.*, 2016). Regardless of the fact that Pinus species, in general, are significantly resilient considering fungal colonization as they invest in resin; a pivotal component of their defence system, which provides them both short-term and long-term response in balance with other physiological functions (e.g. growth) (Kopaczyk *et al.*, 2020). The constant resin collection in our studied trees, increased their susceptibility, as more than half of the trees showed fungal signs. The logistic regression model for the resin-tapped trees presented both high discriminatory performance (91.5 %) and explanatory power (81 %) indicating that the probability in predicting fungal presence can be accurately estimated by the use of common forestry tools and non-invasive diagnostics, while at the same time its emphasizing the importance of the mean growth rate after the resin extraction process (**Table C5**). It is noted that, when focusing on a larger sample of trees including the resin-tapped and the non-tapped, the classification accuracy remained extremely high, both in the case of architectural and vitality traits (91.5 %) and regarding the thermal and humidity indices (90.3 %), as well as when we used those traits in combination (94.9 %). In all models, their explanatory power was quite high, ranging from .766 to .896. Looking at the models discreetly, it is understood that variables describing tree size and its canopy (DBH, CR, LAI_{resin}, LAI_{range}) are important contributors in estimating fungal presence. From the perspective of evaluating fungal presence using the thermal and humidity indices, it is quite clear that H_{IQR} is an ideal index for detecting infection in pine trees, suggesting that the non-invasive method of IRT and in particular the use of the humidity pallete, can be a valuable tool for identifying biotic stresses in pine trees. After all, favourable microclimate conditions, such as high humidity in the tree trunks stimulate fungal pathogen development, reproduction, and persistence (Sudakova *et al.*, 2021).

In conclusion, our results provided evidence of the effect of resin extraction on pines' growth as well as detecting fungal presence in both resin-tapped and non-tapped pine trees. This was accomplished by obtaining phenotypic information from *P. brutia* trees by combining minimal invasive and non-invasive diagnostics. In particular, with the estimation of thermal and humidity indices we demonstrated their importance in estimating pine trees' health state. These indices, along with long-established methodological tools and techniques, showed that the pines' phenotypic traits and indices, can accurately estimate both the effects of the tapping scars in the pines' growth and the presence of fungal pathogens. Overall, this study can contribute to forests management and restoration initiatives by providing the means for a rapid but also precise assessment of the *P. brutia* health state.

References

1. Gamfeldt, L.; Snäll, T.; Bagchi, R.; Jonsson, M.; Gustafsson, L.; Kjellander, P.; Ruiz-Jaen, M.C.; Fröberg, M.; Stendahl, J.; Philipson, C.D.; *et al*. Higher levels of multiple ecosystem services are found in forests with more tree species. *Nat. Commun.* **2013**, 4, doi:10.1038/ncomms2328.
2. Mori, A.S.; Lertzman, K.P.; Gustafsson, L. Biodiversity and ecosystem services in forest ecosystems: a research agenda for applied forest ecology. *J. Appl. Ecol*. **2017**, 54, 12–27, doi:10.1111/1365-2664.12669.
3. Brockerhoff, E.G.; Barbaro, L.; Castagneyrol, B.; Forrester, D.I.; Gardiner, B.; González-Olabarria, J.R.; Lyver, P.O.B.; Meurisse, N.; Oxbrough, A.; Taki, H.; *et al*. Forest biodiversity, ecosystem functioning and the provision of ecosystem services. *Biodivers. Conserv.* **2017**, *26*, 3005–3035, doi:10.1007/s10531-017-1453-2.
4. Watson, J.E.M.; Evans, T.; Venter, O.; Williams, B.; Tulloch, A.; Stewart, C.; Thompson, I.; Ray, J.C.; Murray, K.; Salazar, A.; *et al*. The exceptional value of intact forest ecosystems. *Nat. Ecol. Evol.* **2018**, *2*, 599–610, doi:10.1038/s41559-018-0490-x.
5. Ameztegui, A.; Solarik, K.A.; Parkins, J.R.; Houle, D.; Messier, C.; Gravel, D. Perceptions of climate change across the Canadian forest sector: The key factors of institutional and geographical environment. *PLoS One* **2018**, *13*, 1–18, doi:10.1371/journal.pone.0197689.
6. Li, D.; Wu, S.; Liu, L.; Zhang, Y.; Li, S. Vulnerability of the global terrestrial ecosystems to climate change. *Glob. Chang. Biol.* **2018**, *24*, 4095–4106, doi:10.1111/gcb.14327.
7. Jandl, R.; Spathelf, P.; Bolte, A.; Prescott, C.E. Forest adaptation to climate change—is non-management an option? *Ann. For. Sci.* **2019**, *76*, 1–13, doi:10.1007/s13595-019-0827-x.
8. Morecroft, M.D.; Duffield, S.; Harley, M.; Pearce-Higgins, J.W.; Stevens, N.; Watts, O.; Whitaker, J. Measuring the success of climate change adaptation and mitigation in terrestrial ecosystems. *Science (80-.).* **2019**, *366*, doi:10.1126/science.aaw9256.
9. Ogawa-Onishi, Y.; Berry, P.M.; Tanaka, N. Assessing the potential impacts of climate change and their conservation implications in Japan: A case study of conifers. *Biol. Conserv.* **2010**, *143*, 1728–1736, doi:10.1016/j.biocon.2010.04.021.
10. Gilliam, F.S. Forest ecosystems of temperate climatic regions: from ancient use to climate change. *New Phytol.* **2016**, *212*, 871–887, doi:10.1111/nph.14255.
11. Bisbing, S.M.; Urza, A.K.; Buma, B.J.; Cooper, D.J.; Matocq, M.; Angert, A.L. Can long-lived species keep pace with climate change? Evidence of local persistence potential in a widespread conifer. *Divers. Distrib.* **2021**, *27*, 296–312, doi:10.1111/ddi.13191.
12. Xie, Y.; Wang, X.; Wilson, A.M.; Silander, J.A. Predicting autumn phenology: How deciduous tree species respond to weather stressors. *Agric. For. Meteorol.* **2018**, *250–251*, 127–137, doi:10.1016/j.agrformet.2017.12.259.
13. Chen, L.; Huang, J.G.; Ma, Q.; Hänninen, H.; Tremblay, F.; Bergeron, Y. Long-term changes in the impacts of global warming on leaf phenology of four temperate tree species. *Glob. Chang. Biol.* **2019**, *25*, 997–1004, doi:10.1111/gcb.14496.
14. Piao, S.; Liu, Q.; Chen, A.; Janssens, I.A.; Fu, Y.; Dai, J.; Liu, L.; Lian, X.; Shen, M.; Zhu, X. Plant phenology and global climate change: Current progresses and challenges. *Glob. Chang. Biol.* **2019**, *25*, 1922–1940, doi:10.1111/gcb.14619.
15. Dyderski, M.K.; Paź, S.; Frelich, L.E.; Jagodziński, A.M. How much does climate change threaten European forest tree species distributions? *Glob. Chang. Biol.* **2018**, *24*, 1150–1163, doi:10.1111/gcb.13925.
16. Peterson, M.L.; Doak, D.F.; Morris, W.F. Incorporating local adaptation into forecasts of species' distribution and abundance under climate change. *Glob. Chang. Biol.* **2019**, *25*, 775–793, doi:10.1111/gcb.14562.
17. Morin, X.; Fahse, L.; Jactel, H.; Scherer-Lorenzen, M.; García-Valdés, R.; Bugmann, H. Long-term response of forest productivity to climate change is mostly driven by change in tree species composition. *Sci. Rep.* **2018**, *8*, 1–12, doi:10.1038/s41598-018-23763-y.

18. Holopainen, J.K.; Virjamo, V.; Ghimire, R.P.; Blande, J.D.; Julkunen-Tiitto, R.; Kivimäenpää, M. Climate Change Effects on Secondary Compounds of Forest Trees in the Northern Hemisphere. *Front. Plant Sci.* **2018**, *9*, 1–10, doi:10.3389/fpls.2018.01445.
19. Lahive, F.; Hadley, P.; Daymond, A.J. The physiological responses of cacao to the environment and the implications for climate change resilience. A review. *Agron. Sustain. Dev.* **2019**, *39*, doi:10.1007/s13593-018-0552-0.
20. Boa, E. *An illustrated guide to the state of health of trees Recognition and interpretation*; FAO, Ed.; CABI Bioscience, London, UK., 2003; ISBN 9251050201.
21. Teshome, D.T.; Zharare, G.E.; Naidoo, S. The Threat of the Combined Effect of Biotic and Abiotic Stress Factors in Forestry Under a Changing Climate. *Front. Plant Sci.* **2020**, *11*, doi:10.3389/fpls.2020.601009.
22. Anderegg, W.R.L.; Hicke, J.A.; Fisher, R.A.; Allen, C.D.; Aukema, J.; Bentz, B.; Hood, S.; Lichstein, J.W.; Macalady, A.K.; Mcdowell, N.; *et al*. Tree mortality from drought, insects, and their interactions in a changing climate. *New Phytol.* **2015**, *208*, 674–683, doi:10.1111/nph.13477.
23. IPCC *IPCC Special Report on the impacts of global warming of 1.5°C*; 2018; Vol. 2.
24. Brown, K.A.; Flynn, D.F.B.; Abram, N.K.; Ingram, J.C.; Johnson, S.E.; Wright, P. Assessing natural resource use by forest-reliant communities in madagascar using functional diversity and functional redundancy metrics. *PLoS One* **2011**, *6*, doi:10.1371/journal.pone.0024107.
25. Siry, J.P.; Cubbage, F.W.; Potter, K.M.; McGinley, K. Current Perspectives on Sustainable Forest Management: North America. *Curr. For. Reports* **2018**, *4*, 138–149, doi:10.1007/s40725-018-0079-2.
26. Nerfa, L.; Rhemtulla, J.M.; Zerriffi, H. Forest dependence is more than forest income: Development of a new index of forest product collection and livelihood resources. *World Dev.* **2020**, *125*, 104689, doi:10.1016/j.worlddev.2019.104689.
27. Walmsley, J.D.; Jones, D.L.; Reynolds, B.; Price, M.H.; Healey, J.R. Whole tree harvesting can reduce second rotation forest productivity. *For. Ecol. Manage.* **2009**, *257*, 1104–1111, doi:10.1016/j.foreco.2008.11.015.
28. Pretzsch, H.; Biber, P.; Uhl, E.; Dauber, E. Long-term stand dynamics of managed spruce-fir-beech mountain forests in Central Europe: Structure, productivity and regeneration success. *Forestry* **2015**, *88*, 407–428, doi:10.1093/forestry/cpv013.
29. Gardner, C.J.; Bicknell, J.E.; Baldwin-Cantello, W.; Struebig, M.J.; Davies, Z.G. Quantifying the impacts of defaunation on natural forest regeneration in a global meta-analysis. *Nat. Commun.* **2019**, *10*, 1–7, doi:10.1038/s41467-019-12539-1.
30. Hao, L.; Pan, C.; Fang, D.; Zhang, X.; Zhou, D.; Liu, P.; Liu, Y.; Sun, G. Quantifying the effects of overgrazing on mountainous watershed vegetation dynamics under a changing climate. *Sci. Total Environ.* **2018**, *639*, 1408–1420, doi:10.1016/j.scitotenv.2018.05.224.
31. Piponiot, C.; Rödig, E.; Putz, F.E.; Rutishauser, E.; Sist, P.; Ascarrunz, N.; Blanc, L.; Derroire, G.; Descroix, L.; Guedes, M.C.; *et al*. Can timber provision from Amazonian production forests be sustainable? *Environ. Res. Lett.* **2019**, *14*, doi:10.1088/1748-9326/ab195e.
32. Zhang, Q.; Li, Y.; Yu, C.; Qi, J.; Yang, C.; Cheng, B.; Liang, S. Global timber harvest footprints of nations and virtual timber trade flows. *J. Clean. Prod.* **2020**, *250*, 119503, doi:10.1016/j.jclepro.2019.119503.
33. Lopez-Toledo, L.; Perez-Decelis, A.; Macedo-Santana, F.; Cuevas, E.; Endress, B.A. Chronic leaf harvesting reduces reproductive success of a tropical dry forest palm in northern Mexico. *PLoS One* **2018**, *13*, 1–16, doi:10.1371/journal.pone.0205178.
34. Tieminie, R.N.; Loh, C.E.; Tieguhong, J.C.; Nghobuoche, M.F.; Mandiefe, P.S.; Tieguhong, M.R. "Non-timber forest products and climate change adaptation among forest dependent communities in Bamboko forest reserve, southwest region of Cameroon." *Environ. Syst. Res.* **2021**, *10*, doi:10.1186/s40068-020-00215-z.
35. Ticktin, T. The ecological implications of harvesting non-timber forest products. *J. Appl. Ecol.* **2004**, *41*, 11–21, doi:10.1111/j.1365-2664.2004.00859.x.

36. Gaoue, O.G.; Ticktin, T. Impacts of bark and foliage harvest on Khaya senegalensis (Meliaceae) reproductive performance in Benin. *J. Appl. Ecol.* **2008**, *45*, 34–40, doi:10.1111/j.1365-2664.2007.01381.x.
37. Gaoue, O.G.; Horvitz, C.C.; Ticktin, T.; Steiner, U.K.; Tuljapurkar, S. Defoliation and bark harvesting affect life-history traits of a tropical tree. *J. Ecol.* **2013**, *101*, 1563–1571, doi:10.1111/1365-2745.12140.
38. Endress, B.A.; Gorchov, D.L.; Berry, E.J. Sustainability of a non-timber forest product: Effects of alternative leaf harvest practices over 6 years on yield and demography of the palm Chamaedorea radicalis. *For. Ecol. Manage.* **2006**, *234*, 181–191, doi:10.1016/j.foreco.2006.07.020.
39. Matsuhashi, S.; Hirata, A.; Akiba, M.; Nakamura, K.; Oguro, M.; Takano, K.T.; Nakao, K.; Hijioka, Y.; Matsui, T. Developing a point process model for ecological risk assessment of pine wilt disease at multiple scales. *For. Ecol. Manage.* **2020**, *463*, 118010, doi:10.1016/j.foreco.2020.118010.
40. Santini, A.; Battisti, A. Complex insect-pathogen interactions in tree pandemics. *Front. Physiol.* **2019**, *10*, 1–7, doi:10.3389/fphys.2019.00550.
41. Prospero, S.; Botella, L.; Santini, A.; Robin, C. Biological control of emerging forest diseases: How can we move from dreams to reality? *For. Ecol. Manage.* **2021**, *496*, doi:10.1016/j.foreco.2021.119377.
42. Garrett, K.A.; Nita, M.; Wolf, E.D.D.; Gomez, L.; Sparks, A.H. *Plant Pathogens as Indicators of Climate Change*; 1st ed.; Elsevier B.V., 2016; ISBN 9780444533012.
43. Papadopoulos, A.M. Resin Tapping History of an Aleppo Pine Forest in Central Greece. *Open For. Sci. J.* **2013**, *6*, 50–53, doi:10.2174/1874398601306010050.
44. Camarero, J.J.; Álvarez-Taboada, F.; Hevia, A.; Castedo-Dorado, F. Radial growth and wood density reflect the impacts and susceptibility to defoliation by gypsy moth and climate in radiata pine. *Front. Plant Sci.* **2018**, *871*, 1–12, doi:10.3389/fpls.2018.01582.
45. Trapp, S.; Croteau, R. Defensive resin biosynthesis in conifers. *Annu. Rev. Plant Biol.* **2001**, *52*, 689–724, doi:10.1146/annurev.arplant.52.1.689.
46. Garcia-Forner, N.; Campelo, F.; Carvalho, A.; Vieira, J.; Rodríguez-Pereiras, A.; Ribeiro, M.; Salgueiro, A.; Silva, M.E.; Louzada, J.L. Growth-defence trade-offs in tapped pines on anatomical and resin production. *For. Ecol. Manage.* **2021**, *496*, doi:10.1016/j.foreco.2021.119406.
47. Rodrigues-Corrêa, K.C. da S.; de Lima, J.C.; Fett-Neto, A.G. Pine oleoresin: Tapping green chemicals, biofuels, food protection, and carbon sequestration from multipurpose trees. *Food Energy Secur.* **2012**, *1*, 81–93, doi:10.1002/fes3.13.
48. Palma, A.; Pereira, J.M.; Soares, P. Resin tapping activity as a contribution to the management of maritime pine forest. *For. Syst.* **2016**, *25*, doi:10.5424/fs/2016252-08925.
49. Calama Sainz, R.; Tome, M.; Sánchez-González, M.; Miina., J.; Spanos, K.; Palahi, M. Modelling Non-Wood Forest Products in Europe: a review. *For. Syst.* **2011**, *3*, 69, doi:10.5424/fs/201019s-9324.
50. Gershenzon, J. Metabolic costs of terpenoid accumulation in higher plants. *J. Chem. Ecol.* **1994**, *20*, 1281–1328, doi:10.1007/BF02059810.
51. Züst, T.; Agrawal, A.A. Trade-Offs Between Plant Growth and Defense Against Insect Herbivory: An Emerging Mechanistic Synthesis. *Annu. Rev. Plant Biol.* **2017**, *68*, 513–534, doi:10.1146/annurev-arplant-042916-040856.
52. Magnuszewski, M.; Tomusiak, R. Effect of resin-tapping on the radial increment of Scots pine (Pinus sylvestris L.) – case study of a stand from Lidzbark Forest District. *For. Res. Pap.* **2013**, *74*, 273–280, doi:10.2478/frp-2013-0026.
53. van der Maaten, E.; Mehl, A.; Wilmking, M.; van der Maaten-Theunissen, M. Tapping the tree-ring archive for studying effects of resin extraction on the growth and climate sensitivity of Scots pine. *For. Ecosyst.* **2017**, *4*, doi:10.1186/s40663-017-0096-9.
54. Génova, M.; Caminero, L.; Dochao, J. Resin tapping in Pinus pinaster: Effects on growth and

response function to climate. *Eur. J. For. Res.* **2014**, *133*, 323–333, doi:10.1007/s10342-013-0764-4.
55. Chen, F.; Yuan, Y. jiang; Yu, S. long; Zhang, T. wen Influence of climate warming and resin collection on the growth of Masson pine (Pinus massoniana) in a subtropical forest, southern China. *Trees - Struct. Funct.* **2015**, *29*, 1423–1430, doi:10.1007/s00468-015-1222-3.
56. Rodríguez-García, A.; Martín, J.A.; López, R.; Sanz, A.; Gil, L. Effect of four tapping methods on anatomical traits and resin yield in Maritime pine (Pinus pinaster Ait.). *Ind. Crops Prod.* **2016**, *86*, 143–154, doi:10.1016/j.indcrop.2016.03.033.
57. Zeng, X.; Ni, P.; Li, Y.; Wang, W.; Sun, S.; Wang, Y.; Chang, Y.; Tao, X.; Hou, M.; Liu, X. Short-term resin tapping activities had a minor influence on physiological responses recorded in the tree-ring isotopes of Chinese pine (Pinus tabuliformis). *Dendrochronologia* **2021**, *70*, 125895, doi:10.1016/j.dendro.2021.125895.
58. Williams, R. The Effects of Resin Tapping on the Radial Growth of Masson Pine Trees in South China-A Case Study. *Agric. Res. Technol. Open Access J.* **2017**, *8*, doi:10.19080/artoaj.2017.08.555732.
59. Du, B.; Luan, Q.; Ni, Z.; Sun, H.; Jiang, J. Radial growth and non-structural carbohydrate partitioning response to resin tapping of slash pine (Pinus elliottii Engelm. var. elliottii). *J. For. Res.* **2021**, doi:10.1007/s11676-021-01357-1.
60. Moreira, X.; Zas, R.; Solla, A.; Sampedro, L. Differentiation of persistent anatomical defensive structures is costly and determined by nutrient availability and genetic growth-defence constraints. *Tree Physiol.* **2015**, *35*, 112–123, doi:10.1093/treephys/tpu106.
61. Vázquez-González, C.; López-Goldar, X.; Zas, R.; Sampedro, L. Neutral and Climate-Driven Adaptive Processes Contribute to Explain Population Variation in Resin Duct Traits in a Mediterranean Pine Species. *Front. Plant Sci.* **2019**, *10*, 1–12, doi:10.3389/fpls.2019.01613.
62. Phillips, M.A.; Croteau, R.B. Resin-based defenses in conifers. *Trends Plant Sci.* **1999**, *4*, 184–190, doi:10.1016/S1360-1385(99)01401-6.
63. Cheng, A.X.; Lou, Y.G.; Mao, Y.B.; Lu, S.; Wang, L.J.; Chen, X.Y. Plant terpenoids: Biosynthesis and ecological functions. *J. Integr. Plant Biol.* **2007**, *49*, 179–186, doi:10.1111/j.1744-7909.2007.00395.x.
64. Celedon, J.M.; Bohlmann, J. Oleoresin defenses in conifers: chemical diversity, terpene synthases and limitations of oleoresin defense under climate change. *New Phytol.* **2019**, *224*, 1444–1463, doi:10.1111/nph.15984.
65. Wallin, K.F.; Kolb, T.E.; Skov, K.R.; Wagner, M.R. Effects of crown scorch on ponderosa pine resistance to bark beetles in Northern Arizona. *Environ. Entomol.* **2003**, *32*, 652–661, doi:10.1603/0046-225X-32.3.652.
66. Shigo, A.L.; Marx, H.G. *Compartmentalization of decay in trees.*; Department of Agriculture, Forest Service, 1977; Vol. 252;.
67. Fay, N.; de Berker, N. A review of the theory and practice of tree coring on live ancient and veteran trees. *Scottish Nat. Herit.* **2018**, *789*, 843.
68. Pedersen, B.S. the Role of Stress in the Mortality of Midwestern Oaks As Indicated By Growth Prior To Death. *Ecology* **1998**, *79*, 79–93, doi:10.1890/0012-9658(1998)079[0079:trosit]2.0.co;2.
69. Cherubini, P.; Gartner, B.L.; Tognetti, R.; Bräker, O.U.; Schoch, W.; Innes, J.L. Identification, measurement and interpretation of tree rings in woody species from mediterranean climates. *Biol. Rev. Camb. Philos. Soc.* **2003**, *78*, 119–148, doi:10.1017/S1464793102006000.
70. Huang, Y.; Ren, Z.; Li, D.; Liu, X. Phenotypic techniques and applications in fruit trees: A review. *Plant Methods* **2020**, *16*, 1–22, doi:10.1186/s13007-020-00649-7.
71. Leong, E.C.; Burcham, D.C.; Fong, Y.K. A purposeful classification of tree decay detection tools. *Arboric. J.* **2012**, *34*, 91–115, doi:10.1080/03071375.2012.701430.
72. Goh, C.L.; Abdul Rahim, R.; Fazalul Rahiman, M.H.; Mohamad Talib, M.T.; Tee, Z.C. Sensing wood decay in standing trees: A review. *Sensors Actuators, A Phys.* **2018**, *269*, 276–282, doi:10.1016/j.sna.2017.11.038.

73. Burcham, D.C.; Leong, E.C.; Fong, Y.K.; Tan, P.Y. An evaluation of internal defects and their effect on trunk surface temperature in casuarina equisetifolia L. (Casuarinaceae). *Arboric. Urban For.* **2012**, *38*, 277–286, doi:10.48044/jauf.2012.037.
74. Hartmann, H.; Moura, C.F.; Anderegg, W.R.L.; Ruehr, N.K.; Salmon, Y.; Allen, C.D.; Arndt, S.K.; Breshears, D.D.; Davi, H.; Galbraith, D.; *et al*. Research frontiers for improving our understanding of drought-induced tree and forest mortality. *New Phytol.* **2018**, *218*, 15–28, doi:10.1111/nph.15048.
75. Johnstone, D.; Moore, G.; Tausz, M.; Nicolas, M. The Measurement of Wood Decay in Landscape Trees. *Arboric. Urban For.* **2010**, *36*, 121–127, doi:10.48044/jauf.2010.016.
76. Tsen, E.W.J.; Sitzia, T.; Webber, B.L. To core, or not to core: the impact of coring on tree health and a best-practice framework for collecting dendrochronological information from living trees. *Biol. Rev.* **2016**, *91*, 899–924, doi:10.1111/brv.12200.
77. Kozlowski, T.T.; Kramer, P.J.; Pallardy, S.G. *The physiological ecology of woody plants*; Academic Press Inc., 2012;
78. Fahlgren, N.; Gehan, M.A.; Baxter, I. Lights, camera, action: High-throughput plant phenotyping is ready for a close-up. *Curr. Opin. Plant Biol.* **2015**, *24*, 93–99, doi:10.1016/j.pbi.2015.02.006.
79. Torresan, C.; Berton, A.; Carotenuto, F.; Di Gennaro, S.F.; Gioli, B.; Matese, A.; Miglietta, F.; Vagnoli, C.; Zaldei, A.; Wallace, L. Forestry applications of UAVs in Europe: a review. *Int. J. Remote Sens.* **2017**, *38*, 2427–2447, doi:10.1080/01431161.2016.1252477.
80. Safari, A.; Sohrabi, H.; Powell, S.; Shataee, S. A comparative assessment of multi-temporal Landsat 8 and machine learning algorithms for estimating aboveground carbon stock in coppice oak forests. *Int. J. Remote Sens.* **2017**, *38*, 6407–6432, doi:10.1080/01431161.2017.1356488.
81. Pádua, L.; Hruška, J.; Bessa, J.; Adão, T.; Martins, L.M.; Gonçalves, J.A.; Peres, E.; Sousa, A.M.R.; Castro, J.P.; Sousa, J.J. Multi-temporal analysis of forestry and coastal environments using UASs. *Remote Sens.* **2018**, *10*, 1–21, doi:10.3390/rs10010024.
82. Humplík, J.F.; Lazár, D.; Husičková, A.; Spíchal, L. Automated phenotyping of plant shoots using imaging methods for analysis of plant stress responses - A review. *Plant Methods* **2015**, *11*, 1–10, doi:10.1186/s13007-015-0072-8.
83. Catena, A.; Catena, G. Overview of thermal imaging for tree assessment. *Arboric. J.* **2008**, *30*, 259–270, doi:10.1080/03071375.2008.9747505.
84. Bellett-Travers, M.; Morris, S. The relationship between surface temperature and radial wood thickness of twelve trees harvested in nottinghamshire. *Arboric. J.* **2010**, *33*, 15–26, doi:10.1080/03071375.2010.9747589.
85. Vidal, D.; Pitarma, R. Infrared thermography applied to tree health assessment: A review. *Agric.* **2019**, *9*, doi:10.3390/agriculture9070156.
86. Al-doski, J.; Shattri, B.M.; Helmi-Zulhai, B.M.-S. Thermal Imaging for Pests Detecting—a Review. *Int. J. Agric. For. Plant.* **2016**, *2*, 10–30.
87. Asner, G.P.; Martin, R.E.; Keith, L.M.; Heller, W.P.; Hughes, M.A.; Vaughn, N.R.; Hughes, R.F.; Balzotti, C. A spectral mapping signature for the Rapid Ohia Death (ROD) pathogen in Hawaiian forests. *Remote Sens.* **2018**, *10*, doi:10.3390/rs10030404.
88. Zevgolis, Y.G. Detecting, quantifying and mapping urban trees' structural defects using non–destructive diagnostics: implications for tree hazard assessment and management. *Unpubl. manuscript, Biodivers. Conserv. Lab. Dep. Environ. Univ. Aegean* **2022**.
89. Zevgolis, Y.G.; Kamatsos, E.; Akriotis, T.; Dimitrakopoulos, P.G.; Troumbis, A.Y. Estimating Productivity, Detecting Biotic Disturbances, and Assessing the Health State of Traditional Olive Groves, Using Nondestructive Phenotypic Techniques. *Sustainability* **2022**, *14*, 391, doi:10.3390/su14010391.
90. Palaiologou, P.; Kalabokidis, K.; Ager, A.A.; Day, M.A. Development of comprehensive fuel management strategies for reducing wildfire risk in Greece. *Forests* **2020**, *11*, 1–29, doi:10.3390/F11080789.
91. HNMS *Climatic Data for Selected Stations in Greece*; 2021;

92. Pretzsch, H.; Biber, P.; Uhl, E.; Dahlhausen, J.; Rötzer, T.; Caldentey, J.; Koike, T.; van Con, T.; Chavanne, A.; Seifert, T.; *et al*. Crown size and growing space requirement of common tree species in urban centres, parks, and forests. *Urban For. Urban Green.* **2015**, *14*, 466–479, doi:10.1016/j.ufug.2015.04.006.
93. Kontogianni, A.; Tsitsoni, T.; Goudelis, G. An index based on silvicultural knowledge for tree stability assessment and improved ecological function in urban ecosystems. *Ecol. Eng.* **2011**, *37*, 914–919, doi:10.1016/j.ecoleng.2011.01.015.
94. Soares, P.; Tomé, M. GLOBTREE, an individual tree growth model for Eucalyptus globulus in Portugal. In *Modelling Forest Systems*; Amaro, A., Reed, D., Soares, P., Eds.; CAB International, 2003; pp. 97–110 ISBN 0851996930.
95. Radtke, P.J.; Westfall, J.A.; Burkhart, H.E. Conditioning a distance-dependent competition index to indicate the onset of inter-tree competition. *For. Ecol. Manage.* **2003**, *175*, 17–30, doi:10.1016/S0378-1127(02)00118-4.
96. Searle, E.B.; Chen, H.Y.H. Complementarity effects are strengthened by competition intensity and global environmental change in the central boreal forests of Canada. *Ecol. Lett.* **2020**, *23*, 79–87, doi:10.1111/ele.13411.
97. Hegyi, F. A simulation model for managing Jack-pine stands. In *Growth Models for Tree and Stand Simulation*; Fries, J., Ed.; Royal College of Forestry, Department of Forest Yield Research: Stockholm, Sweden, 1974; pp. 74–90.
98. Coops, N.C.; Waring, R.H. The use of multiscale remote sensing imagery to derive regional estimates of forest growth capacity using 3-PGS. *Remote Sens. Environ.* **2001**, *75*, 324–334, doi:10.1016/S0034-4257(00)00176-0.
99. Nakamura, A.; Kitching, R.L.; Cao, M.; Creedy, T.J.; Fayle, T.M.; Freiberg, M.; Hewitt, C.N.; Itioka, T.; Koh, L.P.; Ma, K.; *et al*. Forests and Their Canopies: Achievements and Horizons in Canopy Science. *Trends Ecol. Evol.* **2017**, *32*, 438–451, doi:10.1016/j.tree.2017.02.020.
100. Arbellay, E.; Stoffel, M.; Sutherland, E.K.; Smith, K.T.; Falk, D.A. Changes in tracheid and ray traits in fire scars of North American conifers and their ecophysiological implications. *Ann. Bot.* **2014**, *114*, 223–232, doi:10.1093/aob/mcu112.
101. Smiley, E.T.; Fraedrich, B.R. Determining strength loss from decay. *J. Arboric.* **1992**, *18*, 201–204.
102. Briscoe, N.J.; Handasyde, K.A.; Griffiths, S.R.; Porter, W.P.; Krockenberger, A.; Kearney, M.R. Tree-hugging koalas demonstrate a novel thermoregulatory mechanism for arboreal mammals. *Biol. Lett.* **2014**, *10*, doi:10.1098/rsbl.2014.0235.
103. Minkina, W.; Dudzik, S. Algorithm of Infrared Camera Measurement Processing Path. In *Infrared Thermography*; John Wiley & Sons, Ltd: Chichester, UK, 2009; pp. 41–60 ISBN 9780470747186.
104. Nicolotti, G.; Gonthier, P.; Guglielmo, F. Advances in Detection and Identification of Wood Rotting Fungi in Timber and Standing Trees. In *Molecular Identification of Fungi*; Springer Berlin Heidelberg: Berlin, Heidelberg, 2010; pp. 251–276 ISBN 9783642050411.
105. Luana, G.; Fabiano, S.; Fabio, G.; Paolo, G. Comparing visual inspection of trees and molecular analysis of internal wood tissues for the diagnosis of wood decay fungi. *Forestry* **2015**, *88*, 465–470, doi:10.1093/forestry/cpv015.
106. Youden, W.J. Index for rating diagnostic tests. *Cancer* **1950**, *3*, 32–35, doi:10.1002/1097-0142(1950)3:1<32::AID-CNCR2820030106>3.0.CO;2-3.
107. Zarate-valdez, J.L.; Whiting, M.L.; Lampinen, B.D.; Metcalf, S.; Ustin, S.L.; Brown, P.H. Author ' s personal copy Prediction of leaf area index in almonds by vegetation indexes Author ' s personal copy. **2012**, *85*, 24–32.
108. Musau, J.; Patil, S.; Sheffield, J.; Marshall, M. Spatio-temporal vegetation dynamics and relationship with climate over East Africa. *Hydrol. Earth Syst. Sci. Discuss.* **2016**, 1–30, doi:10.5194/hess-2016-502.
109. Bréda, N.J.J. Ground-based measurements of leaf area index: A review of methods, instruments and current controversies. *J. Exp. Bot.* **2003**, *54*, 2403–2417, doi:10.1093/jxb/erg263.
110. Liu, Y.; Gong, W.; Xing, Y.; Hu, X.; Gong, J. Estimation of the forest stand mean height and

aboveground biomass in Northeast China using SAR Sentinel-1B, multispectral Sentinel-2A, and DEM imagery. *ISPRS J. Photogramm. Remote Sens.* **2019**, *151*, 277–289, doi:10.1016/j.isprsjprs.2019.03.016.

111. Van Hees, A.F.M. Growth and morphology of pedunculate oak (Quercus robur L) and beech (Fagus sylvatica L) seedlings in relation to shading and drought. *Ann. des Sci. For.* **1997**, *54*, 9–18, doi:10.1051/forest:19970102.
112. López-Bernal, Á.; Alcántara, E.; Testi, L.; Villalobos, F.J. Spatial sap flow and xylem anatomical characteristics in olive trees under different irrigation regimes. *Tree Physiol.* **2010**, *30*, 1536–1544, doi:10.1093/treephys/tpq095.
113. Johnson, D.M.; Wortemann, R.; McCulloh, K.A.; Jordan-Meille, L.; Ward, E.; Warren, J.M.; Palmroth, S.; Domec, J.C. A test of the hydraulic vulnerability segmentation hypothesis in angiosperm and conifer tree species. *Tree Physiol.* **2016**, *36*, 983–993, doi:10.1093/treephys/tpw031.
114. Leverenz, J.W.; Hinckley, T.M. Shoot structure, leaf area index and productivity of evergreen conifer stands. *Tree Physiol.* **1990**, *6*, 135–149, doi:10.1093/treephys/6.2.135.
115. Sarris, D.; Christodoulakis, D.; Körner, C. Recent decline in precipitation and tree growth in the eastern Mediterranean. *Glob. Chang. Biol.* **2007**, *13*, 1187–1200, doi:10.1111/j.1365-2486.2007.01348.x.
116. Sarris, D.; Christodoulakis, D.; Körner, C. Impact of recent climatic change on growth of low elevation eastern Mediterranean forest trees. *Clim. Change* **2011**, *106*, 203–223, doi:10.1007/s10584-010-9901-y.
117. Quintana-Seguí, P.; Martin, E.; Sánchez, E.; Zribi, M.; Vennetier, M.; Vicente-Serrano, S.; Vidal, J.-P. Drought: observed trends, future projections. *Mediterr. Reg. under Clim. Chang.* **2016**, 123--131.
118. Christopoulou, A.; Sazeides, C.I.; Fyllas, N.M. Size-mediated effects of climate on tree growth and mortality in Mediterranean Brutia pine forests. *Sci. Total Environ.* **2021**, *812*, 151463, doi:10.1016/j.scitotenv.2021.151463.
119. Xu, K.; Wang, X.; Liang, P.; An, H.; Sun, H.; Han, W.; Li, Q. Tree-ring widths are good proxies of annual variation in forest productivity in temperate forests. *Sci. Rep.* **2017**, *7*, 1–8, doi:10.1038/s41598-017-02022-6.
120. Crouchet, S.E.; Jensen, J.; Schwartz, B.F.; Schwinning, S. Tree Mortality After a Hot Drought: Distinguishing Density-Dependent and -Independent Drivers and Why It Matters. *Front. For. Glob. Chang.* **2019**, *2*, 1–14, doi:10.3389/ffgc.2019.00021.
121. Belokopytova, L. V; Zhirnova, D.F.; Meko, D.M.; Babushkina, E.A.; Vaganov, E.A.; Krutovsky, K. V Tree Rings Reveal the Impact of Soil Temperature on Larch Growth in the Forest-Steppe of Siberia. **2021**, 1–16.
122. Grulke, N.; Bienz, C.; Hrinkevich, K.; Maxfield, J.; Uyeda, K. Quantitative and qualitative approaches to assess tree vigor and stand health in dry pine forests. *For. Ecol. Manage.* **2020**, *465*, 118085, doi:10.1016/j.foreco.2020.118085.
123. Kopaczyk, J.M.; Warguła, J.; Jelonek, T. The variability of terpenes in conifers under developmental and environmental stimuli. *Environ. Exp. Bot*. **2020**, 180, 104197, doi:10.1016/j.envexpbot.2020.104197.
124. Sudakova, M.; Terentyeva, E.; Kalashnikov, A. Assessment of health status of tree trunks using ground penetrating radar tomography. *AIMS Math*. **2021**, 7, 162–179, doi:10.3934/geosci.2021010.

Συζήτηση

Στο πλαίσιο της παρούσης διδακτορικής διατριβής επιχειρήθηκε η σύνδεση διαφορετικών μη-επεμβατικών μεθοδολογιών και μετρήσεων πεδίου που στόχο είχε τη δημιουργία ενός ολοκληρωμένου μεθοδολογικού πλαισίου που να περιγράφει τη συνολική κατάσταση της υγείας των δέντρων σε αστικά, αγροτικά και δασικά οικοσυστήματα, σε επίπεδο είδους, πληθυσμού και ατόμου. Ο συνδυασμός των τριών διακριτών αλλά ταυτόχρονα άμεσα σχετισμένων περιπτώσεων που περιγράφονται, αποτελεί ένα λειτουργικό διεπιστημονικό πλέγμα, μεθόδων, τεχνικών και τεχνολογιών αιχμής που ισορροπημένα φιλοδοξεί να καλύψει ολιστικά, ως ένα βαθμό, την έννοια της υγείας της δενδρώδους βλάστησης.

Στρατηγικό άξονα και της παρούσης διατριβής αποτελεί ο συνδυασμός διαφορετικών μεθοδολογικών προσεγγίσεων: (α) μιας ταχέως αναπτυσσόμενης (υπέρυθρη θερμογραφία), (β) της μέτρησης των τυπικών, και μη, φαινοτυπικών, φασματικών και χωρικών χαρακτηριστικών των δέντρων και (γ) της δημιουργίας δεικτών υγείας που προκύπτουν από τη σύνδεση αυτών των μεθόδων. Επιπρόσθετα, η μελέτη 910 ιστάμενων δέντρων, από 9 διαφορετικά είδη, προσδίδει τη δυνατότητα σύγκρισής τους τόσο σε διαφορετικά επίπεδα οργάνωσης της βιοκοινότητας (άτομο, πληθυσμός) όσο και σε διαφορετικά επίπεδα ταξινόμησης (είδος). Στο επίπεδο της εφαρμοσμένης έρευνας πεδίου, καινοτομία αποτέλεσε τόσο η χρήση της υπέρυθρη θερμογραφίας για τη μελέτη των δομικών ελαττωμάτων των ιστάμενων δέντρων (**Γράφημα 1**) όσο και η σύνδεση των θερμικών και υγρασιακών δεικτών που εξήχθησαν, με κοινά αποδεκτούς δείκτες υγείας και παραγωγικότητας των δέντρων.

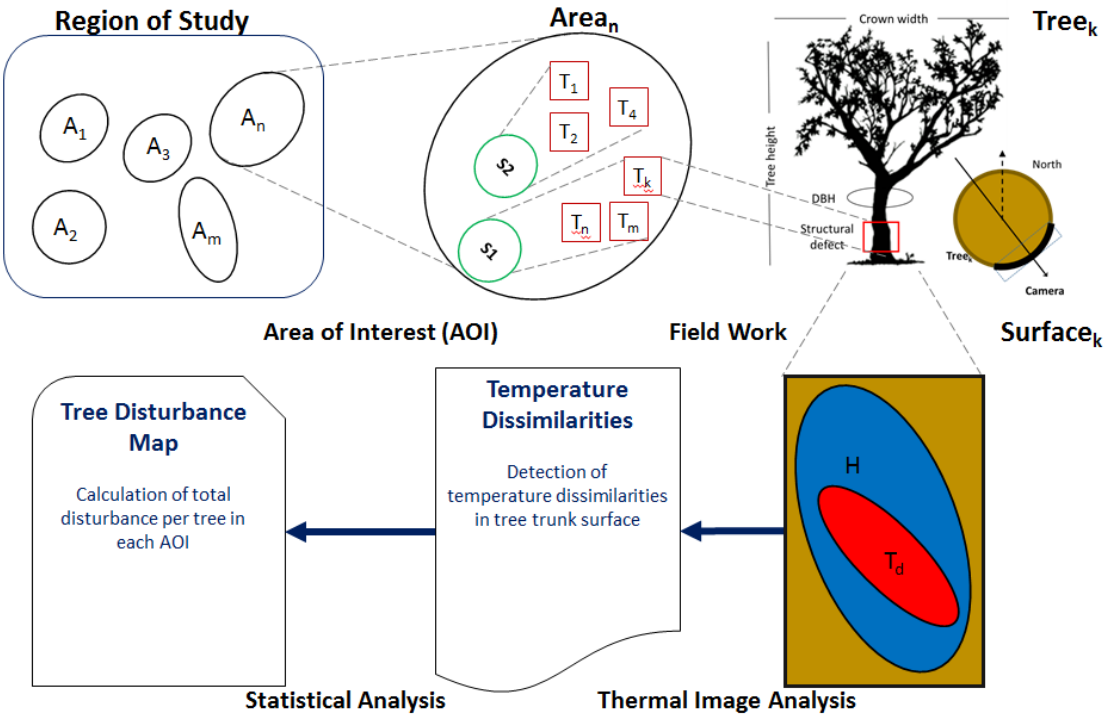

A: Area, S: Species, T: Tree, Td: Tree surface temperature dissimilarities, H: Healthy tree surface

Γράφημα 1: Μεθοδολογικό πλαίσιο για την εκτίμηση της κατάστασης της υγείας ιστάμενων δέντρων σε αστικά, αγροτικά και φυσικά συστήματα.

Ο καθορισμός του μεθοδολογικού πλαισίου που περιγράφεται είχε ήδη διερευνηθεί σε πιλοτικό επίπεδο με τη μελέτη 373 δέντρων από πέντε διαφορετικά είδη (*Pinus Brutia, Cupressus sempervirens, Olea europaea var. media oblonga, Juniperus macrocarpa, Juniperus phoenicea*), ώστε να διασφαλιστεί η επιτυχής περάτωσή του στα τρία συστήματα μελέτης. Συνολικά, εφαρμόστηκε σε 1253 δέντρα γεγονός που ενισχύει ακόμα περισσότερο τα ευρήματα της παρούσης διατριβής. Επιπρόσθετα, η επιλογή και εφαρμογή ευρέως χρησιμοποιούμενων πρωτοκόλλων δειγματοληψίας πεδίου βοήθησε τόσο στην ορθή λήψη πρωτογενών δεδομένων όσο και στη δυνατότητα επιμέρους σύγκρισης μεταξύ τους.

Στα αστικά οικοσυστήματα, η αξιολόγηση της υγείας των δέντρων μέσω της ανίχνευσης και ποσοτικοποίησης των δομικών ελαττωμάτων τους καθώς και ο εντοπισμός των δυνητικά επικίνδυνων δέντρων, βοηθάει στη διαχείριση τόσο σε επίπεδο σχεδιασμού αστικών χώρων πρασίνου, ανταποκρινόμενη σε διαφορετικούς στόχους της διοίκησης, όπως η φύτευση ειδών, η δενδροκομική διαχείριση, ο έλεγχος των κινδύνων και η ασφάλεια των ανθρώπων, όσο και σε επίπεδο αξιολόγησης της υγείας των υφιστάμενων δέντρων. Η χρήση διαφορετικών θερμικών δεικτών, εξαγόμενων από την ανάλυση των θερμικών εικόνων, ανέδειξε τη σημασία της υπέρυθρης θερμογραφίας για την κατανόηση διαφορετικών «μοτίβων» υγείας των δέντρων. Ειδικότερα, ο θερμικός δείκτης T_{IQR}, αποδείχτηκε είναι ένας από τους πιο σημαντικούς δείκτες κατά την εξέταση ενός δέντρου τόσο συνολικά όσο και εξειδικευμένα στην περιοχή της δομικής ατέλειας. Οι παρατηρούμενες διαφορές αυτού του δείκτη σχετικά με τους διαφορετικούς τύπους δομικών ελαττωμάτων, τόσο σε απόλυτους αριθμούς όσο και σε στατιστική σημαντικότητα, επιβεβαιώνουν την έννοια του υγιούς δέντρου μέσω της εκτίμησης του θερμικού του προφίλ. Παράλληλα, η εφαρμογή χωρικών στατιστικών μεθόδων, σε επίπεδο κορμού καθώς και η εξαγωγή χωρικών δεικτών, αποτύπωσε με εξαιρετικά υψηλή ακρίβεια την παρουσία δομικών ελαττωμάτων στα δέντρα. Η σύνδεση αυτή αποτελεί και μία από τις καινοτομίες της παρούσης διατριβής, καθώς δεν υπάρχει άλλη μελέτη σχετικά με τη χρήση δεικτών χωρικής αυτοσυσχέτισης και θερμικών δεικτών, για την απόκτηση πληροφοριών για την ανίχνευση δομικών ελαττωμάτων. Σημαντική προσθήκη σε αυτό ήταν και οι παρατηρούμενες υψηλές σχέσεις εξάρτησης του δείκτη από τα φαινοτυπικά και χωρικά χαρακτηριστικά των δέντρων. Όλα τα παραπάνω έδωσαν τη δυνατότητα εκτίμησης της παρουσίας των διαφορετικών τύπων δομικών ατελειών και της αποτύπωσης αυτών χωρικά, προσφέροντας εξειδικευμένη πληροφορία τόσο για τη δυνητική ιεράρχηση των δέντρων σε επικίνδυνα και μη, όσο και για την ταξινόμηση των περιοχών που φύονται σε υψηλής, μέτριας και χαμηλής επικινδυνότητας.

Στα αγροτικά οικοσυστήματα, η διερεύνηση της συνολικής κατάστασης των παραδοσιακών ελαιώνων της Λέσβου, μέσω της μελέτης 80 ελαιόδεντρων, εντός των υψηλής φυσικής αξίας αγροτικών εκτάσεων, πραγματώθηκε βάσει της δημιουργίας συνδυαστικού μεθοδολογικού πλαισίου στο οποίο εισήχθησαν φαινοτυπικοί, θερμικοί και φασματικοί δείκτες. Με τη συνδυασμένη χρήση αυτών, και μέσω των περιγραφόμενων μεταξύ τους σχέσεων ήταν εφικτή η πρόβλεψη της παραγωγικότητας, ως ένας ακόμη δείκτης υγείας, σε επίπεδο δέντρου αλλά και πληθυσμού. Ειδικότερα, οι εξαγόμενες σχέσεις συγκεκριμένων δεικτών όπως του εύρους φυλλικής επιφάνειας (LAI_{range}), του αριθμού δομικών ατελειών (SDV) και των θερμικών δεικτών IQR και OPR, συνδεόμενες με την παραγωγικότητα, αποτελούν μία ακόμα καινοτόμα διαφοροποίηση της παρούσης διατριβής σε σχέση με την υφιστάμενη επιστημονική γνώση. Οι συγκεκριμένοι δείκτες, που περιγράφουν διαφορετικές δομές των ελαιόδεντρων (κόμη και κορμό), όταν ενισχύονται από πληροφορία σε επίπεδο φύλλου (αλλά και κόμης) που να περιγράφει την συγκέντρωση χλωροφύλλης (TCL_T), μπορούν να ανιχνεύσουν με μεγάλη ακρίβεια μία από τις πιο σημαντικές ασθένειες που διαταράσσουν τη ζωτικότητα των ελαιόδεντρων, το κυκλοκόνειο. Η ταξινόμηση των δέντρων, βάσει των αρχιτεκτονικών, λειτουργικών, θερμικών και φασματικών χαρακτηριστικών τους, οδήγησε στην κατηγοριοποίηση της κατάστασης της υγείας τους, η οποία μπορεί να περιγραφεί ικανοποιητικά από συγκεκριμένα εύρη τιμών των δύο εξαγόμενων θερμικών δεικτών,

μεταβαίνοντας από επίπεδο δέντρου, σε επίπεδο πληθυσμού. Οι συγκεκριμένοι δείκτες μπορούν να έχουν ευρύτερη εφαρμογή και σε άλλα είδη δενδρώδους βλάστησης, όταν συνδυαστούν με ένα φάσμα δομικών και λειτουργικών χαρακτηριστικών των δέντρων, αποτελώντας εφαλτήριο για τη γρήγορη αλλά ταυτόχρονα υψηλής ακρίβειας αξιολόγηση της υγείας τους.

Στα δασικά οικοσυστήματα, η διερεύνηση της επίδρασης της ρητίνευσης, μέσω της ποσοτικοποίησης των πληγώσεων, στην αύξηση των πεύκων και η εκτίμηση της παρουσίας ξυλοσηπτικών μυκήτων σε αυτά, συνείσφερε στην αναγνώριση τόσο των διαταραχών όσο και στην αξιολόγηση της κατάστασής τους. Το γενικό συμπέρασμα, ότι η συγκομιδή ρητίνης διαταράσσει τα δέντρα καθώς προκαλεί δομικές βλάβες στον κορμό τους επηρεάζοντας τη ζωτικότητα τους και, κατά συνέπεια, την απόκρισή τους σε μυκητιασικές ασθένειες, ενώ ταυτόχρονα επηρεάζει τον ρυθμό ανάπτυξής τους, προέκυψε, σε αντιστοιχία με τα παραπάνω, από το συνδυασμό ελάχιστα επεμβατικών και μη επεμβατικών προσεγγίσεων. Σημαντική προσθήκη σε αυτές, ήταν η αντιμετώπιση του υπό μελέτη δασικού οικοσυστήματος ολιστικά, καθώς με την καταγραφή όχι μόνο των φαινοτυπικών χαρακτηριστικών τους, αλλά και της θέσης κάθε πεύκου στη συστάδα, ήταν δυνατή η απομόνωση αυτών των χαρακτηριστικών για την εξακρίβωση της πραγματικής επίδρασης της ρητίνευσης στην αύξηση. Παράλληλα, η μέτρηση του δείκτη φυλλικής επιφάνειας τόσο από την περιοχή της πλήγωσης όσο και από την περιοχή του υγιούς στελέχους, η εκτίμηση του εύρους των τιμών αυτών και η δημιουργία θερμικών αλλά και υγρασιακών δεικτών, οδήγησε στην εύρεση σχέσεων που ενδυναμώνουν την επεξηγηματικότητα μοντέλων που σχετίζονται με την αύξηση και κατ' επέκταση με την υγεία των πεύκων. Τόσο οι δείκτες που σχετίζονται με το θερμικό και υγρασιακό προφίλ των πεύκων, όσο και αυτοί που συνδέονται άμεσα ή έμμεσα με την υγεία τους, διαφοροποιούνται σημαντικά όταν συγκρίνονται με υγιή πεύκα εντός των υπό μελέτη συστάδων. Αυτή η διαφοροποίηση, αντίστοιχα και με τα άλλα είδη δενδρώδους βλάστησης που μελετήθηκαν, ενισχύει το επιχείρημα ότι αυτοί οι δείκτες μπορούν να χρησιμοποιηθούν αυτόνομα για τη μελέτη της αύξησης των δέντρων. Επιπροσθέτως, ο σύντομος (σχετικά) χρόνος λήψης των θερμικών εικόνων αλλά και άλλων δεικτών υγείας, προσθέτει μία ακόμα επιλογή στις υπάρχουσες κλασσικές μεθόδους, για τη γρήγορη αλλά με υψηλή ακρίβεια διάγνωση της παρουσίας μυκητιακών παθογόνων στα δασικά οικοσυστήματα. Βάσει όλων των παραπάνω, είναι αντιληπτό ότι πληροφορία όπως η περιγραφόμενη, μπορεί να συμβάλει σε πρωτοβουλίες διαχείρισης και αποκατάστασης δασικών συστημάτων, παρέχοντας τα μέσα για μια ταχεία αλλά και ακριβή αξιολόγηση της κατάστασης της υγείας τους.

Βιβλιογραφία

1. Allen, C.D.; Macalady, A.K.; Chenchouni, H.; Bachelet, D.; McDowell, N.; Vennetier, M.; Kitzberger, T.; Rigling, A.; Breshears, D.D.; Hogg, E.H.; Gonzalez, P.; Fensham, R.; Zhang, Z.; Castro, J.; Demidova, N.; Lim, J.H.; Allard, G.; Running, S.W.; Semerci, A.; Cobb, N.A global overview of drought and heat-induced tree mortality reveals emerging climate change risks for forests, *Forest Ecology and Management*. **2010**, N259: 660–84.
2. Almansoori, T.; Salman, M.; Aljazeri, M. Rapid and nondestructive estimations of chlorophyll concentration in date palm (Phoenix dactylifera L.) leaflets using SPAD–502+ and CCM–200 portable chlorophyll meters. *Emir. J. Food Agric*. **2021**, 33, 532–543
3. Atkins, P. and de Paula, J., (2006) 'Atkins' Physical Chemistry - 8th Edition. Oxford University Press.
4. Ballester C.; Jiménez-Bello M.A.; Castel J.R.; Intrigliolo D.S. Usefulness of thermography for plant water stress detection in citrus and persimmon trees, *Agricultural and Forest Meteorology*. **2013**, 168, 120-129.
5. Balmford, A.; Bruner, A.; Cooper, P.; Costanza, R.; Farber, S.; Green, R.E.; Jenkins, M.; Jefferiss, P.; Jessamy, V.; Madden, J.; Munro, K.; Myers, N.; Naeem, S.; Paavola, J.; Rayment, M.; Rosendo, S.; Roughgarden, J.; Trumper, K.; Turner, R.K. Economic Reasons for Conserving Wild Nature. *Science*. **2002**, 297: 950.
6. Boa, E.R. An illustrated guide to the state of health of trees: recognition and interpretation of symptoms and damage. Food & Agriculture Org. **2003**
7. Boyd, D.S. and Danson, F.M. Satellite remote sensing of forest resources: three decades of research development. *Progress in Physical Geography*. **2005**, 29(1): 1-26.
8. Bréda, N.J.J. Ground-based measurements of leaf area index: A review of methods, instruments and current controversies. *J. Exp. Bot*. **2003**, 54, 2403–2417
9. Briscoe, N.J., Handasyde, K.A., Griffiths, S.R., Porter, W.P., Krockenberger, A. and Kearney, M.R., Tree-hugging koalas demonstrate a novel thermoregulatory mechanism for arboreal mammals, *Biology Letters.* **2014**, 10(6), 201-235
10. Burcham, D.C.; Leong, E.C.; Fong, Y.K.; Tan, P.Y. An evaluation of internal defects and their effect on trunk surface temperature in Casuarina equisetifolia L. (Casuarinaceae), *Arboriculture and Urban Forestry*. **2012**, 38(6), 277-286.
11. Catena, A. and Catena, G. Overview of thermal imaging for tree assessment, *Arboricultural Journal*. **2008**, 30(4), 259-270.
12. Chaerle, L.; Van Caeneghem, W.; Messens, E.; Lambers, H.; Van Montagu, M.; Van Der Straeten, D. Presymptomatic visualization of plant–virus interactions by thermography. *Nature.* **1999**, *biotechnology*, 17(8), 813.
13. Chaerle, L.; De Boever, F.; Montagu, M.V.; Straeten, D. Thermographic visualization of cell death in tobacco and Arabidopsis. *Plant, Cell & Environment*. **2001**, 24(1), 15-25.
14. Cumming, G. and Collier, J. Change and identity in complex systems. *Ecology and Society*. **2005**, 10(1).
15. Day, K.; Berg, J.; Brown, H.; Crow, T.; Morrison, J.; Nowacki, G.; Puckett, D.; Sallee, R.; Schenck, T.; Wood B. Ecosystem restoration: a framework for restoring and maintaining the National Forests and Grasslands. USDA Forest Service. **2006**, Washington, DC, USA.
16. Dragavtsev, V. and Nartov, V.P. Application of thermal imaging in agriculture and forestry. *European Agrophysical Journal*. **2015**, 2(1): 15-23.
17. Dunjó, G.; Pardini, G.; Gispert, M. Land use change effects on abandoned terraced soils in a Mediterranean catchment, NE Spain. *Catena.* **2003**, 52, 23–37
18. Eva, H.; Carboni, S.; Achard, F.; Stach, N.; Durieux, L.; Faure, J.F.; Mollicone, D. Monitoring forest areas from continental to territorial levels using a sample of medium spatial resolution satellite imagery. *ISPRS Journal of Photogrammetry and Remote Sensing*. **2010**, 65(2): 191-197.
19. Eitel, J.U.; Keefe, R.F.; Long, D.S.; Davis, A.S.; Vierling, L.A. Active ground optical remote sensing

for improved monitoring of seedling stress in nurseries, *Sensors*. **2010**, 10(4), 2843-2850.
20. García-Tejero, I.; Durán-Zuazo, V.H.; Arriaga, J.; Hernández, A.; Vélez, L.M.; Muriel-Fernández, J.L. Approach to assess infrared thermal imaging of almond trees under water-stress conditions, *Fruits*. **2012**, 67(6), 463-474.
21. Guo, Y.Y.; Yu, H.Y.; Kong, D.S.; Yan, F.; Zhang, Y.J. Effects of drought stress on growth and chlorophyll fluorescence of Lycium ruthenicum Murr. seedlings. *Photosynthetica.* **2016**, 54, 524–531.
22. Halpern, B.S.; Walbridge, S.; Selkoe, K.A.; Kappel, C.V.; Micheli, F.; D'Agrosa, C.; Bruno, J.F.; Casey, K.S.; Ebert, C.; Fox, H.E.; Fujita, R.; Heinemann, D.; Lenihan, H.S.; Madin, E.M.P.; Perry, M.T.; Selig, E.R.; Spaldin, M.; Steneck, R.; Watson, R. A global map of human impact on marine ecosystems. *Science*. **2008**, 319: 948-952.
23. Hansen, E.M.; Stone, J.K.; Capitano, B.R.; Rosso, P.; Sutton, W.; Winton, L.; Kanaskie, A.; McWilliams, M.G. Incidence and impact of Swiss needle cast in forest plantations of Douglas-fir in coastal Oregon. *Plant Disease*. **2000**, 84, 773–778.
24. Hunt, J.F.; Gu, H.; Lebow, P.K. (2008) Theoretical thermal conductivity equation for uniform density wood cells. *Wood and Fiber Science*, 40(2): 167-180.
25. IPCC. Climate Change 2007: The Physical Science Basis. Contribution ofWorking Group I to the Fourth Assessment Report of the Intergovernmental Panel on Climate Change. Cambridge University Press. **2007b**, Cambridge.
26. Johnstone, D.M.; Moore, G.; Tausz, M.; Nicolas, M. The measurement of wood decay in landscape trees. *Arboriculture & Urban Forestry*. **2010**, 36(3): 121-127.
27. Jones, H.G.; Serraj, R.; Loveys, B.R.; Xiong, L.; Wheaton, A.; Price, A. H. Thermal infrared imaging of crop canopies for the remote diagnosis and quantification of plant responses to water stress in the field. *Functional Plant Biology*. **2009**, 36(11), 978-989.
28. Kerr, J.T. and Ostrovsky, M. From space to species: ecological applications for remote sensing. *Trends in Ecology & Evolution*. **2003**, 18(6): 299-305.
29. Lenthe, J.H.; Oerke, E.C.; Dehne, H.W. Digital infrared thermography for monitoring canopy health of wheat. *Precision Agriculture*. **2007**, 8(1-2), 15-26.
30. Li, W.; Sun, Z.; Lu, S.; Omasa, K. Estimation of the leaf chlorophyll content using multiangular spectral reflectance factor. *Plant. Cell Environ*. **2019**, 42, 3152–3165.
31. McCafferty, D.J. Applications of thermal imaging in avian science, *Ibis*. **2013**, 155(1), 4-15.
32. Mishra, K.B.; Mishra, A.; Klem, K.; Govindjee Plant phenotyping: A perspective. *Indian J. Plant Physiol.* **2016**, 21, 514–527,
33. Musau, J.; Patil, S.; Sheffield, J.; Marshall, M. Spatio-temporal vegetation dynamics and relationship with climate over East Africa. *Hydrol. Earth Syst. Sci. Discuss*. **2016**, 1–30.
34. Nagendra, H.; Lucas, R.; Honrado, J.P.; Jongman, R.H.; Tarantino, C.; Adamo, M.; Mairota, P. Remote sensing for conservation monitoring: Assessing protected areas, habitat extent, habitat condition, species diversity, and threats. *Ecological Indicators*. **2013**, 33: 45-59.
35. Obeidat, W.; Avila, L.; Earl, H.; Lukens, L. Leaf spectral reflectance of maize seedlings and its relationship to cold tolerance. *Crop Sci*. **2018**, 58, 2569–2580.
36. Oerke, E.C.; Steiner, U.; Dehne, H.W.; Lindenthal, M. Thermal imaging of cucumber leaves affected by downy mildew and environmental conditions. *Journal of experimental botany*. **2006**, 57(9), 2121-2132.
37. Ouis, D. Non-destructive techniques for detecting decay in standing trees, *Arboricultural Journal*. **2003**, 27(2), 159-177.
38. Parmesan, C., and G. Yohe. A globally coherent fingerprint of climate change impacts across natural systems. *Nature.* **2003**, 421:37–42.
39. Parmesan, C. Ecological and evolutionary responses to recent climate change. *Annual Review of Ecology, Evolution, and Systematics*. **2006**, 37:637–669.
40. Pavlovic, D.; Nikolic, B.; Djurovic, S.; Waisi, H.; Andjelkovic, A.; Marisavljevic, D. Chlorophyll as a measure of plant health: Agroecological aspects. *Pestic. Fitomed*. **2014**, 29, 21–34.

41. Potter, B.E. and Andresen, J.A. A finite-difference model of temperatures and heat flow within a tree stem. *Canadian Journal of Forest Research*. **2002**, 32: 548- 555.
42. Quattrochi, D.A. and Luvall, J.C. Thermal infrared remote sensing for analysis of landscape ecological processes: methods and applications. Landscape ecology. **1999**, 14(6): 577-598.
43. Rapport, D.J. What constitutes ecosystem health?. *Perspectives in biology and medicine*. **1989**, 33(1), 120-132.
44. Rapport, D.J. Evaluating ecosystem health. *Journal of aquatic ecosystem health*. **1992**, 1(1), 15-24.
45. Richardson, A.D.; Duigan, S.P.; Berlyn, G.P. An evaluation of noninvasive methods to estimate foliar chlorophyll content. *New Phytol*. **2002**, 153, 185–194.
46. Salvati, L.; Ferrara, C. The local–scale impact of soil salinization on the socioeconomic context: An exploratory analysis in Italy. *Catena.* **2015**, 127, 312–322.
47. Sanderson, E.W.; Jaiteh, M.; Levy, M.A.; Redford, K.H.; Wannebo, A.V.; Woolmer, G. The human footprint and the last of the wild. *Bioscience.* **2002**, 52: 891-904.
48. Sánchez–Reinoso, A.D.; Ligarreto–Moreno, G.A.; Restrepo–Díaz, H. Drought–tolerant common bush bean physiological parameters as indicators to identify susceptibility. *HortScience.* **2019**, 54, 2091–2098.
49. Seastedt, T.R.; Hobbs, J.R.; Suding, K.N. Management of novel ecosystems: are novel approaches required? *Frontiers in Ecology and the Environment.* **2008**, 6: 547-553.
50. SER, (2002). The SER primer on ecological restoration. *Society for Ecological Restoration Science and Policy Working Group* **2002**.
51. Steele, M.; Gitelson, A.A.; Rundquist, D. Nondestructive estimation of leaf chlorophyll content in grapes. *Am. J. Enol. Vitic.* **2008**, 59, 299–305.
52. Stenseth, N.C.; A. Mysterud, G.; Ottersen, J.W.; Hurrell, Chan, K.-S.; Lima. M. Ecological effects of climate fluctuations. *Science*. **2002**, 297:1292–1296.
53. Stoll, M.; Schwarz, H.P.; Baecker, G.; Schultz, H.R. Use of infrared thermography towards improving spray application technologies. *Bulletin de l'OIV.* **2008**, 82(941), 331.
54. Su, M.; Fath, B.D.; Yang, Z. Urban ecosystem health assessment: A review. *Science of the Total Environment*. **2010**, 408(12), 2425-2434.
55. Vidal, D.; Pitarma, R. Infrared thermography applied to tree health assessment: A review. *Agric*. **2019**, 9.
56. Walker, B.; Holling, C.S.; Carpenter, S.; Kinzig, A. Resilience, adaptability and transformability in social–ecological systems. *Ecology and society*. **2004**, 9(2).
57. Wang, J.; Wang, T.; Shi, T.; Wu, G.; Skidmore, A.K. A wavelet–based area parameter for indirectly estimating copper concentration in Carex leaves from canopy reflectance. *Remote Sens.* **2015**, 7, 15340–15360.
58. White, P.S. and Pickett, S.T. Natural disturbance and patch dynamics. *Unknown Journal*. **1985**, 3-13
59. Zarate-valdez, J.L.; Whiting, M.L.; Lampinen, B.D.; Metcalf, S.; Ustin, S.L.; Brown, P.H. Author ' s personal copy Prediction of leaf area index in almonds by vegetation indexes Author ' s personal copy. **2012**, 85, 24–32.
60. Zevgolis, Y.G.; Kamatsos, E.; Akriotis, T.; Dimitrakopoulos, P.G.; Troumbis, A.Y. Estimating Productivity, Detecting Biotic Disturbances, and Assessing the Health State of Traditional Olive Groves, Using Nondestructive Phenotypic Techniques. *Sustainability.* **2022**, 14, 391
61. Zhang, W.; Ricketts, T.H.; Kremen, C.; Carney, K.; Swinton, S.M.; Ecosystem services and dis-services to agriculture. *Ecological economics*. **2007**, 64(2), 253-260.

Other publications

Scientific Journals

I. Troumbis A.Y., **Zevgolis Y.G.** (2020), **Biodiversity crime and economic crisis: Hidden mechanisms of misuse of ecosystem goods in Greece**, Land Use Policy, Volume 99, 105061, https://doi.org/10.1016/j.landusepol.2020.105061

II. Zannetos P.S., **Zevgolis Y. G.,** Akriotis T. (2018), **First record of Crested (or Crested–type) Honey Buzzard *Pernis ptilorhynchus* for Greece**, Bulletin of the British Ornithologists' Club, Volume 138(4): 386 – 388, https://doi.org/10.25226/bboc.v138i4.2018.a10

III. Vasios G.K., Troumbis A.Y., **Zevgolis Y.G.,** Hatziantoniou M.N., Balis M.F. (2018), **Environmental choices in the era of ecological modernization: siting of common interest facilities as a multi–alternative decision field problem in insular setups,** Environment Systems and Decisions, Volume 39: 1–16, https://doi.org/10.1007/s10669–018–9690–9

Book chapter

I. Vasios G.K., Antoniadis I., **Zevgolis Y.,** Giaginis C., Troumbis A.Y. (2020)**, Turning a problem into an opportunity through tourism and marketing: The case of wild rabbits in Lemnos Island, Greece.** In: Kavoura A., Kefallonitis E., Theodoridis P. (eds) Strategic Innovative Marketing and Tourism. Springer Proceedings in Business and Economics. Springer, Cham, https://link.springer.com/chapter/10.1007%2F978–3–030–36126–6_75

International Conference Proceedings

i. **Zevgolis Y.G.**, Zannetos S.P., Akriotis T. (2021), **Determining recapture probability of the free–ranging wood mouse using infrared thermography**, In: Abstracts book of the 58th Annual Conference of the Animal Behavior Society, 03–06/08/2021, Virtual Meeting.

ii. Zannetos S.P., **Zevgolis Y.G.**, Akriotis T. (2021), **Post–trapping behavioral sequence analysis of *Apodemus mystacinus* in field conditions,** In: Abstracts book of the 58th Annual Conference of the Animal Behavior Society, 03–06/08/2021, Virtual Meeting.

iii. **Zevgolis Y.G.**, Zannetos S.P., Akriotis T. (2019), **Thermal imaging as a conservation physiology tool for assessing vertebrate physiological stress response during field handling procedures,** In: "Proceedings of the 14th International Congress on the Zoogeography and Ecology of Greece and Adjacent Regions (ICZEGAR)", pp. 180, 27–30/06/2019, Thessaloniki, Greece.

iv. Zannetos S.P., **Zevgolis Y.G.**, Christopoulos A., Akriotis T. (2019), **Habitat composition and distribution of Persian squirrel (*Sciurus anomalus*) in Greece,** In: "Proceedings of the 14th International Congress on the Zoogeography and Ecology of Greece and Adjacent Regions (ICZEGAR)", pp. 176, 27–30/06/2019, Thessaloniki, Greece.

v. Zannetos S.P., **Zevgolis Y.G.**, Christopoulos A., Akriotis T. (2019), **Preliminary results of the Lesvos Wildlife Roadkill Monitoring Scheme: implications for mammal conservation,** In: "Proceedings of the 14th International Congress on the Zoogeography and Ecology of Greece and Adjacent Regions (ICZEGAR)", pp. 178, 27–30/06/2019, Thessaloniki, Greece.

vi. Zannetos S.P., **Zevgolis Y.G.**, Michail V., Akriotis T. (2019), **Preliminary assessment of small mammal species composition, using Barn owl pellet analysis in three different habitats on the island of Lesvos,** In: "Proceedings of the 14th International Congress on the Zoogeography and Ecology of Greece and Adjacent Regions (ICZEGAR)", pp. 177, 27–30/06/2019, Thessaloniki, Greece.

vii. Zannetos S.P., **Zevgolis Y.G.**, Barboutis C., Akriotis T. (2019), **The importance of abandoned crops as stopover areas for a globally threatened species: the case of turtle dove on the South Aegean island of Antikythera**, In: "Proceedings of the 14th International Congress on the Zoogeography and Ecology of Greece and Adjacent Regions (ICZEGAR)", pp. 179, 27–30/06/2019, Thessaloniki, Greece.

viii. Michail V., Zannetos S.P., **Zevgolis Y.G.**, Akriotis T. (2019), **The importance of a Microtus vole for Barn Owl in an Aegean island ecosystem,** In: "Proceedings of the 14th International Congress on the Zoogeography and Ecology of Greece and Adjacent Regions (ICZEGAR)", pp. 114, 27–30/06/2019, Thessaloniki, Greece.

ix. Vasios G.K., Nannou M., Kostopoulos M., **Zevgolis Y.G.**, Tsiftsi D., Mantzorou M., Arkadianos I., Giaginis C. (2018), **Mediterranean diet and biodiversity as synergistic sustainability factors for promoting human well–being,** In: "Abstracts book of the 1st European Lifestyle Medicine Congress", 10–11/11/2018, Geneva, Switzerland.

x. Savvidou E., Chrysafi D., **Zevgolis Y.G.**, Vasios G.K., Troumbis A.Y. (2018), **Meta–analysis of experimental trends and statistical complexity in Biodiversity–Ecosystem Function theory,** In: "Abstracts book of the 1st International Conference in Environmental Science, Policy & Management", 01–03/06/2018, Mytilene, Greece.

xi. Metaxa C., **Zevgolis Y.G.**, Kotrikla A.M., Troumbis A.Y. (2018), **High risk areas for marine biodiversity conservation regarding tanker shipping routes in the Greek seas,** In: "Abstracts book of the 11th International Conference of the Hellenic Geographical Society (ICHGS – 2018)", 12–15/04/18, Lavrion, Greece.

xii. Vasios G.K., **Zevgolis Y.G.**, Troumbis A.Y. (2017), **Monitoring the extraction process of resinous sap from the *Pistacia lentiscus* var. chia using ground IR techniques**, In: "Abstracts book of the 19th International Symposium of MESAEP on Environmental Pollution and its Impact on Life in the Mediterranean Region", pp. 314–315, 04–06/10/17, Rome, Italy.

xiii. Vasios G.K., **Zevgolis Y.G.**, Nasopoulou C., Karantonis H.C., Giaginis C., Troumbis A.Y. (2017), **Perceptions of local community of Lemnos Island on implementing proper management**

actions for wild rabbits' overpopulation control, In: "Abstracts book of the 19th International Symposium of MESAEP on Environmental Pollution and its Impact on Life in the Mediterranean Region", pp. 61–62, 04–06/10/17, Rome, Italy.

xiv. Chrysafi D., Savvidou E., **Zevgolis Y.G.**, Troumbis A.Y. (2017), **Analyzing trends and statistical significance in Biodiversity–Ecosystem Function theory,** In: "Abstracts book of the 19th International Symposium of MESAEP on Environmental Pollution and its Impact on Life in the Mediterranean Region", pp. 64, 04–06/10/17, Rome, Italy.

xv. Metaxa C., **Zevgolis Y.G.**, Troumbis A.Y. (2017), **Assessing the periodicity of pollution incidents on sea routes in Marine Protected Areas in the Greek Exclusive Economic Zone**, In: "Abstracts book of the 19th International Symposium of MESAEP on Environmental Pollution and its Impact on Life in the Mediterranean Region", pp. 52, 04–06/10/17, Rome, Italy.

xvi. **Zevgolis Y.G.**, Grimpylakou L., Theofanellis T. (2017), **Students' prior knowledge and interests as regulators in designing effective Environmental Education Programs: The case of Kalloni Gulf Wetland**, In: "Abstracts book of the 19th International Symposium of MESAEP on Environmental Pollution and its Impact on Life in the Mediterranean Region", pp. 146, 04–06/10/17, Rome, Italy.

xvii. Vasios G.K., **Zevgolis Y.G.**, Nasopoulou C., Karantonis H.C., Giaginis C., Dimitriadis–Kazasis T.G., Tserolas D., Staramou A., Karathanasi I., Miserli E., Mastrogianni E., Gianniodi E., Papazoglou–Dragoumis D., Moutsai C., Papakosta I., Daskalaki A., Filippatou M., Troumbis A.Y. (2017), **Rural communities under Human–Wildlife Conflict: transforming the wild rabbits problem to a food source and an opportunity for local economy**, In: "Proceedings of the 15th International Conference on Environmental Science And Technology", 31/08–02/09/2017, Rhodes, Greece.

xviii. **Zevgolis Y.G.**, Vasios G.K., Dimitrakopoulos P.G., Troumbis A.Y. (2017), **Development of Ecological Restoration Projects on Mediterranean ecosystems: Analyzing trends and statistical complexity**, In: "Abstracts book of the XIV MEDECOS and AEET Conference 2017 on Human driven scenarios for evolutionary and ecological changes", pp. 245, 31/01–04/02/17, Seville, Spain.

xix. **Zevgolis Y.G.**, Chaintarlis K., Troumbis A.Y. (2016), **High risk areas regarding environmental criminality during the "lean years" of Greece**, In: "Abstracts book of the 5th International EcoSummit: Ecological Sustainability: Engineering Change", 29/08–01/09/16, Montpellier, France.

xx. **Zevgolis Y.G.**, Troumbis A.Y. (2016), **Ecological Criminality Index: A novel approach for preventing and monitoring illegal logging**, In: "Abstracts book of the 5th International EcoSummit: Ecological Sustainability: Engineering Change", 29/08–01/09/16, Montpellier, France**.**

xxi. **Zevgolis Y.G.**, Aiggis K., Troumbis A.Y. (2016), **Assessment on priority natural habitat type**

2250 "Coastal dunes with Juniperus spp." conservation status of Alyko, Naxos, In: "Abstracts book of the 14th 'Islands of the World' Conference 2016", pp. 73, 23–27/05/2016, Mytilene, Greece.

xxii. **Zevgolis Y.G.**, Troumbis A.Y. (2015), **Resilience of restored ecosystems as the basic attribute which mitigates the effects of climate change: A review of the literature**, In: "Abstracts book of the 18th International Symposium of MESAEP on Environmental Pollution and its Impact on Life in the Mediterranean Region", pp. 105, 26–30/09/15, Crete, Greece.

xxiii. **Zevgolis Y.G.**, Oikonomou V., Troumbis A.Y. (2015), **Tendencies towards environmental criminality during the recession in Greece**, In: "Abstracts book of the 18th International Symposium of MESAEP on Environmental Pollution and its Impact on Life in the Mediterranean Region", pp. 308, 26–30/09/15, Crete, Greece.

Hellenic Conference Proceedings

i. **Zevgolis Y.G.,** Zannetos P.S., Charea G., Lykogeorgou M., Mikroni O., Akriotis T. (2021), **Trap shy or trap happy? Small mammals' surface temperature as a recapture probability index,** In: "Abstracts book of the 9th Panhellenic Conference on Ecology, pp. 137, 10–14/10/21, Ioannina, Greece.

ii. **Zevgolis Y.G.,** Zannetos P.S., Charea G., Akriotis T. (2021), **Investigation of the behavioural activity of Eastern Broad–toothed Field Mouse under stress,** In: "Abstracts book of the 9th Panhellenic Conference on Ecology, pp. 136, 10–14/10/21, Ioannina, Greece.

iii. **Zevgolis Y.G.**, Zannetos S.P., Malakis A., Antoniou P., Botetzagias I., Akriotis T. (2021), **Thermal imaging as a diagnostic tool for wildlife veterinary clinical applications: a pilot study,** In: "Abstracts book of the 9th Panhellenic Conference on Ecology, pp. 166, 10–14/10/21, Ioannina, Greece.

iv. Christopoulos A., Kouris A., **Zevgolis Y.G.** (2021), **Investigation of reptiles and amphibians road mortality on the island of Lesvos,** In: "Abstracts book of the 9th Panhellenic Conference on Ecology, pp. 249, 10–14/10/21, Ioannina, Greece.

v. Christopoulos A., Vlachopoulos K., Kouris A., **Zevgolis Y.G.** (2021), **Spatiotemporal patterns of reptile and amphibian mortality from vehicles in Lake Karla,** In: "Abstracts book of the 9th Panhellenic Conference on Ecology, pp. 248, 10–14/10/21, Ioannina, Greece.

vi. Kouris A., **Zevgolis Y.G.,** Zannetos P.S., Akriotis T. (2021), **Analysis of terrestrial vertebrate roadkill mortality on main roads on the island of Lesvos**, In: "Abstracts book of the 9th Panhellenic Conference on Ecology, pp. 185, 10–14/10/21, Ioannina, Greece.

vii. Iliou A., **Zevgolis Y.G.,** Zannetos P.S., Akriotis T. (2021), **Estimation of the relative density of the red fox in different habitats on the island of Lesvos,** In: "Abstracts book of the 9th Panhellenic Conference on Ecology, pp. 168, 10–14/10/21, Ioannina, Greece.

viii. Leros M., **Zevgolis Y.G.,** Zannetos P.S., Akriotis T. (2021), **Effect of weather conditions on arrival time during the roosting of corvids in an urban environment,** In: "Abstracts book of the 9th Panhellenic Conference on Ecology, pp. 191, 10–14/10/21, Ioannina, Greece.

ix. Lykogeorgou M., **Zevgolis Y.G.,** Zannetos P.S., Akriotis T. (2021), **Rodent behavioural variability following trapping and handling**, In: "Abstracts book of the 9th Panhellenic Conference on Ecology, pp. 194, 10–14/10/21, Ioannina, Greece.

x. Mikroni O., **Zevgolis Y.G.,** Zannetos P.S., Akriotis T. (2021), **Estimation of acute stress in the Wood Mouse using thermal imaging techniques**, In: "Abstracts book of the 9th Panhellenic Conference on Ecology, pp. 199, 10–14/10/21, Ioannina, Greece.

xi. Zannetos P.S., **Zevgolis Y.G.,** Akriotis T. (2021), **Study of the behavioural sequence of the Eastern broad–toothed field mouse after trapping and handling in its natural environment,** In: "Abstracts book of the 9th Panhellenic Conference on Ecology, pp. 165, 10–14/10/21, Ioannina, Greece.

xii. Alsamail M.Z., Zannetos S.P., **Zevgolis Y.G**., Akriotis T. (2021), **Investigation of soil properties in areas of Harting's vole colonies,** In: "Abstracts book of the 9th Panhellenic Conference on Ecology, pp. 139, 10–14/10/21, Ioannina, Greece.

xiii. Kafetsi D., Zannetos S.P., **Zevgolis Y.G**., Akriotis T. (2021), **Diversity and abundance of small mammals in different habitats of the island of Lesvos**, In: "Abstracts book of the 9th Panhellenic Conference on Ecology, pp. 179, 10–14/10/21, Ioannina, Greece.

xiv. **Zevgolis Y.G**., Michelaki C., Zannetos S.P. (2019), **Composition, structure and regeneration of juniper communities (Juniperus spp.) in coastal dunes: The case of Alyko, Naxos**, In: "Abstracts book of the 16th Panhellenic Scientific Conference of the Hellenic Botanical Society, pp. 69, 10–13/10/2019, Athens, Greece.

xv. **Zevgolis Y.G.,** Zannetos P.S., Akriotis T. (2018), **Investigation of small mammals physiological stress with the use of thermal imaging techniques,** In: "Abstracts book of the 9th Panhellenic Conference on Ecology, pp. 118, 04–07/10/18, Herakleion, Greece.

xvi. Zannetos P.S., **Zevgolis Y.G.,** Akriotis T. (2018), **Density estimation, capture rate and foraging site selection of small mammals in Brutia pine forests in Lesvos Island**, In: "Abstracts book of the 9th Panhellenic Conference on Ecology, pp. 245, 04–07/10/18, Herakleion, Greece.

xvii. **Zevgolis Y.G.,** Zannetos P.S., Akriotis T. (2018), **Assessment of *Acrocephalus Schoenobaenus* physiological status using non – invasive methods during ringing procedure,** In: "Abstracts book of the 9th Panhellenic Conference on Ecology, 04–07/10/18, pp. 250, Herakleion, Greece.

xviii. **Zevgolis Y.G**., Masouras A., Zannetos P.S. (2018), **Estimation of density and detection probability of passerines in priority habitats: the case of Alyko, Naxos,** In: "Abstracts book of the 9th Panhellenic Conference on Ecology, 04–07/10/18, pp. 249, Herakleion, Greece.

xix. Zannetos P.S., Poupou L.L., **Zevgolis Y.G.,** Akriotis T. (2018), **Autumn and spring migration of Passerine birds in Lesvos: Long distance migrants' phenology**, In: "Abstracts book of the 9th Panhellenic Conference on Ecology, pp. 246, 04–07/10/18, Herakleion, Greece.

xx. Zannetos P.S., Literák I., Poupou L.L., **Zevgolis Y.G.,** Raab R., Akriotis T. (2018), **Winter food habits of Imperial Eagle (Aquila heliaca) at Psara island,** In: "Abstracts book of the 9th Panhellenic Conference on Ecology, 04–07/10/18, pp. 247, Herakleion, Greece.

xxi. **Zevgolis Y.G.,** Vasios GK., Palmou A., Dimitrakopoulos P.G., Troumbis A.Y. (2016), **Evolution of statistical complexity in Restoration Ecology,** In: "Abstracts book of the 8th Panhellenic Conference on Ecology: 150 years of Ecology: structures, links, dynamics and survival strategies, pp. 108, 20–23/10/16, Thessaloniki, Greece.

xxii. **Zevgolis Y.G.,** Vasios G.K., Troumbis A.Y. (2016), **Development of methodological framework for addressing illegal logging with the use of socioecological indicators,** In: "Abstracts book of the 8th Panhellenic Conference on Ecology: 150 years of Ecology: structures, links, dynamics and survival strategies, pp. 251, 20–23/10/16, Thessaloniki, Greece.

xxiii. Palmou A., **Zevgolis Y.G.,** Vasios G.K., Troumbis A.Y. (2016), **Diachronic study of Ecological Restoration projects: a literature review,** In: "Abstracts book of the 8th Panhellenic Conference on Ecology: 150 years of Ecology: structures, links, dynamics and survival strategies, pp. 323, 20–23/10/16, Thessaloniki, Greece.

xxiv. Grimpylakou L., Theofanellis T., **Zevgolis Y.G.** (2016), **The Kalloni gulf wetland, a multimedia approach for primary school children,** In: "Abstracts book of the 8th Panhellenic Conference on Ecology: 150 years of Ecology: structures, links, dynamics and survival strategies, pp. 244, 20–23/10/16, Thessaloniki, Greece.

xxv. Tsaligopoulos A., **Zevgolis Y.G,** Economou C., Oikonomou V., Matsinos Y. (2015), **Assessing the possible co–benefit of climate change adaptation using ecological soundscape restoration techniques,** In: "Proceedings of the 8th Panhellenic Conference Environmental Policy and Management", pp. 28–53, 05–07/06/15, Mytilene, Greece.

xxvi. **Zevgolis Y.G.,** Oikonomou V., Troumbis A.Y. (2014), **Holistic Ecological Restoration: Vision or Utopia?,** In: "Abstracts book of the 7th Panhellenic Conference on Ecology: connecting systems, scales and research fields, pp. 91, 09–12/10/14, Mytilene, Greece.

xxvii. **Zevgolis Y.G.,** Oikonomou V., Troumbis A.Y. (2014), **The effects of economic crisis upon biodiversity conservation policies: evidence from Greece,** In: "Abstracts book of the 5th Environmental Conference of Macedonia, pp. 105, 14–16/03/14, Thessaloniki, Greece.

University of the Aegean
Department of Environment
Biodiversity Conservation Laboratory

DOCTORAL THESIS

Assessing the health state of arboreal vegetation in urban, rural, and natural ecosystems, using non–destructive phenotypic techniques: implications for conservation and management

Yiannis G. Zevgolis


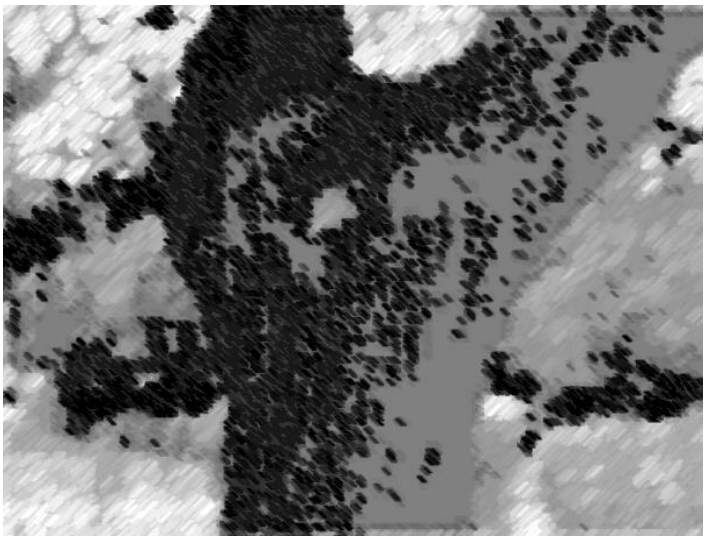

Mytilene, 2022